



HAL
open science

Cortical basis of vocalization in behaving freely moving minipigs

Marie Palma

► **To cite this version:**

Marie Palma. Cortical basis of vocalization in behaving freely moving minipigs. Neuroscience. Université Grenoble Alpes [2020-..], 2021. English. NNT : 2021GRALS013 . tel-03353386

HAL Id: tel-03353386

<https://theses.hal.science/tel-03353386>

Submitted on 24 Sep 2021

HAL is a multi-disciplinary open access archive for the deposit and dissemination of scientific research documents, whether they are published or not. The documents may come from teaching and research institutions in France or abroad, or from public or private research centers.

L'archive ouverte pluridisciplinaire **HAL**, est destinée au dépôt et à la diffusion de documents scientifiques de niveau recherche, publiés ou non, émanant des établissements d'enseignement et de recherche français ou étrangers, des laboratoires publics ou privés.

THÈSE

Pour obtenir le grade de

DOCTEUR DE L'UNIVERSITÉ GRENOBLE ALPES

Spécialité : CIA - Ingénierie de la Cognition, de l'interaction, de l'Apprentissage et de la création

Arrêté ministériel : 25 mai 2016

Présentée par

Marie PALMA

Thèse dirigée par **Blaise YVERT**

préparée au sein du **Laboratoire Grenoble Institut des Neurosciences**
dans l'**École Doctorale Ingénierie pour la Santé la Cognition et l'Environnement**

Bases corticales de la vocalisation chez le miniporc en comportement

Cortical basis of vocalization in behaving freely moving minipigs

Thèse soutenue publiquement le **29 juin 2021**,
devant le jury composé de :

Monsieur BLAISE YVERT

DIRECTEUR DE RECHERCHE, INSERM DELEGATION AUVERGNE-RHONE-ALPES, Directeur de thèse

Madame CELINE TALLET

CHARGE DE RECHERCHE HDR, INRAE CENTRE BRETAGNE-NORMANDIE, Rapporteure

Monsieur EMMANUEL PROCYK

DIRECTEUR DE RECHERCHE, CNRS DELEGATION RHONE AUVERGNE, Président

Madame VERONIQUE COIZET

CHARGE DE RECHERCHE HDR, INSERM DELEGATION AUVERGNE-RHONE-ALPES, Examinatrice

Monsieur JEAN-MARC EDELIN

DIRECTEUR DE RECHERCHE, CNRS DELEGATION ILE-DE-FRANCE SUD, Examinateur



Abstract

Investigating the fundamental cortical dynamics underlying vocal and speech production requires access to multiple cortical areas simultaneously. Such access is partly possible in humans when patients are implanted for clinical purpose with intracortical electrodes, but such cases are rare, with usually only partial coverage of involved brain areas. For this reason, animal models are useful to detail the dynamics of cortical networks underlying vocal production. To date, non-human primates, birds and recently rodents have been used, with increasing data showing that non-human primate network model of vocal production shares strong similarities with that of human speech production. The extent to which such model generalizes to other species remains however unclear. In this context, the main purpose of this thesis was to develop a novel experimental paradigm to investigate the cortical bases of vocal production using cortical electrode arrays in minipigs, a large non-primate species very keen in producing vocalizations and easy to handle by humans. This work was conducted in part within the frame of the Graphene Flagship aiming at developing low-noise cortical probes. Such implants were firstly tested in rats' auditory cortex in response to pure sounds.

To explore minipigs' cortical bases of vocalizations, we firstly characterized the vocalizations produced by these animals in a housing pen, in a context similar to their daily life during the experiment. The results showed 6 categories of calls, with different occurrence situations and acoustic characteristics, allowing us to explore the vocal repertoire of minipigs. Secondly, we developed an experimental setup to record cortical activity along with vocalizations in freely behaving minipigs. We used three minipigs implanted in different cortical areas of the left hemisphere of the animals. We identified key regions activated during vocal production in minipigs, including motor and premotor cortices and inferior frontal gyrus. Minipigs are hence a promising model to study vocal production cortical networks.

Résumé

L'étude des dynamiques corticales fondamentales sous-tendant la production vocale et le langage nécessite l'accès à plusieurs zones corticales simultanément. Un tel accès est en partie possible chez l'Homme lorsque des patients sont implantés à des fins cliniques avec des électrodes intracrâniennes, mais ces cas sont rares, avec en général une couverture partielle des zones du cerveau impliquées. Pour cette raison, les modèles animaux sont utilisés pour détailler la dynamique des réseaux corticaux sous-jacents à la production vocale. À ce jour, les primates non humains, les oiseaux et plus récemment des rongeurs ont été étudiés, et de plus en plus de données montrent que les réseaux corticaux de production vocale des modèles de primates non humains ont de fortes similitudes avec ceux de la production de la parole humaine. La mesure avec laquelle ce modèle se généralise à d'autres espèces demeure toutefois incertaine. Dans ce contexte, le but principal de cette thèse était de développer un nouveau paradigme expérimental pour étudier les bases corticales de la production vocale à l'aide d'électrodes corticales chez les mini-porcs, une espèce domestique non-primate très encline à produire des vocalisations et facile à manipuler par les humains.

Ce travail a été réalisé en partie dans le cadre du Graphene Flagship visant à développer des électrodes corticales permettant des enregistrements bas bruit. Ces implants ont d'abord été testés dans le cortex auditif du rat en réponse à des sons purs.

Pour explorer les bases corticales de la vocalisation chez le mini-porc, nous avons d'abord caractérisé les vocalisations produites par ces animaux dans un enclos de stabulation, en situation de vie quotidienne. Les résultats ont montré 6 catégories de vocalisations, avec différentes situations d'occurrence et caractéristiques acoustiques, nous permettant d'explorer le répertoire vocal des mini-porcs. Deuxièmement, nous avons développé un paradigme expérimental permettant d'enregistrer chez ces animaux, leur activité corticale en lien avec les vocalisations qu'ils produisent en comportement. Notre étude porte sur trois mini-porcs implantés dans différentes zones corticales de l'hémisphère gauche. Nous avons identifié les régions clés activées lors de la production vocale chez les mini-porcs, incluant les cortex moteur et pré-moteur et le gyrus frontal inférieur. Ces résultats suggèrent que les mini-porcs sont un modèle prometteur pour étudier les réseaux corticaux de la production vocale.

Acknowledgements

Key words

Minipig, Vocalization, ElectroCorticoGraphy, Premotor Cortex, SensoriMotor Cortex, Inferior Frontal Gyrus

Mots clés

Miniporc, Vocalisations, ElectroCorticoGraphie, Cortex Premoteur, Cortex SensoriMoteur, Gyrus Frontal Inférieur

Table des matières

ABSTRACT	2
RÉSUMÉ.....	2
LIST OF FIGURES.....	7
LIST OF TABLES	12
ACRONYMS AND TERMS	13
1. GOAL OF THE THESIS AND ORGANIZATION OF THE MANUSCRIPT	15
1.1. Motivation of the thesis	15
1.2. Organization of the manuscript	16
2. STATE OF THE ART	17
2.1. Animal Communication	17
2.1.1. Producing signals.....	19
Chemical	19
Visual	19
Acoustical.....	19
2.1.2. Transmitting signals.....	20
2.1.3. Perceiving signals	20
Chemoreceptors	20
Mechanoreceptors	20
Photoreceptors.....	21
2.2. Vocal communication	21
2.2.1. The roles of vocalizations	22
2.2.2. Language characteristics found in animal communication	22
Semanticity	23
Productivity	23
Symbolic	23
Recursivity / Grammar	23
Displacement	24
Prevarication	24
Traditional transmission.....	24
2.2.3. Suidae vocalizations	25
2.3. Methods for brain recording.....	27

2.3.1.	Neuronal activity	27
	Postsynaptic currents.....	29
	Action Potentials	29
	Neural oscillations.....	30
2.3.2.	General approaches for neural activity recording	32
	Metabolic signals recording	32
	Electrophysiological Recording.....	34
2.4.	Cortical bases of vocalizations.....	37
2.4.1.	Cortical bases of perception of vocalization in animals	40
2.4.2.	Cortical bases of production of vocalization in animals	41
2.4.3.	Minipigs cortical organization.....	42
3.	ASSESSMENT OF GRAPHENE CORTICAL IMPLANTS IN RATS.....	43
3.1.	Materials and methods.....	45
3.1.1.	Animals	45
3.1.3.	Auditory Stimulation	47
3.1.4.	Data aquisition	47
3.1.5.	Data analysis	47
	Local Field Potentials analysis.....	47
	Multi Unit and Single Unit activity analysis	48
3.2.	Results.....	48
3.2.1.	Acoustic contamination	49
3.2.2.	Local Field potentials	49
	Animal 1 – Penetrating NeuroNexus probe	50
	Animal 2 – Surface NeuroNexus μ ECoG	50
	Animal 2 –Graphene surface μ ECoG	50
3.2.3.	Single Unit and Multi Unit Activity	53
	Decoding pure tone frequency from fast events.....	54
3.3.	Discussion and perspectives.....	55
4.	CHARACTERIZATION OF MINIPIGS SPONTANEOUS VOCALIZATIONS.....	57
4.1.	Method.....	58
4.1.1.	Animals	58
4.1.2.	Recording Setup	58
4.1.3.	Analyzing minipig vocalization	59
4.2.	Results.....	60
4.2.1.	Grunts (n = 738).....	61
4.2.1.1.	Common Grunt (n = 591)	63

4.2.1.2.	Long Grunt (n = 93)	64
4.2.1.3.	Repeated Common Grunt (n = 54 individual grunts).....	66
4.2.2.	Trumpet (n=96)	68
4.2.3.	Rattle (n = 16)	69
4.2.4.	Grunt-Squeal (n = 5)	71
4.2.5.	Bark (n = 1)	72
4.2.6.	Blast (n = 421)	73
4.2.7.	Vocal behavior of minipigs.....	75
4.3.	Discussion and perspectives	78
5.	CORTICAL ACTIVITY UNDERLYING VOCAL PRODUCTION IN BEHAVING MINIPIGS.....	80
5.1.	Methods.....	81
5.1.1.	Animals	81
5.1.2.	Socialization program	82
5.1.3.	Anatomical imaging (CT-scan and T1 MRI)	84
5.1.4.	Surgery preparation using 3D modeling and printing	84
5.1.5.	Implantation surgery	85
5.1.6.	Simultaneous electrophysiological, audio and video recordings	89
5.1.7.	Audio data processing	91
5.1.8.	Neural data processing.....	91
5.2.	Results.....	91
5.2.1.	Evolution of the frontal sinuses over the motor cortex after 6 months	91
5.2.2.	Vocalizations.....	93
5.2.2.1.	YU254 vocalizations	93
5.2.2.2.	CH596 vocalizations.....	95
5.2.2.3.	GI2028 vocalizations	96
5.2.3.	Vocal production activates motor and premotor regions	97
5.2.4.	Vocal production activates temporal gyrus, inferior frontal gyrus and sensori motor cortex 100	
5.3.	Discussion and perspectives	104
6.	GENERAL CONCLUSION AND PERSPECTIVES.....	106
8.	REFERENCES.....	108

List of figures

Figure 1. Sonographs of the calls of adult pigs (Kiley, 1972). The categories were mostly made by hearing vocalizations and inspection of the sonograms.	26
Figure 2. Acoustic parameters retained for classification of vocalizations in the wild boar (Garcia et al., 2016). Mean values (\pm SD) of the four features used for classification are displayed for the four call types identified.	27
Figure 3. Structure of a neuron and sodium-potassium pump. (a) The neuron is composed of the soma, or cell body, the axon and the dendrites. At the end of the axon, many ramifications connect other neurons with synapses. The conduction of action potentials along the axon is made step by step from one node of Ranvier to another. Oligodendrocytes sometimes wrap axons with myelin sheath. The more myelinated an axon is, the faster the conduction. (b) Basic principle of a Na^+/K^+ ionic pump. Ionic exchanges are made between extracellular fluid and intracellular medium. The sodium-potassium pump actively brings potassium (K^+) inside the cell and expulses sodium (Na^+) away. This phenomenon requires the consumption of glucose and oxygen for the adenosine triphosphate (ATP) degradation into adenosine diphosphate (ADP)	28
Figure 4. Electroencephalography recording of brain waves. Different brain waves (left) and a sample of human electroencephalography recording with prominent resting state activity - alpha-rhythm (adapted from Sittiprapaporn, 2018 and Cherninskyi, 2015)	31
Figure 5. Electrophysiological recording methods. (Adapted from Mamun, 2012).....	34
Figure 6. NeuroGrid structure and spike recordings in freely moving rats (adapted from (Khodagholy et al., 2015)). (a) High-pass filtered ($f_c = 500\text{Hz}$) time traces recorded in a freely moving rat from the surface of cortex (left) and hippocampus (right) in black. Corresponding postmortem filtered traces ($\text{rms noise} = 3 \mu\text{V}$ at spike bandwidth) are in red (scale = 10 ms by 50 μV). (b) Examples of the spatial extent of extracellular action potentials in cortex (left) and hippocampus (right) over the geometry of the NeuroGrid by spike-triggered averaging during the detected spike times (scale = 1.5 ms by 50 μV).	36
Figure 7. A schematic view of the dual-stream model (Hickok & Poeppel, 2004) of the functional anatomy of language. The dorsal pathway is involved in sensory and phonological representations of speech. The ventral pathway links words to their semantic.	38
Figure 8. The dual-network model (Hage & Nieder, 2016). (A) Simplified circuit diagram (B) Anatomical locations and connections of the structures comprising the dual-network	39
Figure 9. Dorsal, lateral and medial (left hemisphere) views of the brain of a Large White-Landrace pig weighing 30 kg, with schematic representations of the cortical areas (adapted from Sauleau et al., 2009).....	43
Figure 10. Stereotaxic surgery in rat auditory cortex. (a) The screws are placed near the craniotomy in order to glue a custom head holder. The bone from the craniotomy was replaced during the glueing process to protect the brain. (b) The custom bar is glued to the skull with dental cement and the bone is removed. A reference electrode is glued under the piece to allow precise measures. (c) At the bottom of the craniotomy, the primary auditory cortex, represented by the yellow area, can be localized between two veins.	46
Figure 11. Different electrode types used. Left panel : intracortical NeuroNexus probe in animal 1. Center panel : surface NeuroNexus probe in animal 2. Right panel : graphene surface probe in animal 2.	47
Figure 12. Correlations between sound and $\mu\text{-ECoG}$ spectrograms during pure tones perception in an anesthetized rat. (Roussel et al., 2020). (a) Photograph of a $\mu\text{-ECoG}$ grid	

positioned over the left auditory cortex of a rat. Directions: a = anterior, p = posterior, d = dorsal, v = ventral. (b) On the upper panel, each blue curve represents, at all frequency bins, the value of the correlation coefficients between the spectrogram of one electrode signal and the spectrogram of the audio signal. The red curve represents the mean power spectral density (PSD) of the audio signal (a.u.). The lower panel represents a heat map of the correlation coefficient between audio and neural data for all electrodes and frequency bins. Correlation coefficients not statistically significant are displayed in grey.49

Figure 13. Auditory evoked responses in animals 1 and 2. (a) Bootstrapped (n = 1000) auditory evoked responses to pure tones of different frequencies (in lines, ascending order). Red bars indicate stimulus onset. Horizontal bars indicate stimulus duration (200 ms). (b) Bootstrapped (n = 1000) auditory evoked responses to 100 pure tones of 8kHz on one electrode located on A1. (c) Electrode in (b) represented on pictures of the cortex. 51

Figure 14. Spectrograms of the activities for animals 1 and 2. (a) 64 channels representation of the averaged evoked responses to all pure tone frequencies. Each panel represents the electrode layout of the implants. (b) Averaged spectrogram of the activity for all electrodes and all pure tone frequencies. Red bars represent stimulus onset.52

Figure 15. Multi Unit and Single-Unit-like activity recorded in response to pure tones with graphene probe on the surface of the left primary auditory cortex of rat No 2. (a) Pure tone presentation and bursting activity recorded on one electrode. (b) An example of four waveforms extracted from two different electrodes. (c) Waveform extraction and analysis using Plexon OFFLINE sorter. Superimposed waveforms are displayed on the left panel and principal component analysis (PCA) on the right panel. The PCA is visualized in 3 dimensions and the waveforms cluster are represented in pink and blue according to the colors on the left panel.53

Figure 16. Raster plots and peristimulus histograms for 4 units. Red bars represent the number of waveforms detected during the 50ms following stimulus onset. Unit 14, 16 and 32 present ON-OFF pattern of response. Unit 31 shows a sustained activity for pure tones of 2000Hz.54

Figure 17. Decoding pure tone frequencies based on cortical activity. (a) Example of a peristimulus histogram for Unit 32 in response to 12kHz pure tone. The colored bars on the peristimulus histogram are the features used for decoding (from stimulus onset to 450ms after stimulus onset, corresponding to 9 features of 50ms). (b) Confusion matrix of the decoding. Predicted frequencies are presented in columns and true frequencies in lines. The data are in percentages. Green cases indicate the right classification percentages. Red cases are the classification errors.55

Figure 18. AudioMoth recording session setup. The setup of one recording session allowed the acoustic logging of two separated minipigs FAJ758 and FIG776. The most distant AudioMoths were AudioMoth 1 and AudioMoth 6 (circled in red), vocalizations from the minipig FAJ758 were much more loudly recorded by AudioMoth 1 than by AudioMoth 6 and reciprocally.59

Figure 19. Spike 2 Interface for the classification of vocalizations of minipigs FAJ758 and FIG776. A1 and A6 waveforms were analyzed sequentially. Both visual inspection and hearing allowed the choice of locutor. The spectrograms were performed on Spike 2 with a Hanning window (block size = 4096). Memory ticks were the detection of sounds which were going to be classified after removing all the parasitic noises with spectrogram and hearing inspection. FAJ758 vocalizations are represented in red and FIG776 in blue.60

Figure 20. Six types of vocalizations recorded during the session. Top panel : Acoustic waveforms of averaged vocalizations for each recorded call type. Bottom panel : narrow band spectrograms of averaged vocalizations for each recorded call type. The spectrograms were generated in Matlab using the following parameters : 150ms window size, frequency range :

0-10kHz, frequency steps : 300. Grunt and Blast spectrogram scales range from 0 to 1E-6 $\mu\text{V}/\sqrt{\text{Hz}}$. The other vocalizations spectrogram scales range from 0 to 1E-5 $\mu\text{V}/\sqrt{\text{Hz}}$. Temporal scale of 400ms is common to all the panels. Amplitude scale of 1V is common to all the acoustic waveforms.....61

Figure 21. Histogram of the durations of Grunts vocalizations. (a) Histogram of the durations of Grunts for FAJ758 and FIG776. The distribution has a bimodal pattern representing different Grunt types. (b) Histogram of the durations of Grunts for FAJ758. (c) Histogram of the durations of Grunts for FIG776.62

Figure 22. Common Grunt. (a) Acoustic waveforms and narrow band spectrograms of a sample of Common Grunt for FAJ758 and FIG776. (b) narrow band spectrograms of the averaged Common Grunts for FAJ758 and FIG776. The spectrograms were generated in Matlab using the following parameters : 150ms window size, frequency range : 0-1000Hz, frequency steps : 300.63

Figure 23. Common Grunt characterization. Left panel : number of Common Grunts produced by FAJ758 and FIG776. Center panel : histogram of the intervals between two Common Grunts. Right panel : histogram of durations for Common Grunts.64

Figure 24. Long Grunt. (a) Acoustic waveforms and narrow band spectrograms of a sample of Long Grunt for FAJ758 and FIG776. (b) Narrow band spectrograms of the averaged Long Grunts for FAJ758 and FIG776. The spectrograms were generated in Matlab using the following parameters : 150ms window size, frequency range : 0-1000Hz, frequency steps : 300.65

Figure 25. Long Grunts characterization. Left panel : Number of Long Grunts produced by FAJ758 and FIG776. Center panel : histogram of the intervals between two Long Grunts. Right panel : histogram of durations for Long Grunts65

Figure 26. Repeated Grunt. (a) Acoustic waveforms and narrow band spectrograms of 3 samples of Repeated Grunts for FAJ758 and FIG776. (b) Narrow band spectrograms of the averaged Repeated Grunts for FAJ758 and FIG776. The spectrograms were generated in Matlab using the following parameters : 150ms window size, frequency range : 0-1000Hz, frequency steps : 300.66

Figure 27. Repeated Grunt characterization. Left panel : Number of Repeated Grunts produced by FAJ758 and FIG776. Center panel : histogram of the intervals between two Repeated Grunts. Right panel : histogram of durations for Repeated Grunts.67

Figure 28. Time intervals within a Repeated Grunts sequence. The average intervals between two repeated grunts within a sequence was 300ms.67

Figure 29. Trumpet. (a) Acoustic waveforms and narrow band spectrograms of a sample of Trumpet for FAJ758 and FIG776. (b) Narrow band spectrograms of the averaged Trumpets for FAJ758 and FIG776. The spectrograms were generated in Matlab using the following parameters : 150ms window size, frequency range : 0-4000Hz, frequency steps : 300.68

Figure 30. Trumpet characterization. Left panel : Number of Trumpets produced by FAJ758 and FIG776. Center panel : histogram of the intervals between two Trumpets. Right panel : histogram of durations for Trumpets.69

Figure 31. Rattle. (a) Acoustic waveforms and narrow band spectrograms of a sample of Rattle for FAJ758 and FIG776. (b) Narrow band spectrograms of the averaged Rattles for FAJ758 and FIG776. The spectrograms were generated in Matlab using the following parameters : 150ms window size, frequency range : 0-4000Hz, frequency steps : 300.70

Figure 32. Rattle characterization. Left panel : Number of Rattles produced by FAJ758 and FIG776. Center panel : histogram of the intervals between two Rattles. Right panel : histogram of durations for Rattles.70

- Figure 33. Grunt Squeal.** Top panel : acoustic waveform of a sample of Grunt Squeal. Center panel : narrow band spectrogram of a sample of Grunt Squeal. Bottom panel : narrow band spectrogram of the averaged Grunt Squeals. The spectrogram were generated in Matlab using the following parameters : 150ms window size, frequency range : 0-4000Hz, frequency steps : 300.71
- Figure 34. Grunt Squeal characterization.** Left panel : Number of Grunt Squeals produced by FAJ758 and FIG776. Center panel : histogram of the intervals between two Grunt Squeals. Right panel : histogram of durations for Grunt Squeals.....72
- Figure 35. Bark.** Left panel : narrow band spectrogram and acoustic waveform of the call Bark. The orange rectangle represent a Grunt produced by FIG776 just before the Bark of FAJ758. The spectrogram was generated in Matlab using the following parameters : 150ms window size, frequency range : 0-2000Hz, frequency steps : 300. Right panel : Number of Barks produced by FAJ758 and FIG776.....73
- Figure 36. Blast.** (a) Acoustic waveforms and narrow band spectrograms of 2 and 3 samples of Blasts for FAJ758 and FIG776 respectively. (b) Narrow band spectrograms of the averaged Blasts for FAJ758 and FIG776. The spectrograms were generated in Matlab using the following parameters : 150ms window size, frequency range : 0-4000Hz, frequency steps : 300.74
- Figure 37. Blast characterization.** Left panel : Number of Blasts produced by FAJ758 and FIG776. Center panel : histogram of the intervals between two Blasts. Right panel : histogram of durations for Blasts.....74
- Figure 38. Proportion of vocalizations produced during the morning (AM) and the afternoon (PM).** The six types of vocalizations were recorded during the morning but only two types were recorded on the afternoon. FAJ758 proportion of vocalizations are displayed in red and FIG776 in blue.....75
- Figure 39. Histogram of vocalizations during all the day.** Top panel : histogram of vocalizations during the morning (AM). Four types of vocalizations were represented : Grunts in blue (regardless of Grunt type), Trumpets in orange, Rattles in yellow and Blasts in purple. The red vertical bar correspond to the time of distribution of the food ration (9h40 that day). Bottom panel : histogram of vocalizations during the afternoon (PM). The two types of vocalizations represented are the only two recorded during the afternoon : Grunts in blue (regardless of Grunt type) and Blasts in purple.....76
- Figure 40. Pie chart of the proportion of Mixed calls (two locutors vocalizing at the same time) relatively to FAJ758 and FIG776 vocalizations.** FAJ758 calls represented 47% of all vocalizations and FIG776 46%. Mixed calls accounted for 7% of the total recording.77
- Figure 41. General pattern of answers between one vocalization and the previous vocalization for both FAJ758 and FIG776.** Blue rectangles represent percentages of times the current vocalization is preceded by the same type of vocalization (Grunt preceded by Grunt, Rattle preceded by Rattle, etc...). Light red rectangles represent percentages of times the current vocalization is preceded by another type of vocalization (Grunt preceded by Blast, Grunt preceded by Trumpet, etc...)78
- Figure 42. Surgery planning using personalized 3D modeling.** (a) 3D modeling of a minipig's brain based on T1 MR images. (b) 3D representation of the protecting chamber. (c) 3D model of a minipig's skull based on a CT-Scan. (d) The brain model is aligned with the skull model and the craniotomy coordinates were planned. (e) Full 3D model with the protecting chamber and the skin of the animal to prepare the surgery (f) Lateral view of the full 3D model with the resin hood installed.85
- Figure 43. Electrode registration of soft ECoGs over the left hemisphere in three minipigs.** (a) Flexible EcoG array placed surgically on the surface of the brain of CH596. (b), (d), (f) 3D reconstruction of CH596, YU254 and GI2028 brains respectively, with electrodes

placement. (c), (e) X-ray projection of the head of YU254 and GI2028 respectively after implantation of clinical ECoG grids.86

Figure 44. Surgical procedure for the implantation process of a soft ECoG over premotor and motor cortices in CH596. (a) The craniotomy area was drawn over the left hemisphere of the skull based on CT-scan. (b) The bone flap was lifted away from the skull. (c) The dura mater was cut with micro-dissecting scissors. (d) The implant was positioned to cover the premotor and motor cortices. (e) Duraplasty was performed. (f) the bone flap was placed back and fixed on the skull using titanium strips and screws. (g). The titanium chamber was fixed on the skull and the interior space of the chamber was filled with bone cement. The cemented connector is indicated by the red arrow. (h) Implanted animal several days after surgery with protective cap closing the chamber. (i) Explanted animal CH596 (middle pointed by arrow) rehomed with congeners in a farm after ending its investigation. All panels refer to animal CH596 except panel f corresponding to animal BA638 (the same approach was used for CH596 but no picture of this step was taken during the surgery).88

Figure 45. Setup for both vocalizations and cortical data recordings in freely moving minipigs. (a) Roof of the recording pen with the recording setup. (b) 3D representation of the recording pen, roof view from the door. (c) The recording cap is screwed to the protecting chamber during recording sessions to protect the wireless devices. (d) 3D modeling of the recording cap with a representation of a wireless headstage (in blue). (e) Raw recordings of vocalizations (purple lines) and cortical data (blue lines) visualized with Spike2.90

Figure 46. Development of frontal sinus in minipigs between 3 and 12 months of age. Top row: Mid-sagittal CT images of the whole head at various ages. Middle row: close-up of the brain area, with a representation of a typical craniotomy over the motor cortex (white lines). Bregma is represented by the red cross. Bottom row: 3D reconstructions of the skulls. Bregma is represented by the red dot. a=Aachener minipigs, g=Göttingen minipigs.92

Figure 47. Evolution of sinus following implantation. From left to right : 5 ½ months Ellegaard minipig after implantation at 4 months, 9 months Aarchener minipig after implantation at 7 months, 1 year Ellegaard minipig without implantation. The sinusal cavities are represented in red.93

Figure 48. Characterization of vocalizations for all the animals. For each panel, a trace of an example of each type of vocalization is represented with its spectrogram (parameters identical to the parameters used in Chapter 4). The middle histogram represents the intervals between two vocalizations of the same type, except for Scream vocalizations in panel CH596, which displays the patterns of production of Screams 1, 2 and 3 (red rectangles) surrounded by Grunt Squeals (blue rectangles). The bottom histogram shows the durations of the vocalizations. (a) Vocalizations of YU254. (b) Vocalizations of CH596. (c) Vocalizations of GI2028.94

Figure 49. Cortical activity recorded during Grunt vocalizations in CH596. (a) spatiotemporal activity of different electrodes (one electrode is represented as one line, the vertical black line represents vocalization onset). Seven electrodes were selected and the bootstrap (n = 1000) evoked potentials are represented in (b). The horizontal blue bars represent the timings at which spatiotemporal mapping is illustrated on **Figure 50** (c) electrodes mapping over the left hemisphere in CH596. The 7 selected electrodes are displayed in white. (d),(e),(f) Characterization of peaks McP1, PMcN1 and PMcN2 from bootstrap averages. Left panels : Latencies of the peaks in seconds. Right panels : Amplitudes of the peaks in μ V.98

Figure 50. Spatiotemporal mapping of the cortical activity in CH596. The timings are those indicated by the blue horizontal bars in **Figure 49**.99

Figure 51. Cortical activity recorded during Grunt vocalizations in YU254. (a) spatiotemporal representation of the activity. (one electrode is represented as one line, the

vertical black line represents vocalization onset). Three electrodes were selected and the bootstrap ($n = 1000$) evoked potentials are represented in (b). The horizontal blue bar represent the timings at which spatiotemporal mapping is illustrated on **Figure 52**. (c) electrodes mapping over the left hemisphere in YU254. The 3 selected electrodes are displayed in white. (d),(e) Characterization of peaks TempN1 and FrontInfP1 from bootstrap averages. Left panels : Latencies of the peaks in seconds. Right panels : Amplitudes of the peaks in μV101

Figure 52. Spatiotemporal mapping of the cortical activity in YU254. The timings are those indicated by the blue horizontal bars in **Figure 51**.102

Figure 53. Cortical activity synchronized with Grunt vocalizations of GI2028. (a) spatiotemporal representation of the activity. (one electrode is represented as one line, the vertical black line represents vocalization onset). Four electrodes were selected and the bootstrap ($n = 1000$) evoked potentials are represented in (b). The horizontal blue bar represent the timings at which spatiotemporal mapping is illustrated on **Figure 54**. (c) electrodes mapping over the left hemisphere in GI2028. The 4 selected electrodes are displayed in white. (d), (e) Characterization of peaks SensMotP1 and FrontInfP2 from bootstrap averages. Left panels : Latencies of the peaks in seconds. Right panels : Amplitudes of the peaks in μV103

Figure 54. Spatiotemporal mapping of the cortical activity of GI2028. The timings are those indicated by the blue horizontal bar in **Figure 53**.104

List of tables

Table 1. Characteristics of different communication channels (adapted from Higham & Hebets, 2013).....	17
Table 2. Properties of signals and cues in animal communication (adapted from Ruxton & Schaefer, 2011).....	18
Table 3. Summary of the latencies of the different peaks in animals 1 and 2.	51
Table 4. Summary table of the types of vocalizations recorded with their principal characteristics.	79
Table 5. Summary table of the vocalizations produced by the 3 animals.....	96

Acronyms and terms

ADP	Adenosine DiPhosphate
AEP	Auditory Evoked Potentials
AM	Ante Meridiem (morning)
ATP	Adenosine TriPhosphate
A1	Primary Auditory Cortex
BAEP	Brainstem Auditory Evoked Potential
CAEP	Cortical Auditory Evoked Potential
CT	Computed Tomography
DICOM	Digital Imaging and COmmunications in Medicine
ECoG	ElectroCorticoGraphy
EEG	ElectroEncephaloGraphy
EPSP	Excitatory PostSynaptic Potential
FLB	Faculty of Langage in a Broad Sense
FLN	Faculty of Language in a Narrow Sense
fDOI	Functional Diffuse Optical Imaging
fMRI	functional Magnetic Resonance Imaging
F0	Fundamental Frequency
IFG	Inferior Frontal Gyrus
IM	Intramuscular
IP	Intraperitoneal
IPSP	Inhibitory PostSynaptic Potential
LAEP	Long Latency Auditory Evoked Potential
LFP	Local Field Potentials
MAEP	Middle Latency Auditory Evoked Potential
MEA	Micro-Electrode Array
MEG	MagnetoEncephaloGraphy
MRI	Magnetic Resonance Imaging
MUA	MultiUnit Activity
M1	Primary Motor Cortex
NA	Ambigual Nucleus
NHP	Non Human Primate

NRA	RetroAmbigual Nucleus
NREM	Non-Rapid Eye Movement Sleep
PAG	Periaqueductal Grey
PB	Parabrachial Nucleus
PCA	Principal Component Analysis
PET	Positron Emission Tomography
PM	Post Meridiem (afternoon)
PMv	Ventral Premotor Cortex
PSTH	PeriStimulus Time Histogram
PVMN	Primary Vocal Neural Network
REM	Rapid Eye Movement sleep
SC	SubCutaneous
SD	Standard Deviation
sEEG	stereotaxic ElectroEncephaloGraphy
SEM	Standard Error of the Mean
SPECT	Single-photon emission computed tomography
STG	Superior Temporal Gyrus
SUA	Single Unit Activity
SVM	Support Vector Machine
VAMN	Volitional Articulatory Motor Network
VH	Ventral Horn of the spinal tract
vIPFC	ventrolateral Prefrontal Cortex
3D	Three-Dimensional
μECoG	micro ElectroCorticoGraphy

1. Goal of the thesis and organization of the manuscript

1.1. Motivation of the thesis

Animal models are necessary to highlight the cortical dynamics involved in vocal production when not accessible in humans. The investigation of these cortical networks is limited in humans since it requires access to large cortical areas, which is only partly and rarely possible in human patients. To date, animal models used to this aim are non-human primates and birds, and more recently rodents. The organization of vocal production network of non-human primates show strong analogies with that of speech production networks in humans. However, the extent to which this model generalizes to another species remains unclear. My thesis thus aimed to develop a novel experimental paradigm to investigate the cortical bases of vocalizations using cortical electrode arrays in a large behaving mammal species: the minipig. This animal shares physical and physiological similarities with humans, is very talkative and easy to handle by humans. Since my PhD thesis was partly funded by the Graphene Flagship, we also had to assess the performances of graphene-based surface implants in rats and eventually minipigs before translation to humans. The minipig graphene-based electrode array is still in fabrication so all minipigs studies were carried with other implants. Thus, the specific aims of my thesis were the following:

- Assess the recording capabilities of graphene-based electrode arrays in rats (we chose the rat auditory cortex as a model)
- Record and classify minipigs vocalizations during housing, allowing to obtain a first assessment of the vocal repertoire of these animals
- Contribute to the development of an experimental set up to investigate cortical activity in freely vocalizing minipigs
- Identify key cortical regions activated during vocal production in minipigs

1.2. Organization of the manuscript

There were several difficulties to overcome in order to reach this aim. First, minipigs' cortical anatomy was not precisely defined or mapped in the literature, even less when it came to vocal production. Facing this issue, we had to use an exploratory method for the implantations. Secondly, very little was known about minipigs' vocalizations and behavior in general, so we had to investigate by recording the animals' vocal productions during long recording periods. Third, the frontal sinus cavities of minipigs develop fast over the early age of the animal, engendering a risk of infection if brain surgery is performed after this growth. We thus created a new methodology to implant minipigs in the prefrontal cortex before the development of these sinuses. In parallel, we developed an experimental setup that allowed the simultaneous recordings of vocalizations and cortical activity in freely moving minipigs. The global organization of the manuscript is the following:

- **Chapter 2** summarizes the context of the thesis, describing the bases of animal communication along with methods for brain recordings and the known literature on the cortical networks of vocalizations in animals
- **Chapter 3** presents the assessment of low-noise graphene-based cortical probes obtained within the frame of the Graphene Flagship project (implants for minipigs are still in fabrication so all minipigs studies were carried out with other implants)
- **Chapter 4** presents a first characterization of the minipig vocal repertoire obtained by the manual labeling of over 14h of audio recordings from behaving animals in their housing facility
- **Chapter 5** outlines the development of a novel experimental paradigm and setup that allowed the simultaneous recordings of vocalizations and cortical activity in behaving minipigs, and presents several cortical regions that were found to be activated

2. State of the art

2.1. Animal Communication

Animal communication has been extensively studied over the years, with an increasing interest from ethologists and bioacousticians since the 50s. In 1872, Charles Darwin initiated the current of thought placing animal communication at the center of emotions' expression. In *The Expression of the Emotions in Man and Animals* (Darwin, 1877), the famous naturalist highlighted the parallels between human and animal emotional expressions. Despite the major interest for this book, the subject of animal communication has been neglected for about 50 years after its publication. In 1932, Konrad Lorenz used the word 'sign stimulus' to describe (generally quite simple) a species-specific signal that triggers in congeners some mechanisms of responses adapted to that stimulus. Lorenz laid the bases for an ethological view of animal communication. These sign stimuli are often considered as social triggers, as for example in the case of parent-offspring relationships and feeding behavior. One of the most known examples of such instinctive behaviors is the study of Niko Tinbergen in 1951 on herring gulls chicks (*Larus argentatus*).

In general, animal communication can be defined by the ability to produce, transmit and receive relevant signals that convey information by stimulating sensorial systems in the receiver. For any animal, it is essential to be capable of such communication in order to survive. Individual or specific information can be transmitted through various transmission channels (see **Table 1**). The environment is the interface between animals and their signals: it can facilitate or hinder their spread.

Characteristics of the Signal					
Type of signal	Range	Speed of change	Obstacles passage	Localization	Energetical cost
Chemical	Long/Short	Slow	Good	Variable	Low
Visual	Long	Fast	Bad	Good	Low
Tactile	Short	Fast	Bad	Good	Low
Acoustical	Long	Fast	Good	Medium	High

Table 1. Characteristics of different communication channels (adapted from Higham & Hebets, 2013)

In a more specific way, signals have to be differentiated from cues. Technically, both signals and cues fit the previous definition, but only the signal is voluntarily produced and has evolved because of its effect on the perceiver (see **Table 2**). The cue is inadvertently transmitted, like for example the emission of CO₂ by mammals. This cue, detected by mosquitos, is involuntarily produced by the bitten animal (Laidre & Johnstone, 2013). Another major difference between signals and cues is that only signals benefit on average both the informer and the perceiver. An example of signal is foot drumming by kangaroo rats (*Dipodomys spectabilis*). These small rodents strike their feet on the ground to create mechanical vibrations to alert congeners when predators are nearby (Randall, 1997). We will hence distinguish cue-communication from real communication, with the definition of Ruxton & Schaefer: “Animal communication can best be seen as an attempt to influence or manipulate others from the viewpoint of the informers and as providing information from the viewpoint of the perceivers. We see communication (signalling) as a subset of sensory interactions where (on average) both informer and perceiver benefit from the outcome of the interaction between an informer and a perceiver.” (Ruxton & Schaefer, 2011)

Types of communication		
Characteristics	Cues	Signals
Production	Inadvertent	Voluntary
Benefits	Only the perceiver benefits on average from cues	Both perceiver and informer benefit on average from signals
Evolution	Do not evolve to elicit a response in a perceiver	Evolve because of their effects on the perceiver behavior
Effect on perceiver	Changes the behavior of the perceiver	

Table 2. Properties of signals and cues in animal communication (adapted from Ruxton & Schaefer, 2011)

As seen in **Table 1**, There are many different communication channels, and animals use them for various activities like foraging, mating, etc... When used together, these channels allow a multimodal communication. For example, birds-of-paradise display an ornamental plumage and perform display songs when involved in courtship (Irestedt et al., 2009).

2.1.1. Producing signals

Chemical

Chemical communication is the principal way of communication in all living organisms. From the cell level to living organisms, chemical communication is essential and efficient. This type of animal communication uses molecules such as pheromones secreted or excreted by glands. Pheromones are volatile or soluble and are released directly in the environment and impact the behavior or physiology of the receiving individuals. Depending on the animal species, pheromones are produced by skin, sebaceous, exocrine and sweat glands, saliva, urine or feces. These molecules are perceived by smell or by direct contact. There are many different types of pheromones like territorial ones, like in mice to mark the perimeter of the territory (Jones & Nowell, 1973), or sexual pheromones to indicate the female availability for breeding (Gower, 1972).

Visual

Communication can also be exerted by light production realized by cells called photocytes that are responsible for the bioluminescence effect. This phenomenon is widespread in many species, especially in marine organisms. Light production can have various functions like camouflage, predation or mate attraction. Counter-illumination camouflage is used by several squids to match their nearby environment and hide from predators. Bioluminescence is also used by these animals for hunting strategies implying startling preys (Harvey, 1952).

Visual communication can be performed by color too. Skin and eye color in animals including fish, reptiles, amphibians, are produced by chromatophores. In mammals and birds, these cells are called melanocytes. Chromatophores and melanocytes contain pigment that are responsible for skin patterns. Some species like octopus can rapidly change color by translocating pigments within their chromatophores to camouflage (Lane, 1960). The pattern of pigment distribution in chromatophores can vary under hormonal or neuronal control. These color changes allow the animal to be more or less visible depending on its need.

Acoustical

There are many different types of sound communication such as stridulation, wing hums, percussion or vocalization. Producing a sound implies a vibration that propagates as an acoustic wave through the environment. This vibration can be emitted by the movement of a body part pressed against another solid either external or belonging to the animal's body. It is for instance the case for grasshoppers that stridulate by rubbing their leg scrapers against the adjacent forewing (Perdeck, 1958) or with some birds that clap their beaks (Tinbergen, 1959). The sound can also be produced by deforming body membranes like in cicadidae. Moreover, a vibration can be obtained by the passage of a fluid inside a body part. In vertebrates, the air

from the lungs makes vocal folds vibrate before resonating when passing through the vocal tract.

2.1.2. Transmitting signals

Animal signals are influenced by the physical environment in which they are produced and perceived. The nature of this environment is of major importance because it will intrinsically modify the signal itself. As a consequence, the perceiver might not receive the signal exactly as it was emitted by the informer. Two of the main problems in the propagation of signals are distortion and attenuation. For sounds, distortion is due to the dispersion of the wave reverberating over solid bodies like trees, rocks, etc... Attenuation of the sound will be highly dependent on atmospheric conditions and vegetation density (Catchpole & Slater, 2003) but also strongly impacted by a very noisy habitat. In marine mammals for example, underwater noise partly produced by human activity is responsible for strong interferences in communication, a phenomenon called auditory masking. Distortion is also problematic for light waves that can be filtered and scattered, reducing their contrast with the background.

2.1.3. Perceiving signals

A signal is only efficient if it is adapted to the sensory apparatus of the receiver. A stimulus is perceived by specific receptors that transforms it into a nervous input for the brain to analyze.

Chemoreceptors

Chemical receptors are of two types: distance and direct. The distance chemoreceptor detects odors and pheromones in the nasal cavity in vertebrates: Air is drawn inside the cavity and chemicals in the gaseous state are detected. In invertebrates, olfactory organs differ, such as in insects with antennae (Chapman, 1998). Direct receptors include taste and contact chemoreceptors. Insect have conical projections or hairs that allow chemicals to pass through. They use them to perceive certain nutrients and potential toxic materials.

Mechanoreceptors

Perception of various vibrations is made through mechanoreceptors, sensory cells that respond to mechanical pressure. There are many different types of mechanoreceptors. In invertebrates, campaniform sensilla are a class of cells that detect mechanical resistance to muscle contraction. In mammals, there are mechanoreceptors in both hairy and glabrous skin. These cells are part of the mechanisms of somatosensation and audition. The external vibration (sound signal, liquid vibration, etc...) is transduced into a neural signal. In the ear, sound waves impact the eardrum, causing its vibration. The vibration is then conducted into

the inner ear that contains an epithelium tissue studded with hair cells that are mechanoreceptors (Gaudin, 1968; Rosowski, 2003) within the organ of Corti, a receptor organ that is responsible of the transduction of the auditory signal into a neural signal made of action potentials activating in turn subcortical and cortical areas to eventually elicit the conscious perception of the auditory signal.

Photoreceptors

In some arthropods, the organ of vision is a compound eye, which is composed of many simple facets that are very sensitive to motion. Every facet has its own lens and photoreceptors. The Mantis shrimp (*Odontodactylus scyllarus*) is known to have the world's most complex color vision system, with compound eyes made up of tens of thousands of clusters of photoreceptor cells (Dingle & Caldwell, 1969).

Another type of eye is the ocelli, or eye spots, that possess a single lens and without an elaborate retina. This kind of eyes can be found in many snails, worms and sea stars for example.

In most mammals, light enters the eye through the cornea and the lens projects an image onto the retina at the back of the eye. The photoreceptors in the retina are cones and rods. Cones are used for day-time vision when rods primarily contribute to night-time vision. They transmit information to several neural layers of the retina, at the output of which are the ganglion cells projecting to the thalamus. Some retinal ganglion cells are also intrinsically photosensitive and play a role in the circadian rhythm and pupillary reflex.

Eyes in animals adapt to their requirements, and their differences are examples of parallel evolution.

2.2. Vocal communication

Vocal communication in animals and especially in mammals is one of the most widespread socio-behavioral system. This complex pattern requires integration and treatment of many different systems, from the central nervous system to muscular effectors. Vocalizations are an efficient way of sending reliable information, independently from one animal's environment and obstacles to their diffusion (see **Table 1**). They can be expressed without being related to sight or olfactory senses. Vocal communication can have many functions, and it is found ubiquitously in mammals.

In this manuscript, we will adopt the position presented by M.D. Hauser, N. Chomsky and W. T. Fitch in 2002 concerning the faculty of language. A distinction is made between the faculty of language in a broad sense (FLB) and in a narrow sense (FLN). "FLB includes a sensory-motor system, a conceptual-intentional system, and the computational mechanisms for recursion, providing the capacity to generate an infinite range of expressions from a finite set of elements. [...] FLN only includes recursion and is the only uniquely human component of the faculty of language." (Hauser et al., 2002) . This human specificity for FLN could explain the fact that when taught to apes, fluent speech could not be acquired beyond a few words,

even when integrated to the daily life of a family for years as a human child would be (Hayes & Hayes, 1951). Sign language could be taught at the price of intense efforts to bonobos (Savage-rumbaugh & Lewin, 1996) or chimpanzees (R. A. Gardner & Gardner, 1969a) but not spoken language.

2.2.1. The roles of vocalizations

One of the most important roles of vocalization is to carry essential information about the environment, including foraging or signaling dangers. In vervet monkeys, alarm calls were identified as designating a specific type of predator (leopard, eagle and snake), and the behavioral responses following these calls were adapted to the type of predator (leopard alarm made the vervet monkeys run into trees, eagle alarm made them look up and snake alarms look down) (Seyfarth et al., 1980). Many non-human mammals are limited by small vocal repertoires, but a way to overcome this problematic is by combining calls (Arnold & Zuberbuhler, 2006). Hence, two or more call types can be combined to form a new one. In animals, this combination is syntactic and not semantic, as the meaning of the sentence that is formulated cannot be assessed by individual meanings of each word. Thus, in putty-nosed monkeys, some males combine two types of vocalizations in small sequences. Regardless of context, these combinations triggered a behavior in the entire group of monkeys (Arnold & Zuberbuhler, 2017). In dingos as well, combinations of bark and howl vocalizations were related to human presence and increased the pack's vigilance (Déaux et al., 2016).

Another role of vocalization is to inform congeners of one animal's internal state (hunger, distress, rut, etc), identity (male, female, pup), or territorial occupation. This role takes also place in the parent-pup relationship and is particularly well documented in pinnipeds with the mother-pup highly efficient recognition (Aubin et al., 2015).

Vocalizations and their spectral or rhythmic features are also involved in recognition of the environment in parrots (Bradbury & Vehrencamp, 2011) or dolphins (King & Janik, 2013) as in mating and rivalry behaviors like in northern elephant seals (Mathevon et al., 2017). Some species like whales (T. F. Norris, 2012) and parrots (Wright & Dahlin, 2018) even have vocal dialects, geographic variation in the distribution of calls. One animal can be affiliated to a subpopulation given specific vocalizations it produces.

Thus, vocal communication is mainly used in mammals to influence others' behavior, whether congeners of the same species or not, facilitating social interactions by reducing the uncertainty about others' behaviors and intentions (Cheney & Seyfarth, 2018).

2.2.2. Language characteristics found in animal communication

Human language has been and still is broadly studied over the world. In the 1960s, a linguistic anthropologist, Charles F. Hockett, defined a set of features characterizing human language to separate it from animal communication. He called them the design features of

language, and Hockett originally thought that some of these features were exclusively human. However, more recent studies by animal ethologists and bioacousticians have been increasingly showing that a number of Hockett's design features are also found in animal communication. Here we provide some examples of animal communication that match some of Hockett's design features.

Semanticity

Semanticity is the fact that the symbols that are used have particular meanings. In humans, these symbols are phonemes or morphemes. In chestnut-crowned babbler (*Pomatostomus ruficeps*), songs are quite complex structures intended to attract mates. These songs are composed of acoustical elements that can be isolated then rearranged to create functionally distinct vocalizations (Engesser et al., 2015). Such findings suggest a rudimentary form of phonemic structure and recombination in these birds.

Productivity

Productivity is the ability to create new expressions that have not been encountered in previous situation. Research with great apes suggested that they are capable of learning and using a language using productivity to to create new expressions (B. T. Gardner & Gardner, 1975; R. A. Gardner & Gardner, 1969).

Symbolic

This principle means that symbols used do not physically resemble the things they represent. In bees (*Apis mellifera*), one recent study has shown that they could learn the association between a symbol and numerosity (Howard et al., 2019). Basic numerical symbolic representation can be accomplished by an insect brain. Moreover, researchers have taught chimpanzees to use symbolic keyboards to respond to questions or even to transmit information directly. The keyboard is made of buttons representing symbols that stand for different words. When a button is pressed, a computer voice enunciates the word out loud.. One of the chimpanzee named Kanzi learned spontaneously to use the keyboard after seeing his mother being taught (Savage-rumbaugh & Lewin, 1996).

Recursivity / Grammar

Recursivity is the capacity to generate an infinite number of pertinent expressions from a finite number of elements. The elements are not combined randomly and are governed by rule systems called grammars. In human languages, there is a distinction between finite state grammar and phrase structure grammar. The first one, also called weak grammar, defines only local organizational principles and corresponds to calls. Phrase structure grammar is more complex and hierarchical, and allows the construction of structures like sentences, which is crucial for human language. Very few studies were conducted on this subject in animals, but cotton-top tamarin (*saguinus oedipus*) were able to master finite state grammar rules (T. Fitch & Hauser, 2004). Additionally, sequencing complexity has been studied on nonhuman

primates. The relationships between the different vocal sequences can vary in complexity with the use of recursive grammars. As a consequence, two vocal elements separated in time can be linked. Cotton-top tamarin and tamarin monkeys are capable to learn that the first element in a sequence predicts the final element in rapidly presented streams of 3 elements of human speech. They are doing so while ignoring the second element that is not carrying information about the relationship between the first and third element (Newport et al., 2004; Newport & Aslin, 2004).

Displacement

Displacement is the capacity to talk about something that is not immediately present either temporally (the thing happened in the past) or physically (the thing is at a distance). African Weaver Ant (*Oecophylla longinoda*) have been observed to recruit workers to communicate new food sources or defend the territory against intruders (Hölldobler & Wilson, 2004). Such a recruitment requires that the ant passes information about a resource that is not physically present.

Prevarication

This characteristic is the ability to tell things that are false. In Great Tit (*Parus major*), when in groups, some individuals may produce false alarm calls for resource usurpation (Møller, 1988). Dominant great tits used these false alarms with other tits and sparrows, meaning that these calls are inter-specific.

Traditional transmission

Language is not genetic, it is culturally transmitted and socially learned. Vocal dialects were studied in 1962 in White-crowned sparrow (*Zonotrichia leucophrys nuttalli*) (Marler & Tamura, 1964). Similarly, some whales learn their songs by imitating other members of their species (T. Norris et al., 2012).

As seen in these examples, there are many characteristics of language that are shared between human and animal vocalizations. There is a consensus around the fact that human language is more complex and sophisticated than any animal language, but it does not necessarily mean that there is a qualitative difference between human and animal communication.

2.2.3. Suidae vocalizations

The domestic pig (*sus scrofa domesticus*) is a highly social species that produces a large variety of vocalizations in many different situations. Pigs natural communication and vocalizations have been studied mostly in farming and husbandry practices. A large majority of them relate to piglets or sow in estrus during specific situations, those relevant for commercial farming (Signoret et al., 1960; Whittemore & Kyriazakis, 2006). These studies for example focused on vocalizations during food deprivation (Fraser, 1975; Weary & Fraser, 1995), mating (Xin et al., 1989), nest leaving (Jensen & Redbo, 1987) or even suckling (Jensen & Algers, 1984). It obviously improved our understanding of the link between animal vocalizations and their welfare and how they reflect their mental or physical state. Distress vocalizations are considered to be a great indicator of piglets welfare (da Silva Cordeiro et al., 2013; Manteuffel et al., 2004), and automatic recording tools (McLoughlin et al., 2019; Moura et al., 2008) like STREMODDO (Schön et al., 2004) have been developed to help stockbreeders to improve life conditions, avoiding stereotypic behaviors like tail biting which is frequent in industrial breedings. Five decades ago, Kiley (1972) described quite precisely ungulates vocalizations and their causations, and she proposed a classification of adult pigs vocalizations which is now a base for many studies. She highlighted the following four principal types of calls and their situations of occurrence:

Grunt

This is a low amplitude sound, which occurs very frequently. It varies in length between 0.25 and 0.4 seconds and is not repeated within a one-second interval. A common grunt is evoked by any familiar noise or change in the environment.

Bark

This call is given with the mouth open and is very obviously accented with higher amplitude at the beginning. The bark is particularly characteristic of a startle situation, often followed by freezing.

Scream

This call is extremely loud and tonal. Any extremely unpleasant situation will elicit a scream, for example an animal that is squashed by another.

Squeal

Squeals are distinguishable from screams mainly by their constant pitch change, and their higher dominant overtones. The situations in which piglet squeal are apparently very various and this vocalization is non-specific.

Within these four categories, Kiley proposed variations and subcategories like ‘staccato grunts’ which are short repeated grunts, or ‘long grunts’, and even intermediate categories like ‘grunt-squeals’ (see **Figure 1**).

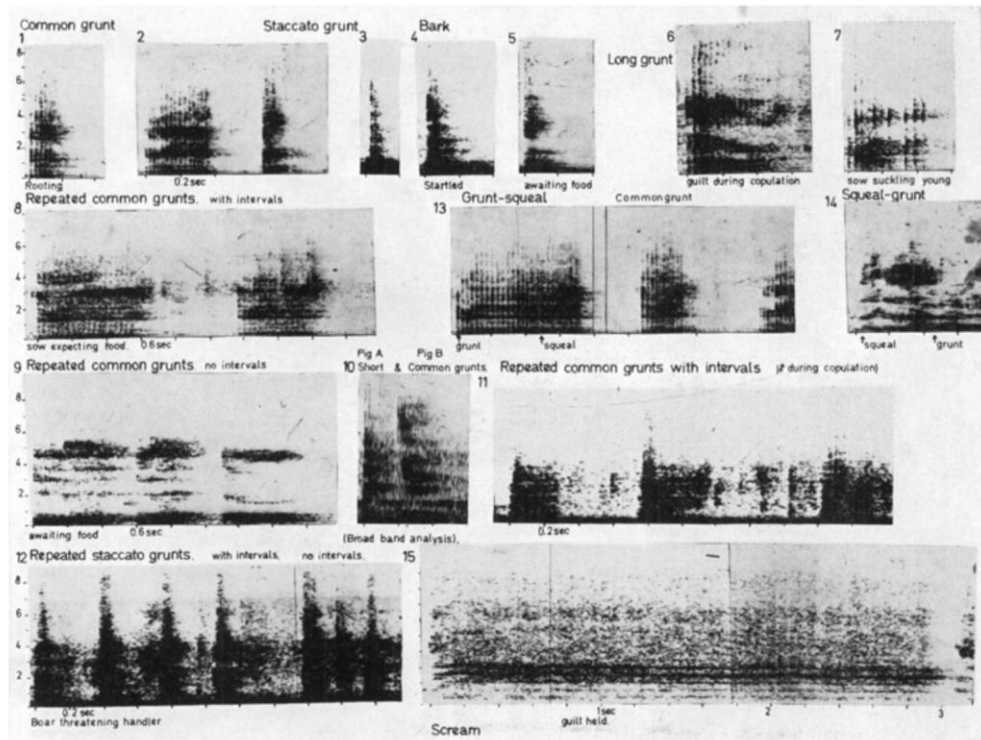


Figure 1. Sonographs of the calls of adult pigs (Kiley, 1972). The categories were mostly made by hearing vocalizations and inspection of the sonograms.

These observations suggest the richness of the pig vocal repertoire, and the difficulty to classify pig calls, but also the fact that the vocalizations might be distributed along a more continuous and constantly varying acoustic spectrum (Tallet et al., 2013), which would mean that calls are likely not fully classifiable. In their study, Céline Tallet and colleagues showed that based on 8 acoustical features it was possible to extract 5 call types clusters, which corresponded to the Kiley classification of 4 call types and 1 call for suckling situation because they were working on piglets before weaning. Kiley’s study relied on visual inspection of the sonograms and lack precision due to the fact that it was conducted in the 70’s with poor structural analysis means. Recent studies focused on spectro-temporal analysis of vocalizations to propose a more reliable classification of pig’s vocalizations. The features exploited in such studies are very numerous, since there are many characteristics in a sound that are relevant to investigate. Garcia and colleagues (Garcia et al., 2016) proposed a classification based on 4 spectro-temporal features they selected among 19 identified acoustic parameters and obtained a 80%-correct classification of the wild boar (*sus scrofa*) repertoire into four main vocalizations: grunts, grunt-squeals, squeals and trumpets (see **Figure 2**).

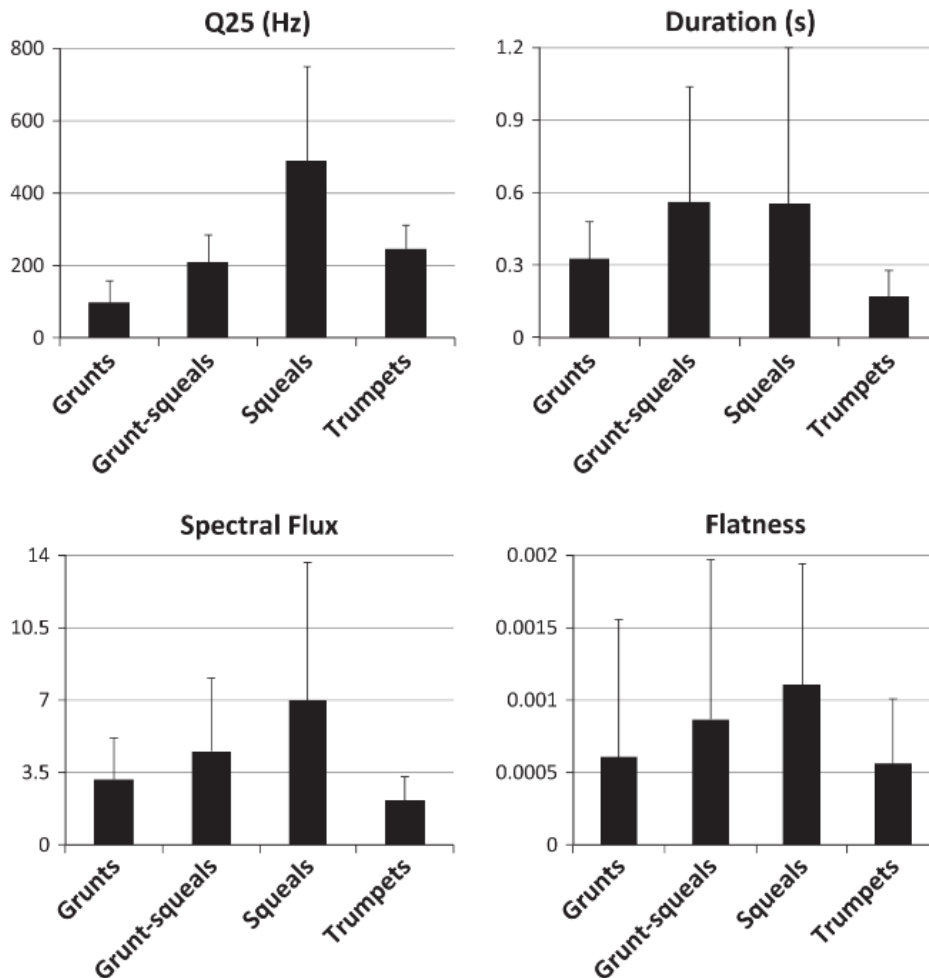


Figure 2. Acoustic parameters retained for classification of vocalizations in the wild boar (Garcia et al., 2016). Mean values (\pm SD) of the four features used for classification are displayed for the four call types identified.

In the face of this regain of interest for their vocalizations, adult pigs and minipigs vocal repertoires need more precise description, and a study where vocalizations and their situation of occurrence would be fully described in acoustic terms with current means of recording and data analysis is still lacking.

2.3. Methods for brain recording

2.3.1. Neuronal activity

Neurons are a type of cells present in every animals, apart from sponges and placozoa (marine multicellular organisms). The average number of neurons in an adult human brain is

estimated between 86 and 100 billions. In adults minipigs, 324 millions have been counted (Jelsing et al., 2006). Neurons possess different functions and mechanisms underlying 2 major physiological properties: excitability and conductivity. Excitability represents the capacity of this nerve cell to integrate incoming information and to induce an impulse response. Conductivity implies that the cell is capable of transmitting information coming from others. A neuron is composed of three parts: the soma, or cell body, the axon and the dendrites. The cell receives electrical information through its dendrites. Depending on the neuron type, there are on average 7000 ramificated dendrites per cell; they are the receptors of the electrical signal. This signal comes from other nerve cells, and is conducted afferently to the soma. Once in the soma, the integrated signal is propagated through the axon of the neuron to other nerve cells. One axon can vary in length from less than 1 mm to more than a meter in humans. The connection sites interfacing axons to others dendrites is called a synapse. At the synapse interface, the signal transmission is often chemical with neurotransmitter releases.

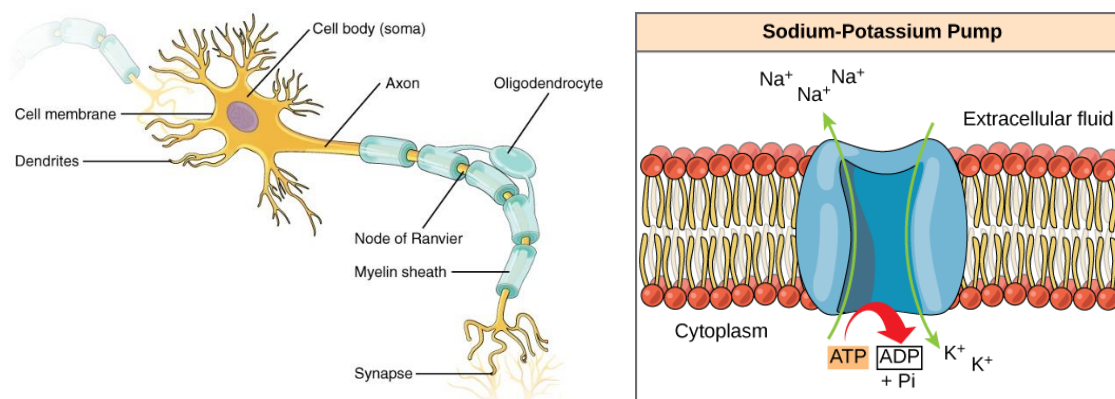


Figure 3. Structure of a neuron and sodium-potassium pump. (a) The neuron is composed of the soma, or cell body, the axon and the dendrites. At the end of the axon, many ramifications connect other neurons with synapses. The conduction of action potentials along the axon is made step by step from one node of Ranvier to another. Oligodendrocytes sometimes wrap axons with myelin sheath. The more myelinated an axon is, the faster the conduction. (b) Basic principle of a Na⁺/K⁺ ionic pump. Ionic exchanges are made between extracellular fluid and intracellular medium. The sodium-potassium pump actively brings potassium (K⁺) inside the cell and expulses sodium (Na⁺) away. This phenomenon requires the consumption of glucose and oxygen for the adenosine triphosphate (ATP) degradation into adenosine diphosphate (ADP)

Sources : licence Creative Commons Attribution 4.0 International
https://commons.wikimedia.org/wiki/File:1206_The_Neuron.jpg
https://upload.wikimedia.org/wikipedia/commons/7/72/Figure_06_04_02.png

At every moment, there are concentration gradients of ions between the inside and the outside of the cell. These gradients vary across species and are made possible by ion pumps and leaky ion channels. The neuron membrane has a selective permeability, and there are active ionic transmembrane currents resulting in permanent modifications of the ionic concentrations inside and outside of the cell. Such gradients induce a negative difference of potential of approximately -60mV to -90mV between the intracellular and the extracellular regions of the

neuron. At rest, the concentration of potassium ions (K^+) is way higher inside the cell than in the extracellular medium. In contrast, the concentration of sodium ions (Na^+) is stronger outside of the cell than inside. Consequently, at resting potential, potassium ions (K^+) tend to leave the inside of the cell to the extracellular medium through opened potassium channels, while sodium ions (Na^+) tend to enter the neuron through sodium channels.

Postsynaptic currents

At the synapse level, microvesicles release neurotransmitters, which are chemical compounds acting like messengers between neural cells. There are various types of neurotransmitters, which action can be either excitatory or inhibitory. Postsynaptic currents stem from the opening of ionic channels on the post-synaptic neuron membrane under the docking of neurotransmitters onto specific receptors. These channel opening induces changes in the membrane potential of the postsynaptic cell that make the postsynaptic neuron more likely to fire an action potential if the synapse is excitatory or less likely in case of an inhibitory synapse. These single currents are extremely small but when several occur simultaneously, the resulting extracellular signals add up to a recordable signal called local field potentials (LFP).

Excitatory postsynaptic potential (EPSP)

EPSPs are caused by the flow of positively charged ions into the postsynaptic neuron. The main excitatory neurotransmitter is the glutamate, it is used for over 90% of the synaptic connections in the human brain and at various percentages in vertebrates' nervous system. Glutamate increases membrane permeability for sodium (Na^+), potassium (K^+) and calcium (Ca^{2+}), thus inducing a depolarization of the membrane potential. A neuron may receive synaptic inputs from hundreds of other neurons, and if the combined activity leads to a sufficient depolarization, the action potential will occur.

Inhibitory postsynaptic potential (IPSP)

IPSPs are the opposite of EPSPs, since they result from the flow of negatively charged ions into the postsynaptic cell. IPSPs make the postsynaptic neuron less likely to generate an action potential by decreasing the membrane potential. The most common inhibitory neurotransmitter is the gamma-Aminobutyric acid, or GABA, which increases the membrane permeability for chloride (Cl^-).

The balance of EPSPs and IPSPs is extremely important in the integration of information in the brain.

Action Potentials

If the sum of all postsynaptic currents reaches a threshold (typically $-40mV$), while the sodium-potassium pumps continue their work, voltage gated sodium channels are opened in response to this initial change of voltage. These voltage gated sodium channels are opened,

allowing a massive flow of Na⁺ into the cell. Hence, the membrane potential fastly rises to a peak of above +30 mV, this phenomena is called depolarisation. Just after that, potassium ions leave the cell through voltage-dependent K⁺ selective channels. As voltage-gated sodium channels close, the potential of the membrane decreases again until it reaches a value lower than the resting potential. This phase is called hyperpolarisation. Then the K⁺ selective channels are closed again and the cell comes back to its resting potential. All this process lasts between 1 and 2 milliseconds and is accompanied by a refractory period during which another action potential cannot be triggered unless in response to a very high stimulus level. These transmembrane currents typically generate an extracellular signal in the form of a negative waveform of a few tens of μV (depending on the distance at which it is recorded).

The action potential, also called spike, is initiated in the axon hillock, the area connecting the axon to the soma. This area presents a particularly dense population of voltage-gated ion channels, and is also called the trigger zone. The action potential then propagates forwardly, step by step along the axon, by saltatory conduction from a node of Ranvier to another. At the end of the axon, the nervous fiber ramificates, enabling communication with many other cells. The axon terminal contains synapses, and the arrival of an action potential can elicit the release of neurotransmitters, thus excite or inhibit another neuron.

Neural oscillations

Neurons are organized into highly interconnected networks, with many feedback connections between them. All this ensemble can give rise to macroscopic oscillations in different frequency bands. Brain waves were first described in 1924 by the psychiatrist Hans Berger, the inventor of electroencephalography. Different rhythms are present in the brain and these oscillations are referred to according to the following taxonomy:

Delta Wave (0.1-4Hz)

Usually associated with deep non-rapid eye movement sleep (NREM), they are the slowest and highest amplitude brainwaves (Steriade, 2006)

Theta Wave (4-7.5Hz)

Theta waves are related to various states of cognition such as memory and spatial navigation, but also rapid eye movement sleep (REM) (Seager et al., 2002)

Alpha Wave (7.5-12Hz)

Also called Berger's waves, they can be recorded during relaxation with eyes closed. They are thought to coordinate neural networks (Palva & Palva, 2007)

Mu Wave (7.5-12.5Hz)

Mu and alpha waves occur at the same frequency range but are not recorded from the same sites. Mu waves are found over the motor cortex. This wave is suppressed (this is called desynchronization) when a motor action is performed or visualized (Cochin et al., 1999). Mu waves are particularly studied in autism and used in non-invasive brain-computer interfaces.

SMR Wave (13-15Hz)

SMR waves appear over the sensorimotor cortex and are decreased in amplitude when the corresponding sensory or motor areas are activated (Arroyo et al., 1993).

Beta Wave (12-30Hz)

Beta waves are commonly associated with normal waking consciousness. They are smaller amplitude, faster waves replacing alpha waves when the eyes are opened and the subject is fully awoken, active, or concentrated (Gevins et al., 1997).

Gamma wave (30-100Hz)

Gamma waves are correlated to working memory and attentive states (McCormick et al., 2015). An impairment in gamma waves activity has been described in neuronal diseases such as epilepsy and Alzheimer (Hughes, 2008; van Deursen et al., 2008). The fast rhythms, known as high-gamma activity, have been described quite recently and are thought to be linked to cognitive processing such as decision-making (Saez et al., 2018). They are supposed to reflect the firing of action potentials by neural populations (Ray & Maunsell, 2011)

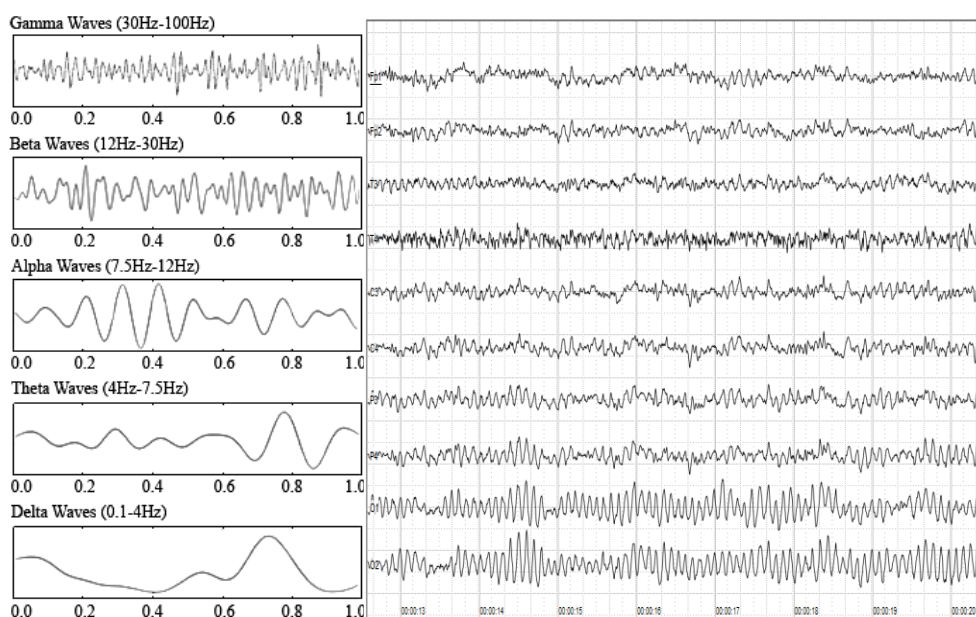


Figure 4. Electroencephalography recording of brain waves. Different brain waves (left) and a sample of human electroencephalography recording with prominent resting state activity - alpha-rhythm (adapted from Sittiprapaporn, 2018 and Cherninskyi, 2015)

2.3.2. General approaches for neural activity recording

Neuronal activity can be measured either indirectly or directly. Indirect ways consist in following the consumption of glucose and/or oxygen in the brain, which represent indirectly the activity of brain cells. Neural activity is highly energy-consuming, particularly on the synaptic transmission. This energy is provided by adenosine triphosphate (ATP) degradation in adenosine-diphosphate (ADP), but has a high cost in glucose and oxygen for the glycolyse. Synaptic activity has been estimated to represent half of the total ATP consumption of the cell. 50% of the energy consumption of a post-synaptic cell is dedicated to the ions pumping to generate synaptic currents. Another large part of the neuron's energy budget is used to regulate ion gradients across the cell membrane with ATP-consuming pumps. 22% of the energy budget is used to restore the Na⁺ gradient due to action potentials. Finally, 20% of the energy budget is used to maintain the resting potential (Vergara et al., 2019). The methods measuring this consumption are metabolic recordings.

Neuronal activity can also be measured directly by recording action potentials and synaptic currents, in the direct environment of the cells or further. This method is named electrophysiology, and it allows the recording of single cells with spikes (or action potentials), or pools of cells with local field potentials (LFPs). LFPs are extracellular signals resulting from the circulation of extracellular currents created by the membrane currents participating to neuronal activity. They can be recorded by electrodes nearby the emitting neurons or at longer distances if currents add up sufficiently.

Metabolic signals recording

As described above, neurons need to consume glucose and oxygen to produce action potentials. These two elements are routed to the brain by a dense network of blood vessels. Hence, an increase in neuronal activity results in a higher blood flow in the brain area concerned (Logothetis et al., 2001). Cerebral circulation of blood is carried through a complex network of veins and arteries. With metabolic signals recordings, oxygenated blood is tracked in arteries. Regarding arterial blood supply, the brain can be divided into 2 parts: anterior and posterior. The internal carotid arteries pair supply the anterior brain, and the vertebral arteries pair supply the brainstem and the posterior brain. At rest, an adult has a cerebral blood flow of about 750 milliliters per minute. Even if this phenomenon is quite slow, blood flow variations, oxygen and glucose metabolism in the working brain reflect the amount of activity in various regions. There are various methods to measure this activity, and each one has its benefits and limitations. We will now describe the main techniques used for functional brain imaging.

Positron emission tomography (PET)

The PET technique tracks in the body radioactive chemicals administered to the patient. Different contrast agents can be injected to measure either blood flow or the consumption of glucose or of other metabolics such as neurotransmitters. In this way, it is used to localize neurologic illnesses or to diagnose brain pathologies, but also in fundamental research like for example to investigate the physiology of motor control (Deiber et al., 1997). However, the majority of contrast agents have a very short half-life (from about 20 minutes for ^{11}C to approximatively one hour for ^{68}Ga), limiting the usage of PET to short experiments. Moreover, the toxicity of radioactive agents makes experiments not repeatable in individual subjects. The temporal resolution of PET is about 0.2 seconds and the intrinsic spatial resolution is about 1 mm (Castermans et al., 2014), which made PET scans the preferred technique of functional brain imaging before fMRI technology became available. PET is a non-invasive technique that is both in clinical and preclinical fields, but its high cost makes cheaper alternatives appealing to provide efficient imagery at a more affordable price.

Single-photon emission computed tomography (SPECT)

This technique called SPECT is related to PET scan in the way that it requires the injection of a radioactive tracer as well. Unlike PET, SPECT detects directly the gamma radiation emitted by the tracer and has a spatial resolution of about 1 cm. The main positive aspect of SPECT is that it is much more affordable than PET. Another benefit is that gamma radio tracers used in SPECT have half-lives of up to six hours while positron emitting radioisotopes have half-lives of up to a couple of minutes. This allows longer imaging procedures, but the use of isotopes is still a disadvantage, since their fabrication is expensive and their storage requires high maintenance.

Functional diffuse optical imaging (fDOI)

Diffuse optical imaging is a technique using near-infrared spectroscopy (fNIRS) that monitors differences of oxygenated and deoxygenated hemoglobin in the cerebral blood flow, known as the blood-oxygen-level dependent (BOLD) response. When an area of the cortex is active, it requires more oxygen for ATP degradation in ADP. The extraction of oxygen is made in the local capillaries near the activated zone. This consumption leads to an initial drop in oxygenated hemoglobin, followed by another flow of oxygenated hemoglobin. The near-infrared light measures the cerebral hemodynamic responses to a task. This method is non-invasive because the optical window used to quantify oxygenated and deoxygenated hemoglobin is from 700 to 900nm. In this range, skin, tissue and bones are mostly transparent, while hemoglobin absorbs light in two different absorption spectra (oxygenated or deoxygenated) (Jobsis, 1977). fNIRS has recently been used in brain-computer interfaces (BCI) as a control signal for left and right wrist hemodynamic responses classification (Nasser & Hong, 2013), demonstrating the feasibility of an fNIRS-based BCI. However, fNIRS cannot be used to record deep cerebral activity, since the lighting power is limited to about 4cm. The spatial resolution of fNIRS is limited to 10mm. While still limited to the temporal resolution of hemodynamic activity, one of the main advantages is that it can be coupled with other scans such as electroencephalographs or magnetic resonance imaging.

Functional Magnetic Resonance Imaging (fMRI)

fMRI detects changes in the magnetic properties of the brain associated with blood flow. As fDOI, fMRI is based on BOLD response, and can localize activity to within millimeters, which is why, despite a relatively poor temporal resolution (around the second), fMRI is quite commonly used in both medical and research fields. fMRI can also be used to measure resting states, showing the subjects' spontaneous BOLD activity without any task. fMRI is a non-invasive technique and is often preferred over methods using radioactive markers. However, MRI is incompatible with numerous metallic implants and medical devices, which limits the use of this technique in individuals with such items in the body.

Electrophysiological Recording

Electrophysiological methods directly record the electrical activity of neurons. The different types of activity (action potentials and field potentials) are recorded with electrodes of many various types, inserted inside the target cell or in the extracellular space. Single-cell recording is possible if the electrode is small enough to be inside or in contact with the neuron. Conversely, an extracellular placement may account for several nearby neurons or pools of neurons. This extracellular signal reflects not only surrounding action potentials, but also synaptic currents, ions leakage, etc. There are many different ways to record electrophysiological signals, and we will describe some of them from the more microscopic to the more macroscopic level.

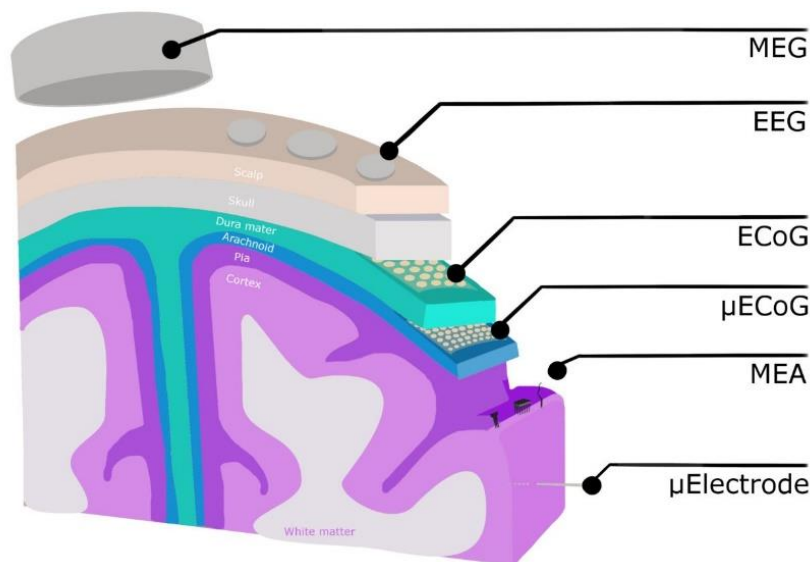


Figure 5. Electrophysiological recording methods. Representation of the different recording methods and their placement (Adapted from Mamun, 2012)

μElectrode (glass micropipettes, metal microelectrodes)

Glass micropipettes are the most commonly intracellular electrodes used for single cell recordings. With a tip diameter inferior to 1μm, the electrode can penetrate the membrane of the neuron and directly allow the recording of the membrane potential and its fluctuations including action potentials. Glass micropipettes can also be positioned in the extracellular space to record extracellular neural signals. Metal microelectrodes are made of different types of metals and are used for measurement of extracellular potentials. These electrodes can be individually implanted in vivo or in vitro at different depths from millimeters in order to record from specific cortical layer to centimeters to record from subcortical regions.

Microelectrode array (MEA) (in vitro and in vivo)

Microelectrode arrays (MEA) can be implanted in vivo or used in vitro, and allow single or multiple cells recordings. In vitro MEAs are usually square shaped with a grid pattern of 60 to 256 electrodes and are often used for cell cultures or measuring acute brain slices activity. High density MEAs are used when a higher spatial resolution is required. The temporal resolution of MEA recordings is very good with recording frequencies of several kHz. In vivo arrays are inserted inside the brain and are either rigid silicone-based devices like the Utah Array model (Blackrock Microsystems, Salt Lake City, UT) or the Michigan Probe (NeuroNexus Technologies, Ann Arbor, MI); or flexible polyimide-based like the MicroFlex Array (Blackrock Microsystems, Salt Lake City, UT). MEAs are used to record extracellular field potentials, reflecting mainly synaptic activity, and also action potentials of single neurons (SUA) or neuron populations (MUA).

Electrocorticography and Microelectrocorticography (ECoG and μECoG)

Electrocorticography is an invasive technique during which recording devices are placed at the surface of the cortex, either over or under the dura. The ECoG signal is mainly composed of postsynaptic potentials that are synchronized. The surgery requires a craniotomy to remove a part of the skull which is invasive, but the spatial resolution (several millimeters for ECoG to typically less than 100μm in μECoG) and the temporal resolution of approximately 1ms allows precise monitoring of brain activity.

Since ECoG recordings are commonly carried out with large arrays of typically 2-3 mm-sized electrodes for clinical ECoG, vast cortical areas can be covered with large neural populations contributing to the signal recorded on each electrode. ECoG signals are a set of combined brainwaves that can be decomposed into several frequency bands described in the previous chapter. This signal, also called local field potential (LFP) is composed of the summation of synaptic currents in the cortical area directly close to the electrode.

Conversely, μECoG have electrodes that are less than 100μm of diameter, allowing both the recording of LFP and MUA and even potentially SUA. The extend to which μECoG can be used to record single unit activity is still debated, but recent data using low-noise μECoG arrays show spiking activity in the surface of the cortex of a freely moving rat (**Figure 6**).

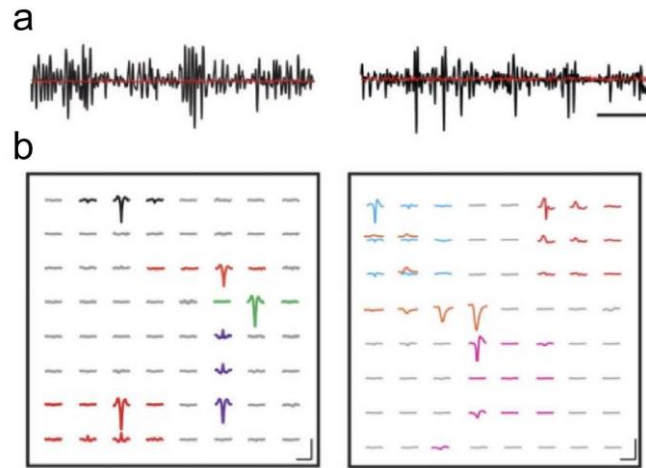


Figure 6. NeuroGrid structure and spike recordings in freely moving rats (adapted from (Khodagholy et al., 2015)). (a) High-pass filtered ($f_c = 500\text{Hz}$) time traces recorded in a freely moving rat from the surface of cortex (left) and hippocampus (right) in black. Corresponding postmortem filtered traces ($\text{rms noise} = 3 \mu\text{V}$ at spike bandwidth) are in red (scale = 10 ms by 50 μV). (b) Examples of the spatial extent of extracellular action potentials in cortex (left) and hippocampus (right) over the geometry of the NeuroGrid by spike-triggered averaging during the detected spike times (scale = 1.5 ms by 50 μV).

Electroencephalography (EEG)

EEG method requires the placement of electrodes on the scalp. These electrodes record electrical signals produced by large neural populations (millions of neurons altogether). Since it is not invasive, not expensive and portable, this technique is widespread in research as in medical use, to diagnose sleep disorders or epilepsy for example. Moreover, it does not involve the exposure of the patient to radioisotope or high-intensity magnetic fields.

Nevertheless, brain activity recorded is located several centimeters below the electrode. Cortical currents have to pass through various layers, and especially the skull, inducing a blurring at the scalp level. As a consequence, at every spatial scalp position, the recorded activity is a mixture (i.e. a weighted sum) of the underlying brain sources (Burle et al., 2015). The poor spatial resolution of scalp EEG (around 6 to 9 cm) results from this phenomenon (Babiloni et al., 2001).

Modeling techniques are thus required to estimate what areas are responsible of the activity measured. Synaptic activity on one neuron is too small to be recorded by EEG, but the summation of synchronous activity of thousands to millions of neurons can. However, the condition for such summation is that neurons shall have a similar spatial orientation, which is the case for pyramidal neurons of the cortex. These particular cells are thought to produce the majority of EEG signal.

Stereotactic EEG (sEEG)

Stereotactic electroencephalography uses penetrating depth electrodes to measure electrophysiological brain activity. The electrodes are localized using stereotactic guidance, and allow recording in deep regions of the brain such as hippocampus or insula. This technique is less invasive than ECoG since only small burr holes (about 1.2mm diameter) are needed instead of a wide craniotomy. Moreover, sEEG offers a signal-to-noise 100 times higher than EEG (Kern et al., 2009).

Magnetoencephalography (MEG)

MEG is a method to record magnetic fields produced by brain activity (Hämäläinen et al., 1993). The patient is placed inside a set of magnetic sensors based on SQUIDs (superconducting quantum interference devices) or SERF (spin exchange relaxation-free). The first MEG systems were both costly and cumbersome, but recent studies installed a MEG magnetometer in a portable 3D-printed helmet (Boto et al., 2018). MEG has a good temporal resolution of about 1 millisecond and a spatial resolution of a few millimeters better than EEG (because magnetic fields are not influenced by the low conductivity of the skull) but lower than subdural ECoG. This technique does not require exposure to radioisotopes.

Choice of a recording technique in minipigs

In minipigs, very little is known about cortical dynamics of prefrontal areas. A wide spatial coverage method is required to map the activity over large cortical regions in order to explore minipigs prefrontal cortex activity during vocalizations. To this intent, a short spatial resolution is also needed to highlight fast transient dynamic changes occurring in the areas of interest. With regards to these requirements, we will use ECoG arrays in minipigs to record cortical activity in the left prefrontal cortex during vocal production.

2.4. Cortical bases of vocalizations

In humans, vocalization takes another dimension with speech. Cortical areas involved in speech processing are situated in frontal, temporal and parietal lobe (See **Figure 7**). The superior temporal gyrus (STG) contains Wernicke's area (Brodmann 22) which is adjacent to auditory area. The STG is associated with comprehension of complex sounds and speech processing (Binder et al., 1997). The inferior frontal gyrus (IFG) is situated above the Sylvian sulcus and is composed of Brodmann areas 44, 45 and 47 (Catani et al., 2005). The IFG, also called Broca's area, is involved in speech production, working memory and lexical or syntactic speech processing (Hickok & Poeppel, 2007; Loh et al., 2020) along with social cognition (Jiang, 2018). To link both Broca and Wernicke's areas, an important pool of neuronal fibers are involved. These fiber tracks are called the arcuate fasciculus, or dorsal pathway (Friederici, 2009) and are considered crucial in human language evolution. In

addition, there is another pathway that runs parallel and lateral to the arcuate fasciculus (dorsal pathway) and connects both Broca and Wernicke in the inferior parietal lobule (Rijntjes et al., 2012), composed by Brodmann area 39 and 40. This ventral pathway plays an important role since it is involved in semantic analysis, but also phonologic and articulatory process. The dorsal pathway constitutes the sensorimotor and articulatory interface, since it integrates sensory or phonological representations of speech sounds to articulatory motor output (Hickok & Poeppel, 2004). The ventral pathway is the interface between phonological and semantic information, linking words to their significations(Hickok & Poeppel, 2004).

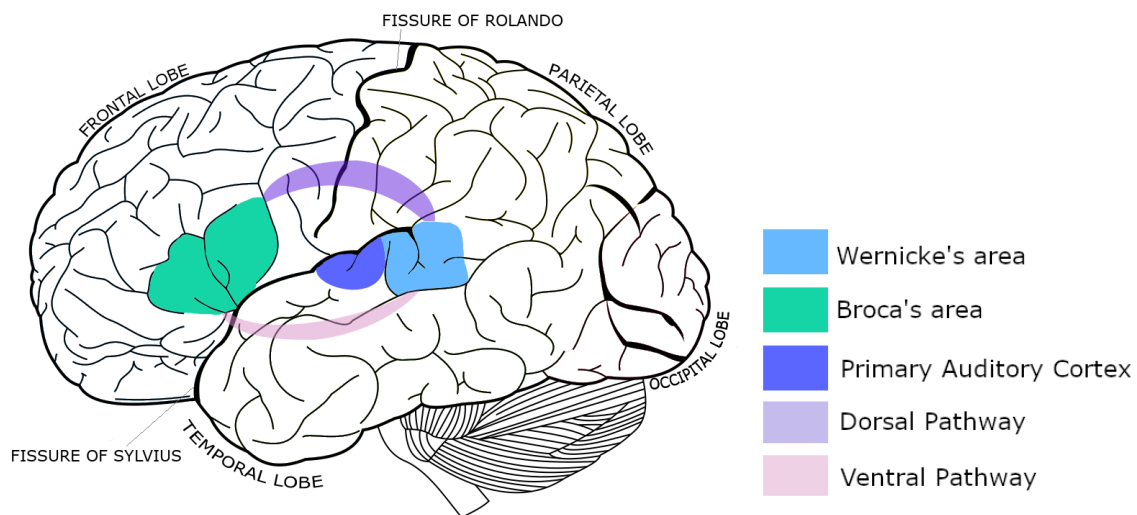


Figure 7. A schematic view of the dual-stream model (Hickok & Poeppel, 2004) of the functional anatomy of language. The dorsal pathway is involved in sensory and phonological representations of speech. The ventral pathway links words to their semantic.

More recently, an anatomical and functional dual-network was presented, synthesizing all relevant anatomical structures involved in vocal production in both humans and monkeys (Hage & Nieder, 2016, see **Figure 8**). This model emphasizes the fact that vocal production is supported by two different interconnected structures. Firstly, The primary vocal motor network (PVMN) is responsible of genetically predetermined vocal patterns linked to affective states. It is considered to be the brainstem vocal pattern-generating system and is composed of the periaqueductal grey (PAG), parabrachial nucleus (PB), and ventrolateral pontine reticular formation (Lateral reg. form.). The PVMN is controlled among other by the anterior cingulate cortex (ACC) and the hypothalamus amygdala. In humans, the PVMN produces non-verbal vocalizations such as laughing and crying (Wild et al., 2003), that are innate vocal productions, considered as the human counterparts of nonhuman primates vocalizations (Ackermann et al., 2014).

Additionally, there is a volitional articulatory motor network (VAMN), composed of the inferior frontal gyrus (IFG), the ventral premotor cortex (PMv) and ventrolateral primary motor cortex (M1). Broca's area is located in the IFG and consists of the granular ventrolateral prefrontal

cortex (vPFC). To date, only primates are known to possess direct connections between M1 and phonatory motoneuron pools controlling respiration, articulation and laryngeal movements. In non primates mammals, these connections are indirect via interneurons (Simonyan, 2014). In humans, the motor cortex is even directly connected to the ambigular nucleus. Such link has not yet been found in another species. VAMN is responsible of speech coordination, modulation of articulation, its role is to receive and process an important amount of information coming from different sensory structures such as the primary auditory cortex or primary visual cortex (Romanski, 2007).

In order to produce vocalizations, several groups of motoneurons are recruited to ensure the major functions involved in vocal production. Articulation, representing the movements of the tongue, the face and the jaw involve the nuclei of cranial nerves V, VII & XII. Respiration, which is used to modulate the vocal output, recruit pools of motoneurons in the ventral horn (VH) of the spinal tract (U Jürgens, 2009). This ventral horn of the spinal tract is also involved in the control of some articulatory movements, such as jaw-closing and jaw-opening via the nucleus hypoglossus. In addition to this respiratory musculature control, the VH also innervates the muscles of the larynx in combination with the ambigular nucleus (NA). All of these structures allow the production of the actual vocal output, and are under direct supervision of the primary vocal motor network.

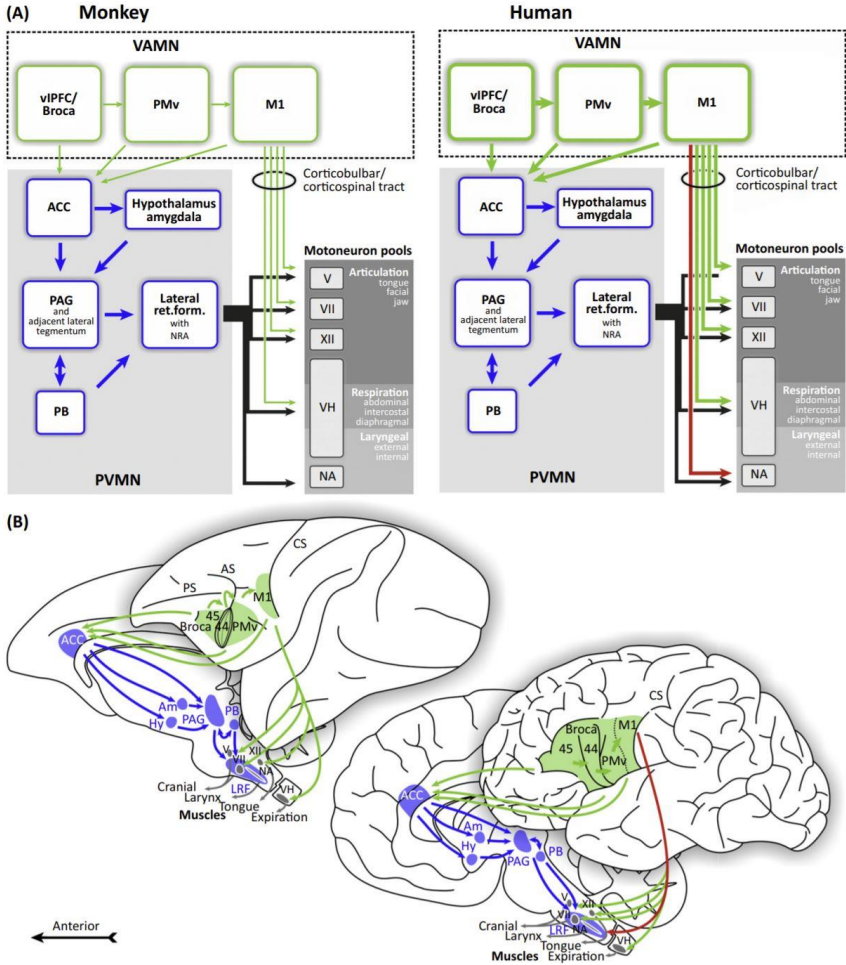


Figure 8. The dual-network model (Hage & Nieder, 2016). (A) Simplified circuit diagram (B) Anatomical locations and connections of the structures comprising the dual-network

2.4.1. Cortical bases of perception of vocalization in animals

Animal models have been widely used in research on the nervous system, and our neurobiological understanding of cognitive systems derive from their use. In contrast to prolific animal research on memory, spacial navigation or sensory processing, the field of speech and vocalizations processing has suffered from a reluctance to use animal models. This reflects the belief that only humans are capable of language processing and as such, animal models would not be relevant. However, this view is no longer supported now, because evidences were found that precursors to the function underlying speech perception can be found in nonhuman animals. For example, temporal cortical ablation in monkeys or in cats led to deficits in auditory discrimination of complex sounds like species-specific calls (Diamond & Neff, 1957; Hefner & Heffner, 1986). In humans, such deficits were observed in Wernicke's aphasia patients or following temporal cortex damages (Ludlow et al., 1986). In nonhuman animals, the left superior temporal gyrus is involved in species-specific vocalizations (R. H. Fitch et al., 1993), suggesting that the left hemisphere specialization for complex sound processing is not only found in humans.

Moreover, nonhuman primates neurons prefer complex sounds, including species-specific vocalizations in nonprimary auditory areas comparable to human superior temporal gyrus and auditory cortex (Broadmann 42 and 22, both in Wernicke's area) (Hackett, 2015). Additionally, macaque and marmosets studies suggested that there are "voice patches" (discrete, interconnected cortical areas supporting increasingly abstract representations of the vocal input) in the primates brain that are highly specialized in the processing of conspecific vocalizations (Belin et al., 2018). This result is in line with the fact that there are subpopulations of neurons that are dedicated to conspecifics vocalizations encoding in both human and animals like dogs or macaques (Andics et al., 2014; Plakke et al., 2013). More generally, the left hemisphere appears to be more involved than the right one for processing of conspecific vocalizations even in animals like pigs or mice (Ehret, 1987; Leliveld et al., 2020).

Additionally, animal research also focused in the perception of speech in animals, to shed light on neurobiological information about mechanisms underlying it. Dogs brains process conspecifics vocalizations and human acoustic cues in auditory areas that overlap, and they are also capable to segregate and integrate lexical information about words (Andics et al., 2016). Despite the complexity and variability of human speech, it appears that the activity of the auditory core is sufficient enough to characterize phonemes (Engineer et al., 2008; M. Steinschneider et al., 1994). These results are in line with behavioral studies showing that numerous animal species are able to discriminate phonemes reliably based on their capacity to detect novelty. For instance, Japanese quails are able to differentiate [b], [d] and [g] in a protocol of reinforcement (Kluender et al., 1987). Other species like chinchillas (Kuhl & Miller, 1975) or rats (Reed et al., 2003) are capable of discriminating phonemes. Moreover, recordings from awake ferrets show that neurons in the primary auditory cortex of these animals have responses that are sufficiently rich to encode and discriminate phoneme classes for sound classification (Mesgarani et al., 2008). Decoding human speech was also possible using intracortical microelectrode arrays in the rostral and caudal parabelt regions of the superior temporal gyrus in macaques (Heelan et al., 2019). Numerous nonhuman species

show behavioral and neurobiological evidences to categorize speech phonemes, proving that categorical perception involved in speech-specific processing is not unique to humans. However, there are persistent differences between animals and humans concerning the cortical bases of perception of vocalizations.

In terms of cortical organization, in human there is an asymmetry in the minicolumns sizes in Wernicke's area. Minicolumns are pools of 80-120 cortical neurons, organized vertically, that have nearly the same receptive field. Compared to chimpanzee and rhesus monkey planum temporale regions, only human revealed wider columns on the left hemisphere (Buxhoeveden et al., 2001). Additionally, the arcuate fasciculus is more developed in humans than in chimpanzees (J. Rilling, 2014).

2.4.2. Cortical bases of production of vocalization in animals

Vocal production is made possible with the complex involvement of three major functions: articulation, respiration and laryngeal or syringeal movements in birds. Vocal production in nonhuman primates and other animals have been classically assumed to be predominantly emotional, and linked to the brainstem or the mesial cortex activities (Allison et al., 1996). Innate vocalizations in animals are controlled by the PVMN that produces genetically determined vocal utterances. Electrophysiological recordings, stimulation or lesion studies show that neuronal activity in brainstem regions are related to vocalizations in squirrel monkeys and macaques (Hage & Jürgens, 2006; Larson & Kistler, 1984; Lütke et al., 2000). The brainstem areas involved in the PVMN in monkeys are the periaqueductal grey, parabrachial nucleus and ventrolateral pontine reticular formation. The latter innervates the different muscles of the larynx and tongue (Hage & Jürgens, 2006; Uwe Jürgens, 2000). These brainstem regions are under control of a limbic network that triggers vocalizations representing affective states. The network is composed of widespread areas, including region in the anterior cingulate cortex (including areas 24, 25 and 32), the hypothalamus, reticular formation of the mesencephalon, and amygdala (Dujardin & Jürgens, 2005, 2006). Electrical stimulation in all the structures involved in this network elicits vocal outputs, especially the anterior cingulate gyrus that triggered species-specific vocalizations in macaques and squirrel monkeys (Kirzinger & Jürgens, 1982; Smith, 1945). Ablation of the anterior cingulate gyrus lead to a decrease in spontaneous vocal behavior but animals were still able to produce vocalizations (Aitken, 1981). Ablation of other limbic regions like the tegmentum seems to suppress spontaneous vocalizations but species-specific calls can still be elicited by electrical stimulation of the periaqueductal grey (U. Jürgens & Pratt, 1979). These results suggest that the brainstem network is responsible of the initiation of a call, depending on its emotional or motivational valence.

As seen previously, VAMN is responsible of voluntary vocal outputs in humans and especially Broca's area. However, in monkeys, electrical stimulation or lesions in area 44 and 45 did not alter the acoustic traits of spontaneous vocalizations in squirrel or macaque monkeys (Green & Walker, 1938; Kirzinger & Jürgens, 1982). The frontal cortex of monkeys have received more attention recently and has been cytoarchitecturally described to assess its differences with

Broca's area in humans (Amiez et al., 2019; M. Petrides & Pandya, 2002). Minicolumns in humans Broca's area appear to be larger than in monkeys area 44 (Schenker et al., 2008), and there is no significant left hemisphere lateralization in nonhuman primates for both area 44 and 45 (J. Rilling, 2014; Schenker et al., 2010). These findings supported the theory that there were no nonhuman counterparts of Broca's area functionally speaking. However, studies show that in monkeys, areas 44 and 45, M1 and the premotor cortex were involved in volitive vocalizations (Ferrari et al., 2011; Gemba et al., 1999). Additionally, tropical singing mice were found to have turn-taking strategies in vocalizations, meaning they are able to interrupt their vocal songs when another speaker is vocalizing (Okobi et al., 2019). These animals are able to volitionally initiate or interrupt vocal production and start it again where it stopped.

Moreover, the premotor cortex of monkeys contains a representation of laryngeal movements, as shown by electrical stimulation studies (Hast et al., 1974; Uwe Jürgens, 2002).

Despite these similarities, there is still a superiority of human language in terms of scope and flexibility. It appears that basic mechanisms underlying a full blown language are present in non-human brains, and that the differences between human speech and animal vocalization can be seen as a matter of degree.

2.4.3. Minipigs cortical organization

Minipigs are very intelligent domestic animals that can easily be trained. There are many similarities between humans and minipigs brains since their gyrifications and morphologies tend to be comparable (Schmidt, 2015). Due to a critical need for large animal model excluding non-human primates, minipigs have been increasingly used in the field of neuroscience (Saikali et al., 2010). Both minipigs and pigs can be particularly pertinent models in biomedical studies such as transplantation or pathological models (Lind et al., 2007). The size of the brain, approximately 6cm, represents an advantage compared to rodent models for brain imagery. The motor cortex is directly caudal to the dorsofrontal prefrontal cortex (**Figure 9**), and adjacent to somatosensory cortex (Jelsing et al., 2006). The prefrontal cortex can be subdivided into four regions : the frontopolar, the anterior insular, the anterior cingulate and the dorsofrontal region (Sauleau et al., 2009). To date, the description of the cortex remains vague and subject to debate, and there are no stereotaxic atlases of good quality of the minipig. . Moreover, since the role of the prefrontal cortex in the production of vocalizations has not been studied yet in minipigs, we can legitimately ask if neuronal subpopulations in prefrontal cortices are specifically coding for vocal productions. In particular, we ask the question whether all vocalizations are controlled by the prefrontal motor cortex or only specific vocalizations, corresponding for instance to specific situations or emotional status of the animal.

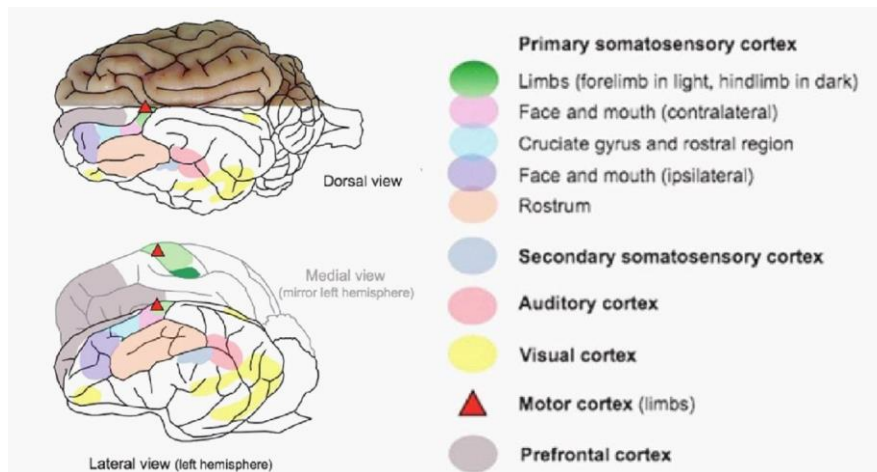


Figure 9. Dorsal, lateral and medial (left hemisphere) views of the brain of a Large White-Landrace pig weighing 30 kg, with schematic representations of the cortical areas (adapted from Sauleau et al., 2009)

3. Assessment of graphene cortical implants in rats

Recording of LFP, single neurons (SUA) and multiple neurons (MUA) activities is made possible with the use of penetrating silicone probes or tetrodes. These electrodes have been used extensively to investigate the neural bases of several behaviors. However, penetrating probes can cause great damage to the brain, along with loss of signal due partly to inflammatory response (Polikov et al., 2005). Moreover, intracortical arrays allow only the recording of small cerebral volumes, which limits the assessment of neural dynamics over large cerebral areas. Surface μ ECoG arrays have electrodes that are less than 100 μ m of diameter, allowing both the recording of LFP and MUA. The possibility that μ ECoG can be used to record single unit activity has been recently proposed (Khodagholy et al., 2015). However, few studies have then confirmed this finding, which is thus still debated. In particular, it is not yet known if the sharp events (or putative single units) recorded from the surface of the cortex contained information that can be decoded to predict behavior.

My PhD thesis was partly funded by the Graphene Flagship, a European project that aims to bring graphene technology into commercial application. Our role was to test graphene-based implants in rats and eventually minipigs afterwards before translation to humans. We tested whether 64 channels surface graphene probe were able to detect both LFPs, MUA and SUA from the surface of the rat brain. Rats were used in first intention to assess whether such type of innovative probes could allow low-noise recordings of LFPs, MUA and possibly SUA, and to test the physical properties of the implant in real conditions. We decided to compare Graphene probes with commercial NeuroNexus penetrating and surface implants in order to understand the differences between evoked responses acquired in deep cortical layers and

those recorded at the surface of the brain. As part of the collaboration with other actors of the Graphene Flagship, graphene-based electrodes have to be studied in preclinical conditions to bring this technological innovation into clinical or commercial applications.

We chose the rat auditory cortex to evaluate the probes. As humans, rats possess a primary auditory cortex (A1) and an antero-associative field (AAF). Rats have developed a highly sensitive hearing range that runs from 200Hz to 76000Hz, which allows them to hear what we consider as ultrasounds (commonly more than 20000Hz). The rat audiogram is considered to be representative of mammals, and therefore it is a convenient animal model to study the neurophysiological aspects of the auditory system. Functional knowledge is available to characterize precisely the rat auditory cortex dynamics. The auditory core is tonotopically organized in V shaped bands with a tonotopic gradient in the postero-anterior axis (Rutkowski et al., 2003). The position of the auditory core is also well identified with brain atlas (Khazipov et al., 2015).

In humans, an auditory stimulus triggers various evoked responses that are distinguishable by their latencies (Picton et al., 1974). The early (or brainstem) auditory evoked potential (BAEP) represents activity in the brainstem auditory pathways and in the eighth nerve. BAEP latency is very short and commonly between 1 and 10ms (Erné et al., 1987). Middle latency evoked potentials (MAEP) reflects both subcortical and cortical auditory activity and have a latency of 10 to 50ms (Liégeois-Chauvel et al., 1994; Mäkelä et al., 1994; Yvert et al., 2001; Yvert et al., 2005). The long latency auditory evoked potential (LAEP) comes from late secondary processes. Additionally, in response to sound stimuli longer than clicks, there is a sustained component of AEPs that occurs during the sound stimulation (Hari et al., 1987). This sustained activity is followed by an OFF response that is time locked to the end of the stimulus (when the sound is longer than 100ms) (Onishi & Davis, 1968).

In rats, homologous of these categories can also be recorded. BAEPs are composed of four waves occurring in the first 6ms after stimulus onset (Poblano et al., 1996). Surface MAEP in rats consists typically of two positive-negative components (Shaw, 1988). The positive peaks are labelled P1 and P2 and have latencies of approximately 8 and 25ms. The two negative peaks are N1 and N2 with latencies of approximately 18 and 35ms respectively (Wang et al., 2001). The later component consists of a slow positive peak at 68ms followed by a large negative peak at 88ms (Lorenzo et al., 1977; Meeren et al., 2001; Simpson & Knight, 1993). In rats, OFF responses could not be at first replicated, and neurons in the primary auditory cortex (A1) of barbiturate-anesthetized animals seemed to only elicit ON responses (Phillips & Hall, 1990). However, as the anesthesia techniques changed, new experiments showed that neurons in cats primary auditory cortex could also respond to tones with OFF activities (Volkov & Galazjuk, 1991). These results were found on ketamine-anesthetized cats, and were replicated later on rats (Kopp-Scheinflug et al., 2018; Qin et al., 2007; Takahashi et al., 2004; Xu et al., 2014), highlighting the fact that previously used barbiturate anesthesia tended to modify deeply the evoked responses in the auditory cortex.

Neurons in auditory cortex are well tuned to sound frequency and are organized into multiple tonotopic maps across the cortical surface. Other relevant animal studies have examined the primary auditory cortex in ferrets to reveal representations of the tonotopy over A1 (David & Shamma, 2013; Thorson et al., 2015). These researches have demonstrated encoding properties based on spectrotemporal receptive fields (STRFs) of the primary sensory neurons in A1. Studies show that the neural responses of the auditory cortex are sufficiently

rich to allow encoding of phonetic acoustic features of speech in monkeys and ferrets (Heelan et al., 2019; Mesgarani et al., 2008; Mitchell Steinschneider et al., 2003).

In this chapter, we setup a paradigm to perform cortical recordings on ketamine-xylazine anesthetized rats' auditory core. We characterized responses to pure tones and decoded pure tone frequency based on the auditory cortex activity.

To do so, we tested three different types of electrodes on two animals. Firstly a penetrating NeuroNexus MEA, secondly a surface NeuroNexus μ ECoG and finally a surface Graphene μ ECoG. These last two probes were tested in the same animal.

3.1. Materials and methods

3.1.1. Animals

Results presented in this chapter report neurophysiological recordings in the left auditory core from 2 adult male rats (OFA, n=2, 400-604 g, Charles River). Animals were housed in pairs in plexiglass cages (25°C, 22 Pa, 12-hour light-dark cycle) with free access to food and water. All experimental procedures were performed under the supervision of a qualified person in accordance with the recommendations of the European Community Council Directive of November 24, 1986 (86/609/EEC) and French legislation for care and use of laboratory animals. The protocols have been approved by the Grenoble ethical committee (ComEth Grenoble number 04815.02).

3.1.2. Surgical procedure

Animals were induced with Isoflurane 4% (Vetflurane 2L/min, 1.8L air + 0.2L O₂) then anesthetized by an intramuscular injection of Xylazine in the thigh (Rompun 2% 2mg/kg) followed by an intraperitoneal injection of Ketamine (Imalgene 90mg/kg). Additional doses (Ketamine 100mg/kg : Imalgene 0.9ml; Xylazine 5mg/kg : Rompun 2% 0.1ml) were provided when necessary in order to suppress hind paw reflex movements and maintain the rat deeply asleep. Temperature was monitored with a heating pad coupled to a rectal thermometer to maintain an average of 36°C rectal temperature (TemSega). The rat was placed in a stereotaxic frame (Narishige, SR-6R-HT) with ear bars to maintain the head horizontal. The lambda and bregma points (lambdoid suture and bregmatic fontanel) were identified to position the craniotomy above the left auditory core. A 40mm skin incision was made following a line starting between the eyes to the neck with a sterile scalpel. The skin and muscles of the left cheek were resected with forceps and scissors. A wide craniotomy was performed using a dental bur (Dremmel) to expose the left auditory core. The craniotomy runs from 2mm to 8mm posterior to bregma (coordinates obtained stereotactically) and from 2mm from the anterior fontanel to the zygomatic arch according to a rat brain atlas (Khazipov et al., 2015). Burr holes were drilled on the four corners of the rectangle shape craniotomy to estimate the bone

thickness. After the craniotomy was made, fixation screws were put (PlasticsOne, diameter: 1.19mm, length: 1.60mm) and glued to the skull. The screws allowed the placement of a custom 3D printed headpole ahead Bregma and far enough from the bregmatic fontanel to avoid damages. The headpole was used to maintain the head in place during recordings since the removing of the ear bars was necessary. A reference wire was glued under the headpole. During this process, the bone was placed back over the craniotomy in order to protect the brain.

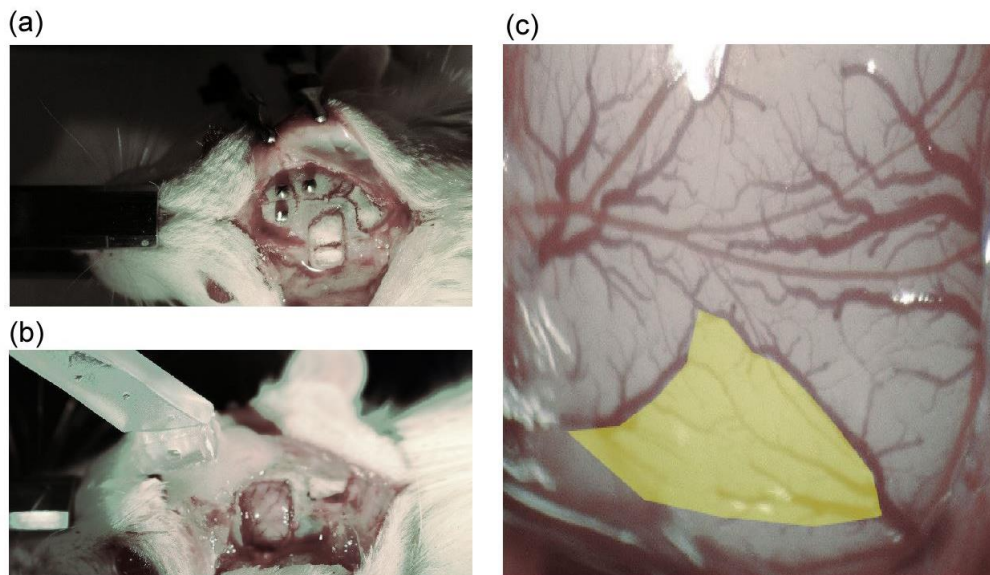


Figure 10. Stereotaxic surgery in rat auditory cortex. (a) The screws are placed near the craniotomy in order to glue a custom head holder. The bone from the craniotomy was replaced during the glueing process to protect the brain. **(b)** The custom bar is glued to the skull with dental cement and the bone is removed. A reference electrode is glued under the piece to allow precise measures. **(c)** At the bottom of the craniotomy, the primary auditory cortex, represented by the yellow area, can be localized between two veins.

Left auditory core was identified with its coordinates given by an atlas of the rat brain (Khazipov et al., 2015) and blood vessels tracking according to literature references (Kalatsky et al., 2005; Sally & Kelly, 1988). Although there is a wide variety of vascular patterns in rat brains, some constant anatomic cues can be seen on the left cortex. It shows a typical blood vessels pattern in the left auditory cortex, and the inclined vessel on the right was always distinguishable over all our surgeries. On the contrary, the left vessel was really difficult to identify on some experiments and its location and form were quite variable. In general, the typical triangle shape shown on **Figure 10** helped us identify the auditory core. The dura was removed with a n°55 plier and micro-scissors around the implantation site.

The first animal was implanted with intracortical electrodes array (NeuroNexus NN64 A8x8-5mm-200-200-703 30 μ m contact diameter) with a 20-degree medio-lateral angle and 2 millimeters depth. The second animal was implanted with a surface NeuroNexus probe and a surface microelectrode array (graphene microelectrode array, 25 μ m electrode diameter, 1kHz of impedance before implantation, 13 μ m polyimide and gold substrate) during the same recording process. To prevent edema and reduce potential bleeding, the cortex was frequently hydrated with physiological liquid. The ear bars were then removed to allow a better hearing

by the animal. At the end of the recording, electrodes were removed and animals were sacrificed with a lethal intracardiac injection of pentobarbital (Doletal 1ml/kg, Vetoquinol).

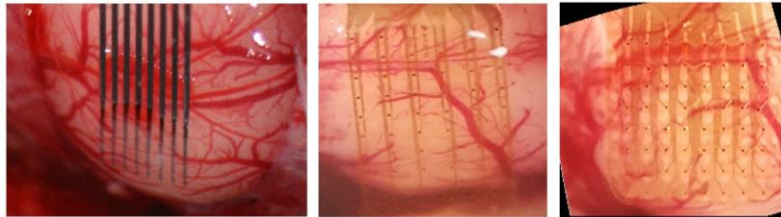


Figure 11. Different electrode types used. Left panel : intracortical NeuroNexus probe in animal 1. Center panel : surface NeuroNexus probe in animal 2. Right panel : graphene surface probe in animal 2.

3.1.3. Auditory Stimulation

The stimulation was composed of eight 200ms pure tones with a 3ms ascending front and 30ms descending front created off-line with Matlab software (Natick, Massachusetts: The MathWorks Inc) at a rate of 50000Hz at different frequencies. We created 500Hz, 1000Hz, 2000Hz, 4000Hz, 6000Hz, 8000Hz, 12000Hz and 16000Hz pure tones presented randomly. Sounds were presented every 1800ms \pm 10 to 20 ms. The frequencies were chosen to cover a wide part of the auditory spectrum of rats and to remain audible by the experimenter so that he can control the smooth progress of the sequence. One recording corresponded to 800 sounds and lasted approximately 30 minutes. (100 sounds of each frequency). The first animal was only exposed to 6 frequencies : 500Hz, 1000Hz, 4000Hz, 8000Hz, 12000Hz and 16000Hz.

3.1.4. Data acquisition

For animal 1, data was recorded with NeuroPXI general user interface (Bonnet et al., 2012) at a sampling rate of 20kHz.

For animals 2, data was recorded with Intan recorder (Intan Technologies) at a sampling rate of 30kHz.

3.1.5. Data analysis

Local Field Potentials analysis

The analysis was performed using Spike2 (Cambridge Electronic Design) and Matlab (Natick, Massachusetts: The MathWorks Inc) softwares. We applied a low pass filter at 500Hz

for local field potentials analysis. Cortical data was low-pass filtered at 500Hz, evoked potentials were computed by averaging single trials locked to the onsets of different frequency pure sounds and correcting the baseline with respect to [-100, -10] ms interval preceding sound onset. To assess the statistical significance of these averages, we first built a distribution of bootstrap averages (Blaise Yvert et al., 2002). If N vocalizations were recorded, N trials were drawn with replacement from the original set of N trials, and averaged and baseline-corrected. This procedure was repeated 1000 times. We further assessed significant sound-induced cortical activations using the following procedure. A rest period void of sound presentation was considered and used to select N resting trials, which were in turn averaged and baseline corrected with the same parameters as the signal. The standard deviations corresponding to both the sounds and the resting averages were also computed and a Welch t-test was performed to compare both distribution at every time point of the average potential. A threshold was set at 0.05 and all time points for which the P-value of the Welch test was below this threshold were considered to correspond to statistically significant activity. This procedure was further retained to build spatiotemporal maps of cortical activity using our previously developed NeuroMap software (freely available at <https://sites.google.com/site/neuromapsoftware/>) (Abdoun et al., 2011). Spectrograms were performed with a window of 250ms and a step of 5ms, and z-scored with the rest period void of sound presentation.

Multi Unit and Single Unit activity analysis

In animal 2, we observed spike-like activity recorded with graphene surface probe, which were in the form of sharp events that we will call “unit” in the following even though no proof that they are actually action potentials have been obtained at this stage. Data were band-pass filtered between 1kHz and 4kHz and analyzed with Offline Sorter application (Plexon, Neurotechnology Research Systems). Pertinent waveforms were extracted and spike sorting algorithm was performed to classify units.

To decode pure tone frequency based on the auditory activity, we considered 9 features of 50ms each ranging from 0 to 450ms after stimulus onset. These features were used to train a support vector machine (SVM) classifier. Firing rates were smoothed using a gaussian convolution (kernel std = 0.05sec, kernel spread = 2sec) then scaled with the standard deviation. The parameters of the SVM were optimized with a grid search on 5 folds.

This spike-like activity was not observed with either penetrating nor surface NeuroNexus probe in animals 1 and 2.

3.2. Results

Electrophysiological data were recorded from rats. Auditory evoked responses to pure tones were acquired in the left auditory cortex with three different types of electrodes: two surface probes and one penetrating probe. The results reported here are LFP activities from two ketamine-xylazine anesthetized animals, along with MUA and SUA in one of the animals.

3.2.1. Acoustic contamination

During the analysis of microelectrocorticographic recordings in rats, it appeared that cortical data contained spectrotemporal features correlated with the pure tone frequencies that were presented, a phenomenon initially observed in human recordings and extensively explored during the PhD thesis of Philemon Roussel. Hence, the audio signal was recorded in the same way as neurophysiological data, suggesting an acoustic contamination, which distorts the analysis of cortical auditory evoked potentials (Roussel et al., 2020). In **Figure 12** (b) and (c) we noted that all the electrodes were strongly correlated to sound spectrograms, especially at the specific pure tones frequencies (500Hz, 1000Hz and 2000Hz)

As a consequence, for the study of local field potentials, we decided to only focus on data frequencies lower to 500Hz in order to avoid acoustic contamination.

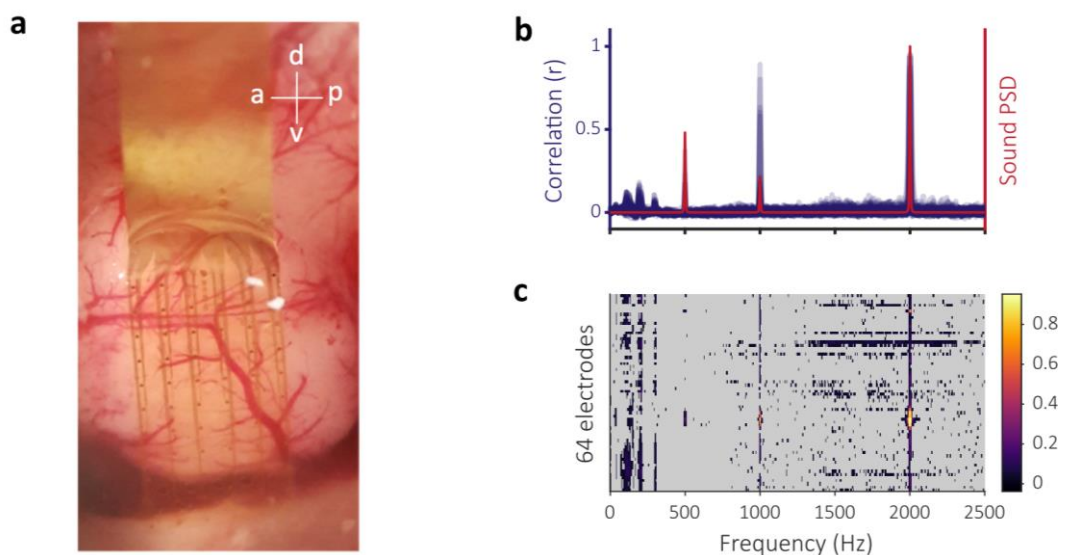


Figure 12. Correlations between sound and μ -ECoG spectrograms during pure tones perception in an anesthetized rat. (Roussel et al., 2020). (a) Photograph of a μ -ECoG grid positioned over the left auditory cortex of a rat. Directions: a = anterior, p = posterior, d = dorsal, v = ventral. (b) On the upper panel, each blue curve represents, at all frequency bins, the value of the correlation coefficients between the spectrogram of one electrode signal and the spectrogram of the audio signal. The red curve represents the mean power spectral density (PSD) of the audio signal (a.u.). The lower panel represents a heat map of the correlation coefficient between audio and neural data for all electrodes and frequency bins. Correlation coefficients not statistically significant are displayed in grey.

3.2.2. Local Field potentials

We used different probes to record auditory evoked potentials for a period of approximately 30 minutes during which several pure tones of different frequencies were

presented to the animal in a pseudo random order. The following chapter show the results for the peaks latencies of the components obtained. Peaks have been labeled according to their polarity and the order of their occurrence in each electrode waveform.

Animal 1 – Penetrating NeuroNexus probe

The first component is composed of a positive peak P1 at 10ms and a negative peak N1 at 22ms. The second component is a positive peak P2 at 60ms. We recorded an OFF response with a similar Positive-Negative-Positive pattern than the ON response. The latencies of the OFF peaks were : 220ms (P1OFF), 260ms (N1OFF) and 317ms (P2OFF) (20ms, 60ms and 117ms after stimulus offset respectively). **Figure 13(a)** left panel shows the pattern of averaged responses on all electrodes to each pure tone given the six frequencies (see auditory stimulation). **Figure 13(b)** left panel represents the bootstrapped waveforms in response to a 8kHz pure tone for one electrode located over the primary auditory cortex (**Figure 13(c)** left panel).

Animal 2 – Surface NeuroNexus μ ECoG

The first positive peak P1 occurred 7ms after stimulus onset, followed by a negative peak N1 at 35ms. P2 occurred at 80ms. We recorded a small amplitude OFF response with POFF at 270ms and NOFF at 290ms (70ms and 90ms after stimulus offset respectively). We averaged responses for each pure tone given the eight frequencies (see auditory stimulation) and obtained averaged local field potentials (**Figure 13(a)** (center panel)). The OFF response was recorded with an amplitude about 4 times smaller than the amplitude of P1. **Figure 13(b)** center panel represents the bootstrapped waveforms in response to a 8kHz pure tone for one electrode located over the primary auditory cortex (**Figure 13(c)** center panel)

Animal 2 – Graphene surface μ ECoG

The first positive peak P1 occurred at 30ms, followed by a large N1 at 162ms. The OFF response consists of a positive peak POFF at 270ms and a negative peak NOFF at 320ms (70ms and 120ms after stimulus offset respectively). For each electrode, we averaged responses for each pure tone given the eight frequencies (see auditory stimulation) and obtained averaged local field potentials. The average auditory evoked response was obtained with bootstrapped responses to each pure tone frequencies (**Figure 13(a)** (right panel)). **Figure 13(b)** right panel shows the bootstrapped evoked response obtained on one electrode located over the auditory cortex (**Figure 13(c)** right panel).

	Animal 1	Animal 2 NeuroNexus	Animal 2 Graphene
P1	10	7	30
N1	22	35	162
P2	60	80	
P1OFF	220	270	270
N1OFF	260	290	320
P2OFF	317		

Table 3. Summary of the latencies of the different peaks in animals 1 and 2.

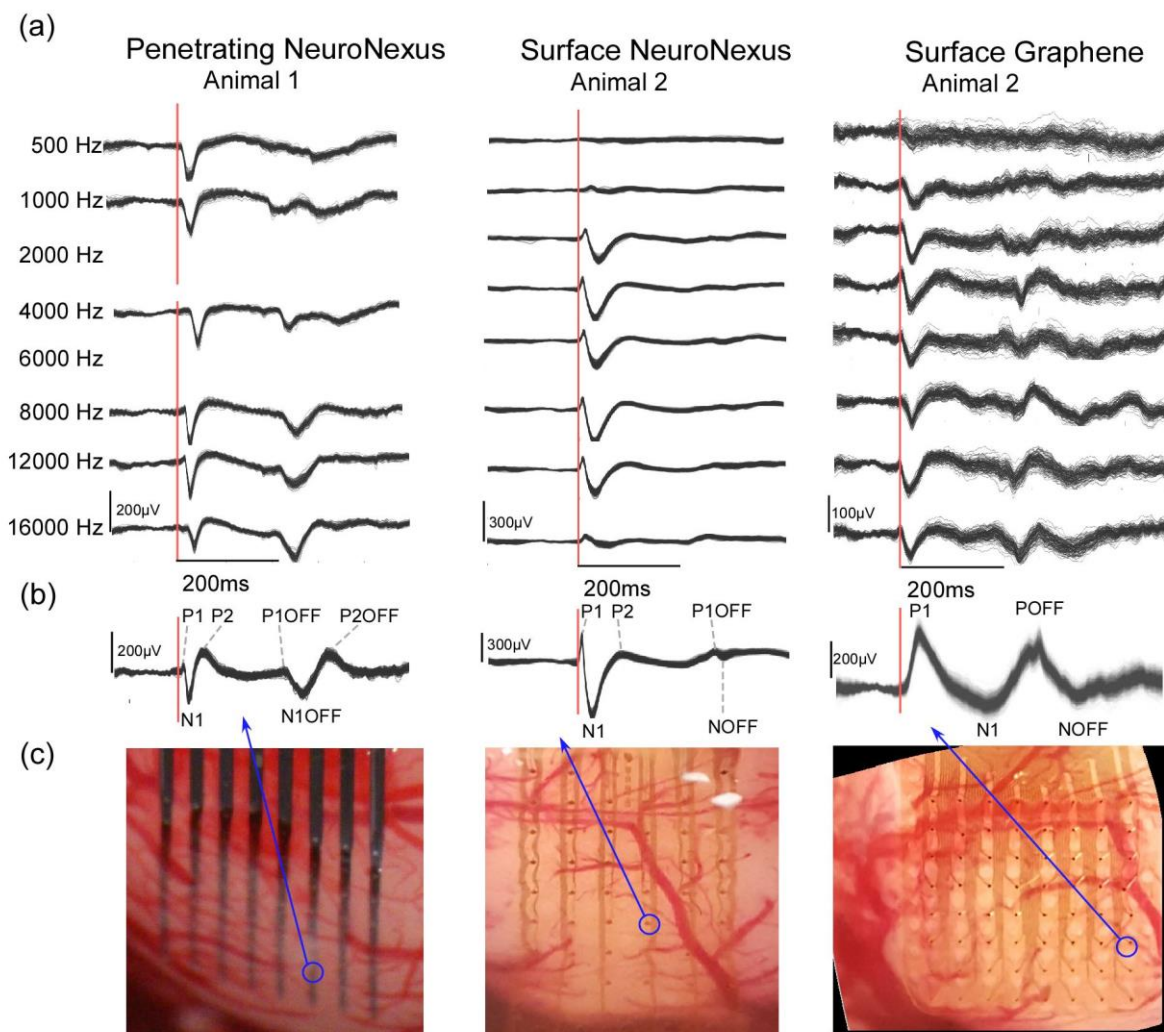


Figure 13. Auditory evoked responses in animals 1 and 2. (a) Bootstrapped ($n = 1000$) auditory evoked responses to pure tones of different frequencies (in lines, ascending order). Red bars indicate stimulus onset. Horizontal bars indicate stimulus duration (200 ms). (b) Bootstrapped ($n = 1000$) auditory evoked responses to 100 pure tones of 8 kHz on one electrode located on A1. (c) Electrode in (b) represented on pictures of the cortex.

We wanted to explore the frequency characteristics of ON and OFF responses in the different animals. To do so, we studied the time-frequency representations of the averaged electrodes for animals 1 and 2 (**Figure 14**). The two responses do not have the same frequency contents.

ON and OFF responses were recorded on both animals, with a lower amplitude of the OFF response in animal 2 with surface NeuroNexus probe (see **Figure 14(b)** middle panel). **Figure 14 (a)** shows the spectrograms of the activity for each electrode of the probe. In animal 1, ON response consists on a broadband activity between 25Hz and 210Hz, which covers beta, gamma and high-gamma bands. OFF response is located around 120Hz (high-gamma band) (**Figure 14 (b)** left panel). In animal 2, ON response show a component in the bands between 32Hz and 80 Hz (gamma band) recorded by both surface NeuroNexus and surface graphene probes. Additionally, surface graphene probes allow the recording of other ON response pools of activity at 150Hz, 240Hz and 440Hz (high-gamma). OFF response presents the same activity between 32Hz and 80Hz, a weaker activity at 240Hz, along with very high frequency components stronger than 400Hz (**Figure 14(b)** right panel).

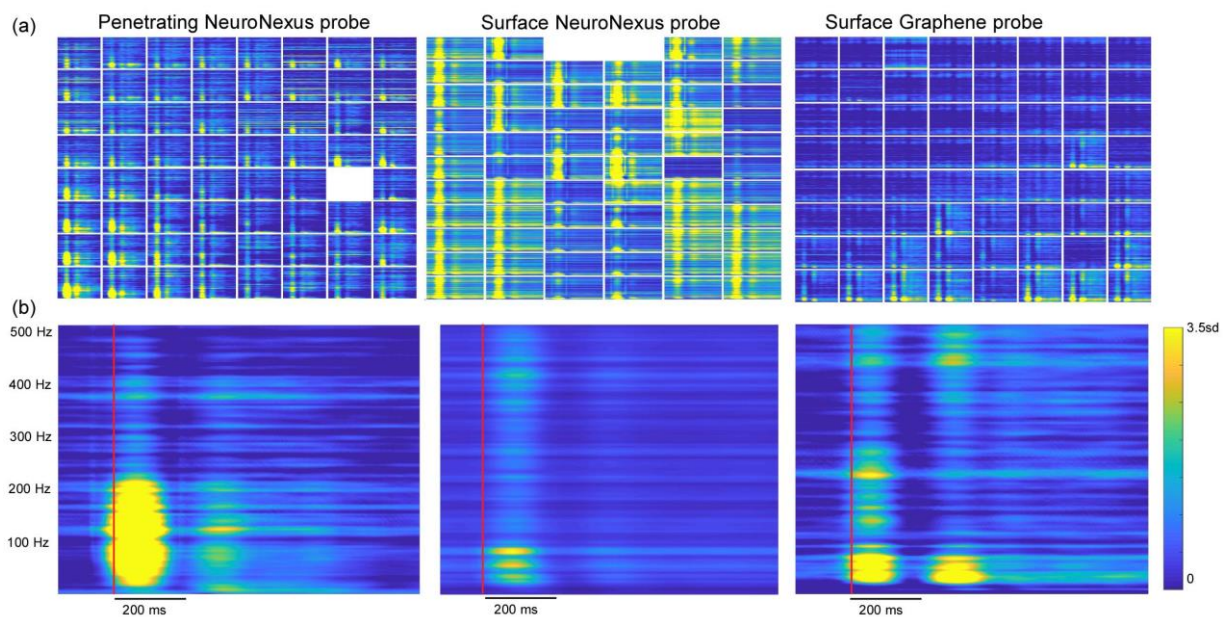


Figure 14. Spectrograms of the activities for animals 1 and 2. (a) 64 channels representation of the averaged evoked responses to all pure tone frequencies. Each panel represents the electrode layout of the implants. (b) Averaged spectrogram of the activity for all electrodes and all pure tone frequencies. Red bars represent stimulus onset.

Both penetrating NeuroNexus, surface NeuroNexus and surface graphene probes allowed the recording of auditory evoked responses of A1 in rats. OFF responses were weaker with surface NeuroNexus probes.

3.2.3. Single Unit and Multi Unit Activity

By observing the raw signals of our Graphene electrodes on animal 2, we noticed the presence of bursting activity in the 50ms following stimulus onset and stimulus offset (see **Figure 15 (a)**). This activity was analyzed and we extracted different waveforms which we considered as fast events and called units. The events were on average 500 μ s long and their amplitude was 5 μ V. As can be seen on **Figure 15(b)**, some of the electrodes recorded several units. We extracted 40 different units in total. **Figure 16** represents the raster plots of four different units. Each panel corresponds to one pure tone frequency, the rasters are the occurrences of the waveforms at each of the 100 presentations of the same stimulus. Unit 31 shows a sustained activity for the pure tone of 2000Hz frequency, and units 14, 16 and 32 show a pattern of ON-OFF responses for pure tones with a frequency superior or equal to 2000Hz. On average, units tended to display a pattern equivalent to those of units 14, 16 and 32 with ON and OFF peaks (see **Figure 16** and **Figure 17 (a)**), suggesting that the cells recorded here are mostly onset-offset neurons, which is in adequacy with previous literature on the auditory cortex of different animal species (Xu et al., 2014).

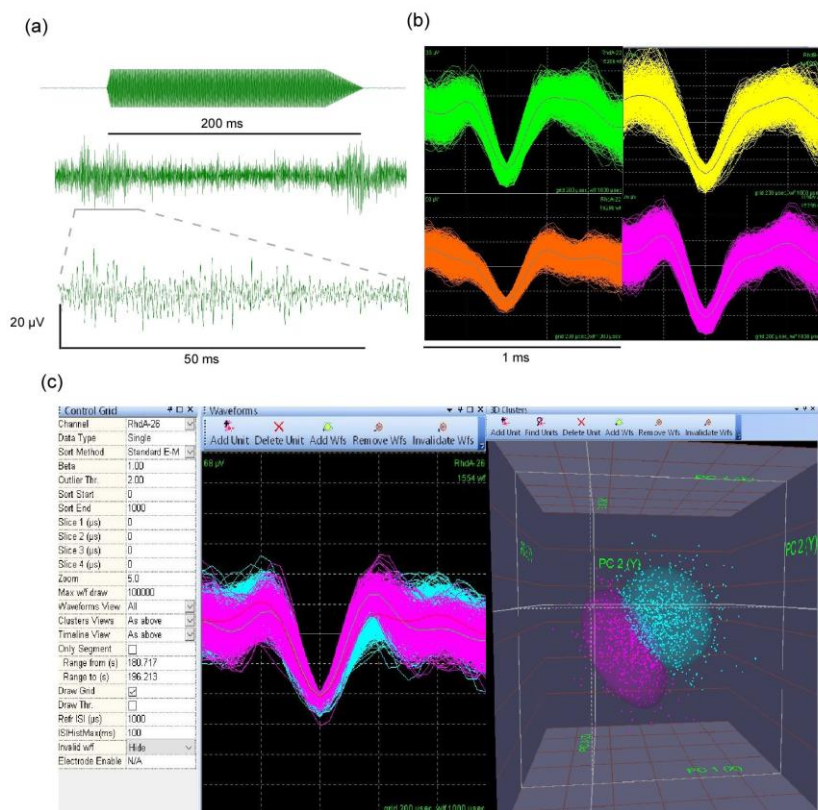


Figure 15. Multi Unit and Single-Unit-like activity recorded in response to pure tones with graphene probe on the surface of the left primary auditory cortex of rat No 2. (a) Pure tone presentation and bursting activity recorded on one electrode. **(b)** An example of four waveforms extracted from two different electrodes. **(c)** Waveform extraction and analysis using Plexon OFFLINE sorter. Superimposed waveforms are displayed on the left panel and principal component analysis (PCA) on the right panel. The PCA is visualized in 3 dimensions and the waveforms cluster are represented in pink and blue according to the colors on the left panel.

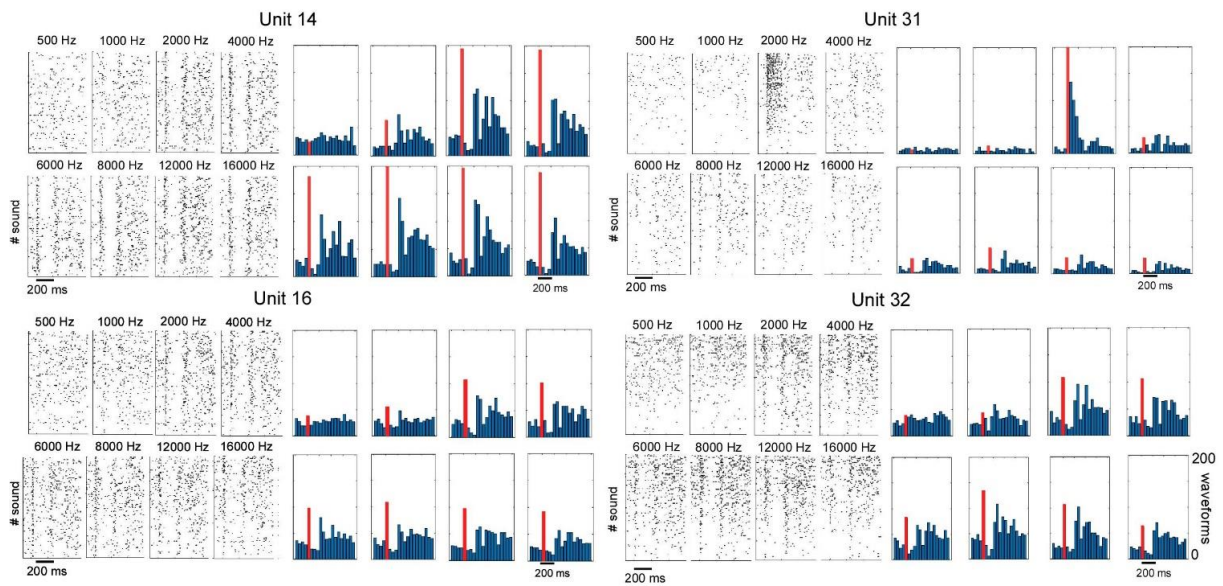


Figure 16. Raster plots and peristimulus histograms for 4 units. Red bars represent the number of waveforms detected during the 50ms following stimulus onset. Unit 14, 16 and 32 present ON-OFF pattern of response. Unit 31 shows a sustained activity for pure tones of 2000Hz.

Decoding pure tone frequency from fast events

Based on the activity of the 40 units recorded on 18 channels of the Graphene μ ECoG, we trained an SVM classifier to decode which pure tone frequency was heard by the animal based on the unit-like sharp events recorded from the surface of the auditory cortex. The features used in this algorithm are illustrated in **Figure 17 (a)** by the red and blue bars on the histogram. They were the firing rate in 50-ms time bins for all units the 450 ms following the stimulus onset, resulting in $9 \times 40 = 360$ features for the 40 units. The decoding accuracy obtained was 47.89% of correct classification for a chance level of 12.5%. **Figure 17 (b)** represents the confusion matrix of the decoding results. For each predicted frequency, it gives the results of the SVM classifier. Best predictions were obtained for the 2000 Hz and 4000 Hz tone frequencies with 80.36% and 89.47% accuracy, respectively. The 500-Hz frequency was likely artifactually well predicted due to the absence of any specific firing of the putative cells for this frequency (see **Figure 16**).

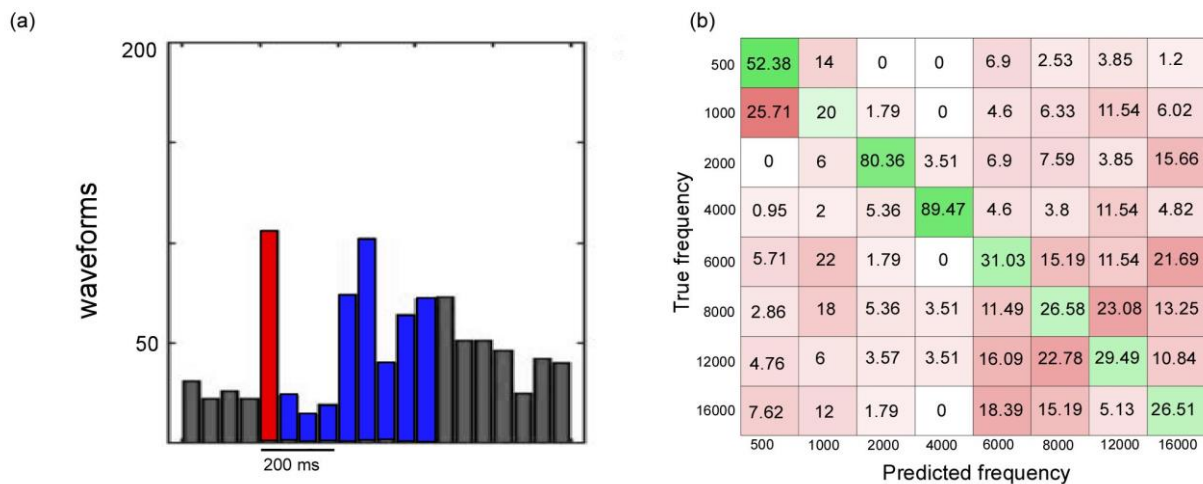


Figure 17. Decoding pure tone frequencies based on cortical activity. (a) Example of a peristimulus histogram for Unit 32 in response to 12kHz pure tone. The colored bars on the peristimulus histogram are the features used for decoding (from stimulus onset to 450ms after stimulus onset, corresponding to 9 features of 50ms). (b) Confusion matrix of the decoding. Predicted frequencies are presented in columns and true frequencies in lines. The data are in percentages. Green cases indicate the right classification percentages. Red cases are the classification errors.

3.3. Discussion and perspectives

The study of this chapter was designed to evaluate the auditory evoked responses to pure tones in two animals implanted with three different probes. Local field potentials were analyzed in response to pure tones of different frequencies. The typical response from the auditory cortex found in the present study showed differences in peak latencies with those found by others in awake or anaesthetized rats (Lorenzo et al., 1977; Meeren et al., 2001; Simpson & Knight, 1993), but the left auditory cortex presented ON and OFF activities recorded by all the different probes. This pattern of response could be significantly recorded with either penetrating NeuroNexus probes or graphene surface probes, but not clearly with NeuroNexus surface probes. Previous studies show that the offset of auditory brainstem responses is influenced by rise and fall times of the stimulus. In particular, the offset response decreased drastically as the fall time increases from 0.2 to 2ms in bats and mice (Grinnell, 2004; Henry, 1985). In our study, we used a very long descending front of 30ms for every pure tone frequency. In another animal recorded with a surface NeuroNexus probe, we experimented differently during another recording and tested the potential effect of this long descending front. We sharpened the sound fall timing to 3ms but no significant OFF response was recorded. Additionally, the lack of recording of an OFF responses with surface NeuroNexus probe might be influenced by anesthesia levels (Plourde, 2006). However, anesthesia levels were similar

in the whole protocole, and the graphene-based electrode implanted in the same animal subsequently allowed the recording of OFF responses.

The extent to which μ ECoG can be used to record single unit activity from the surface of the brain is still debated, but recent data using low-noise μ ECoG arrays show spiking activity in the surface of the cortex of a freely moving rat (Khodagholy et al., 2015). The waveforms were correlated to sound presentation, either in a sustained way or in an ON-OFF pattern. Here, we found that such recordings obtained with graphene probes contain relevant information regarding the animal behavior since they could be used to decode which stimulus has been perceived. This activity was used to decode pure tone frequency with an accuracy of 47.89% (chance level = 12.5%).

This study demonstrated the feasibility of recordings of auditory evoked potentials in rats, in order to apprehend the analysis of cortical results and the adaptation of the protocole to a preclinical model with minipigs. Additionally, new surface Graphene probes are expected to confirm the spike-like recordings in the auditory cortex of rats. The data might be used to improve the performances of the decoding algorithm, especially by the combination of various types of sounds like swipes, rats vocalizations or speech. A previous study on ferrets shown that A1 responses were sufficient to discriminate phoneme classes (Mesgarani et al., 2008) so we might consider to analyze the auditory responses of the rats to various sentences and try to decode phonemes from continuous speech processing.

4. Characterization of minipigs spontaneous vocalizations

The analysis of animal vocalizations is a subject studied extensively. This field is part of bioacoustics, and focuses on the vocal repertoires of animals and their social behaviour.

The domestic pig (*sus scrofa domesticus*) is a highly social species that has been observed to produce a large variety of vocalizations in different situations. Several decades ago, (Kiley, 1972) described ungulates vocalizations and their causations, and she proposed a classification of adult pig vocalizations and highlighted four principal types of calls (grunts, barks, screams and squeals) and their situations of occurrence. She has showed many variations and subcategories, giving an overview of the potential richness of the pig's vocal repertoire. Further ethological studies have later reported the existence of vocal call subcategories such as long grunts (Marchant et al., 2001) or even intermediate call types such as grunt-squeals (Appleby et al., 1999), suggesting that the vocal repertoire of pigs might be more continuous. Recent studies classified vocalizations in ungulate species (Garcia et al., 2016; Tallet et al., 2013) and concluded that a discrete system was adapted, even if there are evidences of gradation between acoustic categories. Beyond these works, a number of studies have been conducted in situations relevant for commercial farming. The vocalizations recorded in these studies are related to husbandry practices like castration (Puppe et al., 2008) or nursing (Algers, 1993), but also to assess and improve the welfare of pigs (da Silva Cordeiro et al., 2013; Fraser, 1975; Jensen & Algers, 1984; Jensen & Redbo, 1987; Manteuffel et al., 2004; Moura et al., 2008; Schön et al., 2004; Weary & Fraser, 1995; Whittemore & Kyriazakis, 2006; Xin et al., 1989). These works have thus improved our understanding of pig vocalizations and how they reflect their mental or physical state, for example hunger, pain, cold or stress in rearing piglets (da Silva Cordeiro et al., 2013).

In minipigs, a study concerning vocal behavior and calls situation of occurrence is still missing. In this study, we aimed to acquire greater knowledge on minipigs vocalizations. We wanted to record as many various calls as possible in a daily housing environment to induce as little stress as possible. We also aim to describe the vocalizations of these animals, in regard to previous knowledge about domestic pigs and wild boars vocal behavior. Such a description was the initial step before studying the cortical bases of vocal production in these animals.

4.1. Method

To record a great number of vocalizations, we placed AudioMoth recording devices in the stabulation pen of two minipigs. We recorded during 14 hours without interfering with the animals typical daily rhythm.

The results of this chapter summarize data from this recording session.

4.1.1. Animals

Animals in this study were two female Aachener minipigs (Carfil Quality) of the same litter called FAJ758 and FIG776. The animals were 13 months old at the recording session time.

4.1.2. Recording Setup

To record the vocalizations of the two minipigs, we used 6 AudioMoth devices (Open Acoustic Devices, 2020) which are small low-cost acoustic loggers. One AudioMoth measures 58 x 48 x 15 mm and is powered by 3 AA batteries. These low-cost audio loggers allow long-time recordings while being inconspicuous, portable and reliable.

We configured the 6 synchronized AudioMoths for 14h of recording per day, from 6am to 1pm for the morning session (AM) and from 1pm to 8pm for the afternoon session (PM). The selected sampling rate was 48kHz and the gain was set to medium (30.6dB). During all this period, animals were placed in two separated stabulations and could see each other through the pens doors. The 6 AudioMoths were placed as pictured in **Figure 18**. We analyzed the data from AudioMoth 1 and 6 (A1 & A6). Due to their spacing, it was possible to assess acoustically which animal vocalized based only on the audio volume. Hence, FAJ758 vocalizations were recorded loudly by A1 and more quietly by A6, and FIG776 vocalization were recorded louder by A6 than by A1. As a consequence, we were able to sort vocalizations by locutor, namely FAJ758 and FIG776.

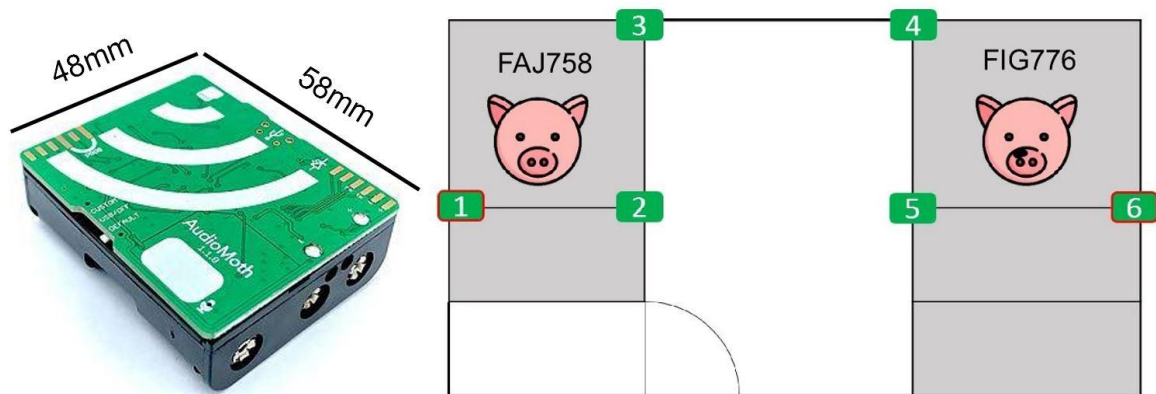


Figure 18. AudioMoth recording session setup. The setup of one recording session allowed the acoustic logging of two separated minipigs FAJ758 and FIG776. The most distant AudioMoths were AudioMoth 1 and AudioMoth 6 (circled in red), vocalizations from the minipig FAJ758 were much more loudly recorded by AudioMoth 1 than by AudioMoth 6 and reciprocally.

4.1.3. Analyzing minipig vocalization

To analyze the minipigs vocalizations, we manually labeled an entire recording session of 14h for both FAJ758 and FIG776 animals. We made a custom script on Spike2 software (CED Corp., Cambridge, UK) to sort vocalizations into different categories of calls. The script detected all sounds rising through a threshold manually placed, then allowed the user to classify it into existing call categories, or new call type. The audio recording could be visualized either in waveforms or in spectrograms, and both A1 and A6 analysis were made simultaneously. As can be seen on **Figure 19**, A1 and A6 waveforms displayed different patterns of sounds depending on the locutor. For example, the second vocalization is recorded more loudly on A1 than on A6 because it is a call of FAJ758, hence produced closer to A1 than A6. The choice of locutor was made essentially by listening to the two audios separately. When in doubt, the acoustic waveforms helped the decision of locutor. When neither of the two technics allowed a decision, the vocalization was noted as 'Doubt' and was not analyzed. The script enabled the creation of new call categories during the analysis.

The spectrogram inspection allowed sorting of vocalizations among other noises. Indeed, the majority of parasitic noises recorded during the day were noises of grinding of teeth of our animals or shaking of the metal feeders. The spectrograms of these noises had a very sharp beginning and a high amplitude, which differed from the vocalizations spectrograms. The classification into call categories was made according to previous studies on ungulates vocalizations mentioned in the introduction.

The further analysis of the calls was done using Matlab software (Natick, Massachusetts: The MathWorks Inc).

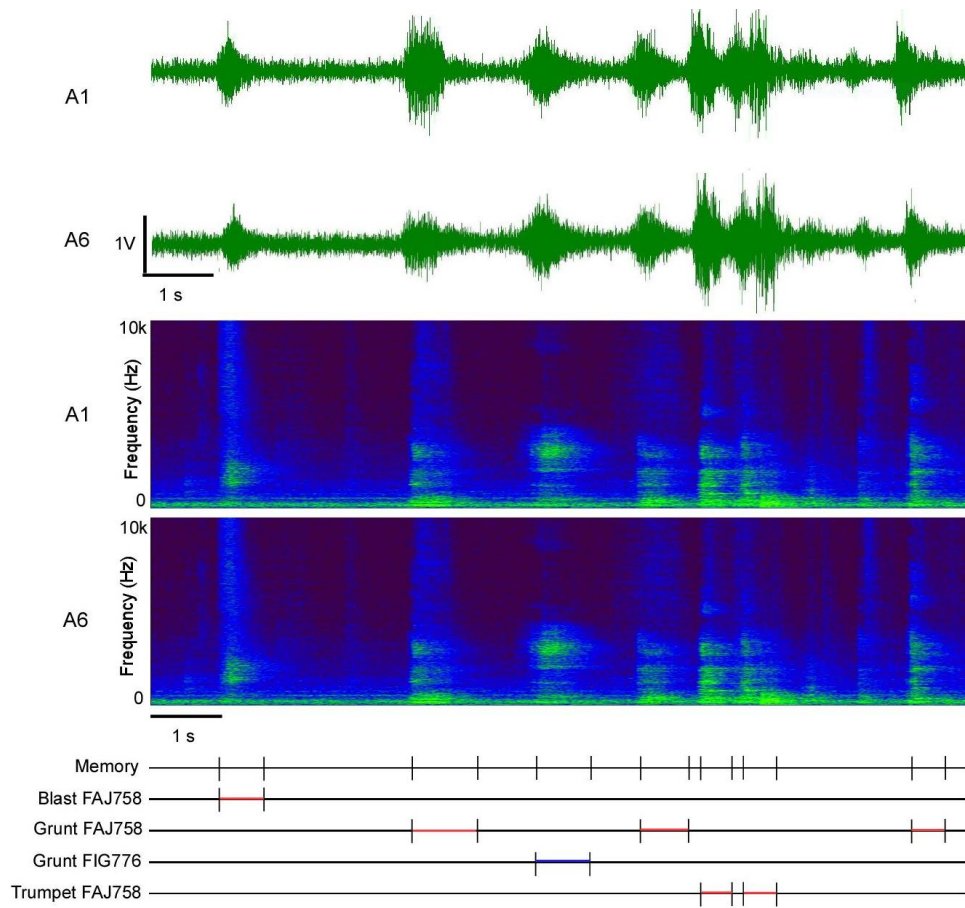


Figure 19. Spike 2 Interface for the classification of vocalizations of minipigs FAJ758 and FIG776. A1 and A6 waveforms were analyzed sequentially. Both visual inspection and hearing allowed the choice of locutor. The spectrograms were performed on Spike 2 with a Hanning window (block size = 4096). Memory ticks were the detection of sounds which were going to be classified after removing all the parasitic noises with spectrogram and hearing inspection. FAJ758 vocalizations are represented in red and FIG776 in blue.

4.2. Results

Totally, we recorded and analyzed 1601 sounds produced for both animals. 1277 vocalizations were split into 6 types of produced calls (Grunt, Blast, Trumpet, Rattle, Grunt Squeal and Bark, see **Figure 20**) with a high acoustic variability. The other 324 sounds were mainly mixed calls and snores which we do not describe here. The vocalizations in which the two animals expressed themselves at the same time (that is to say vocalizing over each other) were annotated as Mixed. The Snores were recorded during the morning of the session, around 6am to 8am.

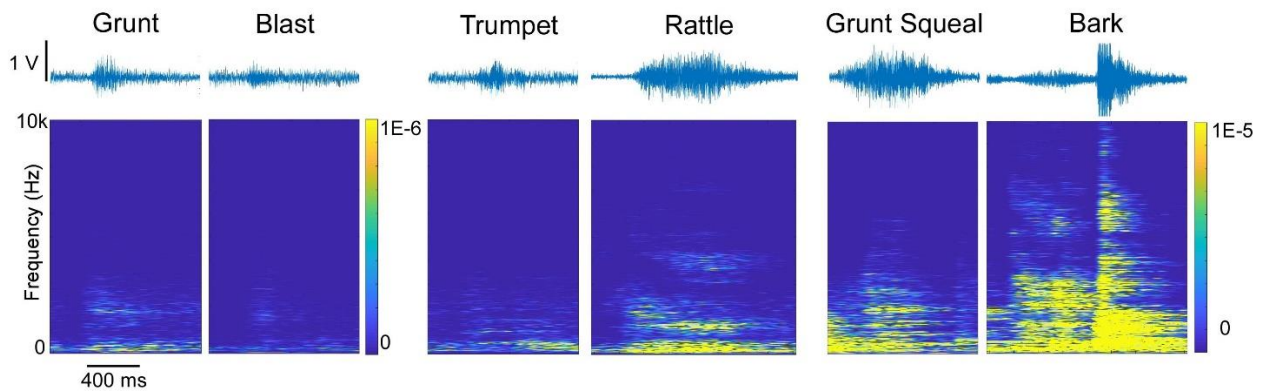


Figure 20. Six types of vocalizations recorded during the session. Top panel : Acoustic waveforms of averaged vocalizations for each recorded call type. Bottom panel : narrow band spectrograms of averaged vocalizations for each recorded call type. The spectrograms were generated in Matlab using the following parameters : 150ms window size, frequency range : 0-10kHz, frequency steps : 300. Grunt and Blast spectrogram scales range from 0 to 1E-6 $\mu\text{V}/\sqrt{\text{Hz}}$. The other vocalizations spectrogram scales range from 0 to 1E-5 $\mu\text{V}/\sqrt{\text{Hz}}$. Temporal scale of 400ms is common to all the panels. Amplitude scale of 1V is common to all the acoustic waveforms.

4.2.1. Grunts (n = 738)

As expected, the most common calls were Grunts (n = 738) and were produced by both FAJ758 and FIG776. On average, Grunts recorded were 607ms long but the histogram of the durations of all the Grunts had a bimodal pattern (see **Figure 21**). This revealed at least two categories of Grunts distinguishable by their durations. Totally, we have distinguished three categories of Grunts described below.

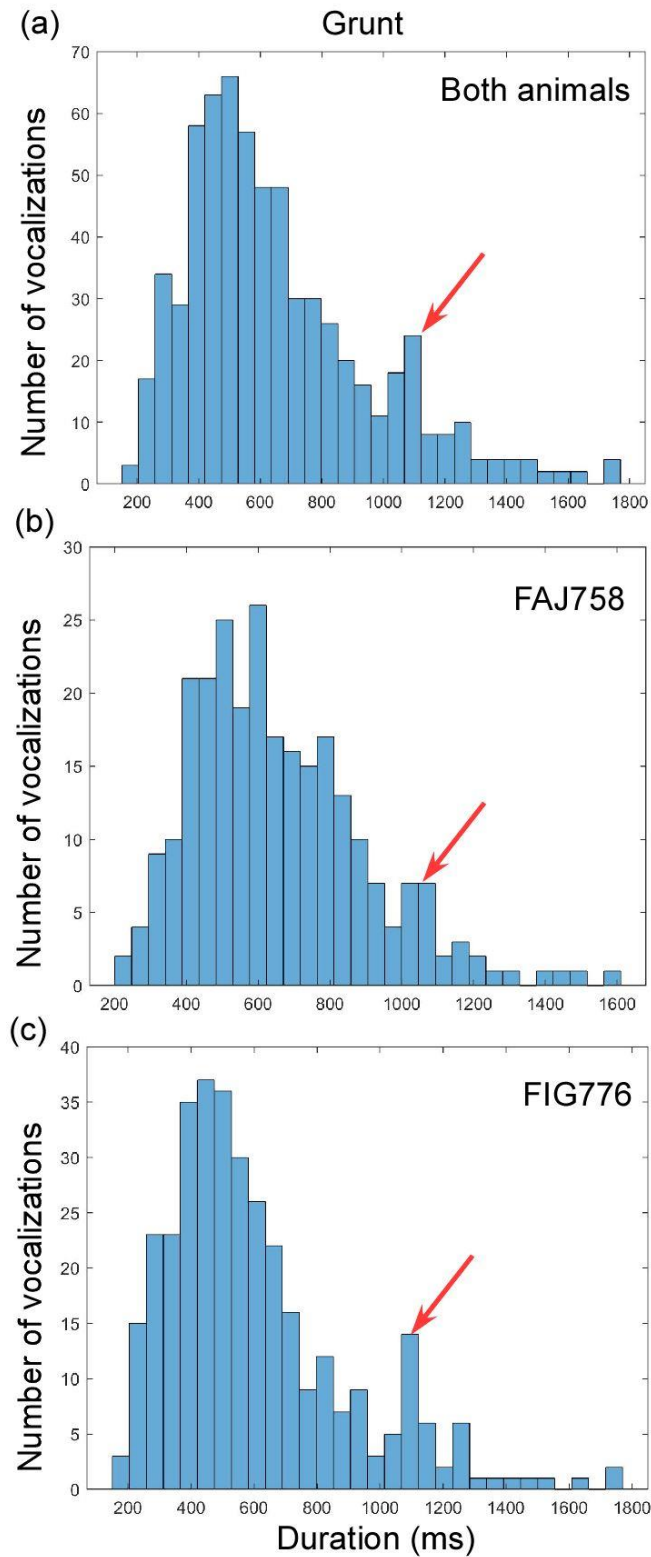


Figure 21. Histogram of the durations of Grunts vocalizations. (a) Histogram of the durations of Grunts for FAJ758 and FIG776. The distribution has a bimodal pattern representing different Grunt types. (b) Histogram of the durations of Grunts for FAJ758. (c) Histogram of the durations of Grunts for FIG776.

4.2.1.1. Common Grunt (n = 591)

Common Grunts lasted an average of 549ms and were the most common of all types of Grunts. We recorded Common Grunts throughout the day, in various occurrence situations such as rooting, playing or waiting for food. Samples of Common Grunts and averaged Common Grunts for animals FAJ758 and FIG776 are shown in **Figure 22**. The lowest frequency peak of Common Grunts produced by FAJ758 is 99Hz (± 12 Hz), and by FIG776 of 125Hz (± 19 Hz). Common Grunts were produced by both FAJ758 and FIG776 and the intervals between two Common Grunts were short (see **Figure 23** left and center panel). The durations of Common Grunts were highly variable (from 200 to 1200ms see **Figure 23** right panel). We sorted vocalizations mainly using auditory waveforms, without taking care of the duration of the call, which could explain the fact that some Common Grunts had a duration that could make them Long Grunts.

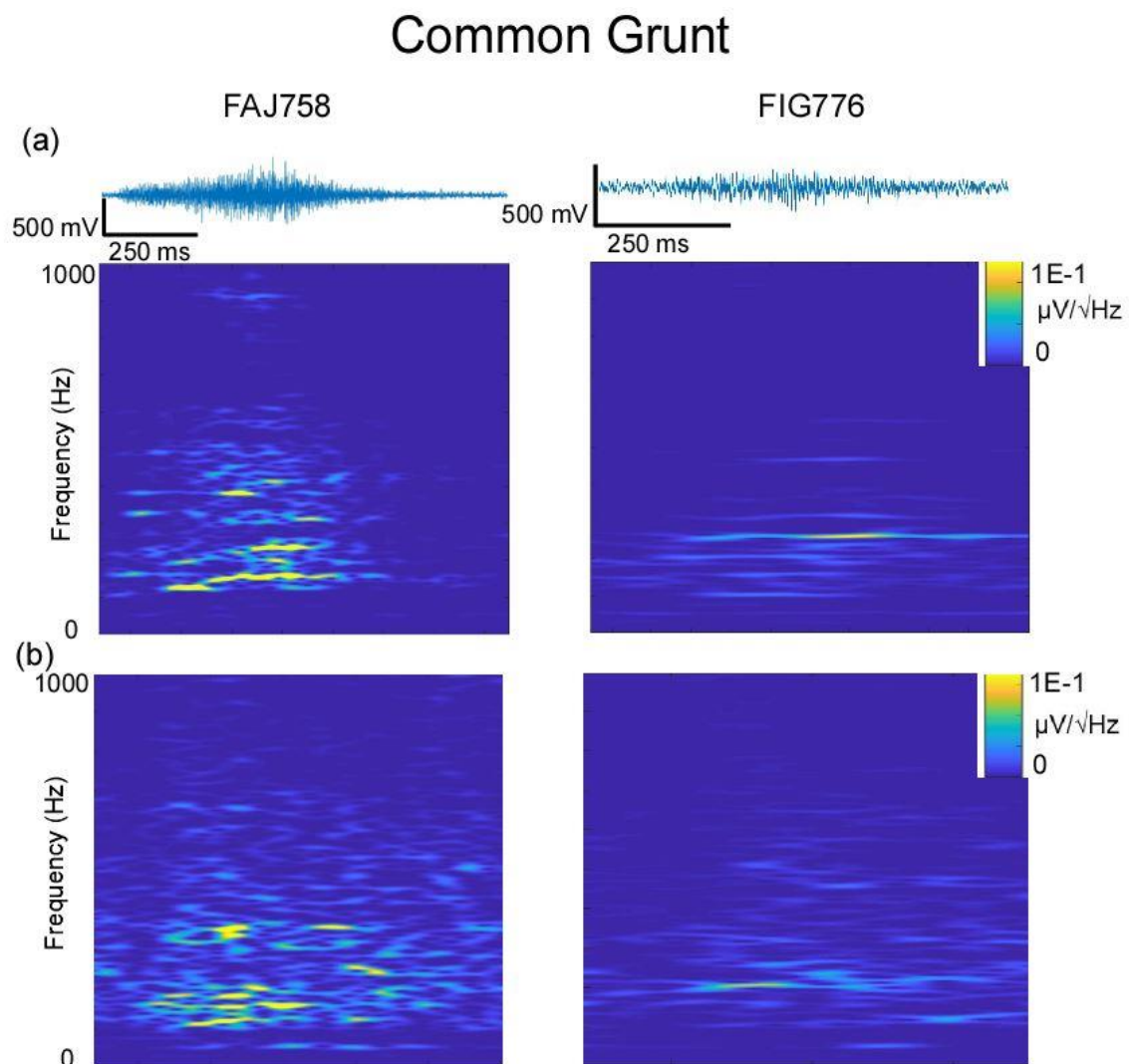


Figure 22. Common Grunt. (a) Acoustic waveforms and narrow band spectrograms of a sample of Common Grunt for FAJ758 and FIG776. (b) narrow band spectrograms of the averaged Common Grunts for FAJ758 and FIG776. The spectrograms were generated in Matlab using the following parameters : 150ms window size, frequency range : 0-1000Hz, frequency steps : 300.

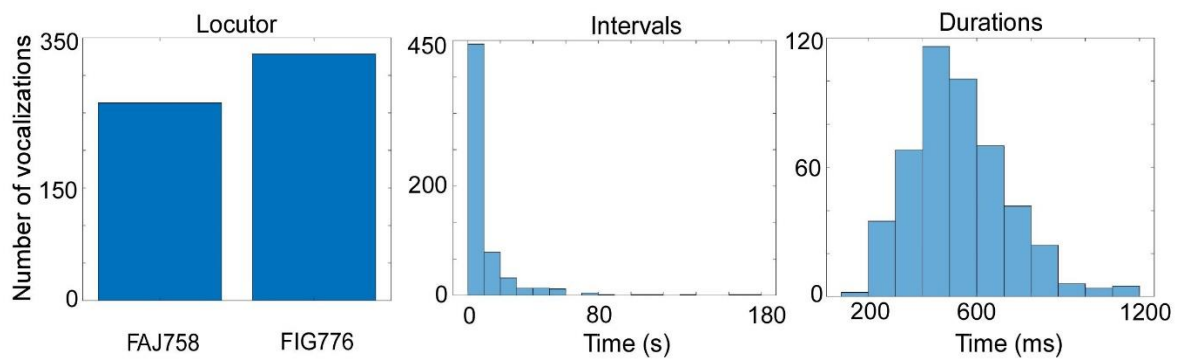


Figure 23. Common Grunt characterization. Left panel : number of Common Grunts produced by FAJ758 and FIG776. Center panel : histogram of the intervals between two Common Grunts. Right panel : histogram of durations for Common Grunts.

4.2.1.2. Long Grunt ($n = 93$)

Long Grunts resembled Common Grunts acoustically but could be differentiated by their much longer duration. Indeed, the average duration of a Long Grunt was 1203ms (see durations on **Figure 25** right panel) , which was more than double that of a Common Grunt (average duration: 549ms). We recorded Long Grunts in the middle of the morning, one hour before the food was distributed to the animals. The Long Grunts were often followed by periods of very loud noises corresponding to demonstrations of impatience of the animals (shaking the feeders, biting the bars of the stall, etc). These vocalizations were produced by FAJ758 and FIG776 (see **Figure 25** left panel) and seemed to indicate agitation in anticipation of food distribution. The lowest frequency peak of Long Grunts produced by FAJ758 was 102Hz (± 10 Hz), and by FIG776 of 125Hz (± 8 Hz).

Long Grunt

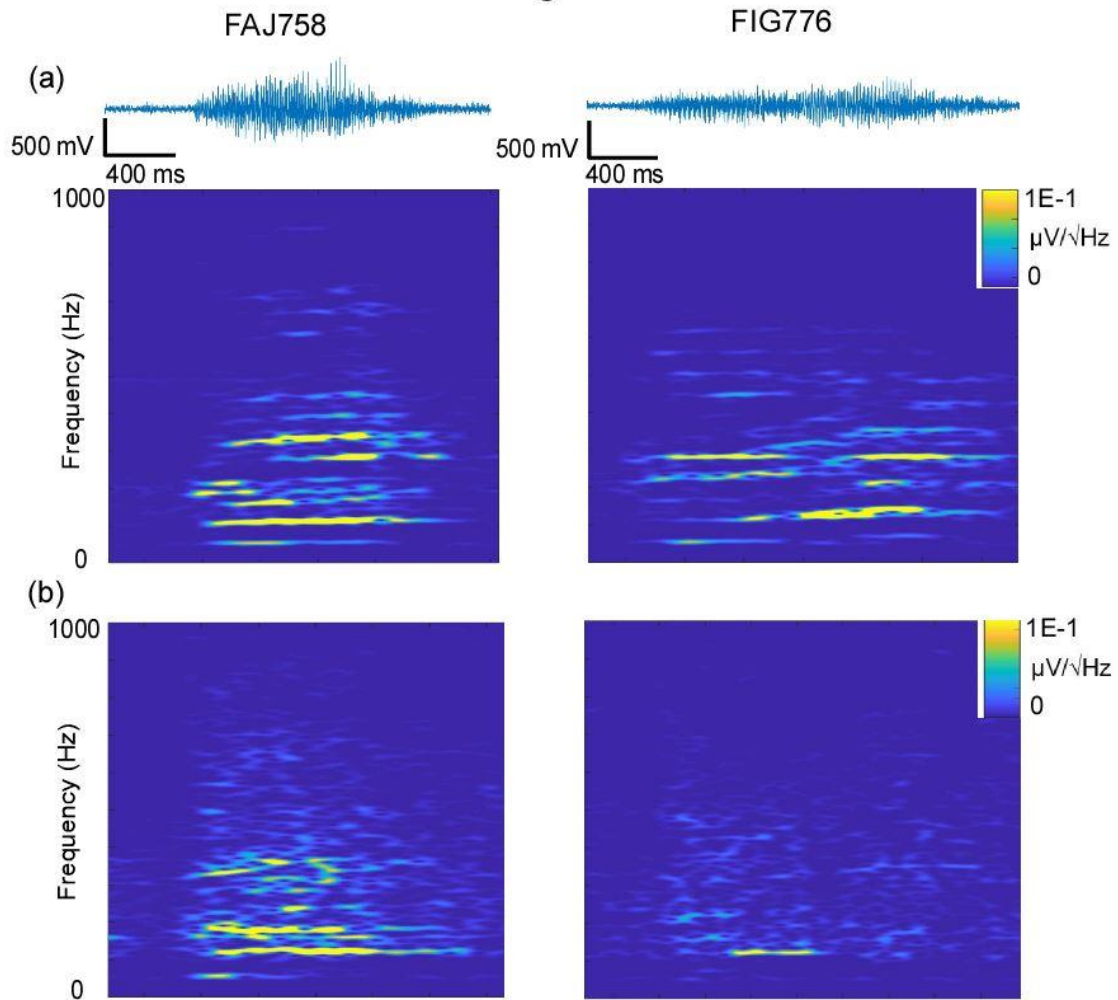


Figure 24. Long Grunt. (a) Acoustic waveforms and narrow band spectrograms of a sample of Long Grunt for FAJ758 and FIG776. (b) Narrow band spectrograms of the averaged Long Grunts for FAJ758 and FIG776. The spectrograms were generated in Matlab using the following parameters : 150ms window size, frequency range : 0-1000Hz, frequency steps : 300.

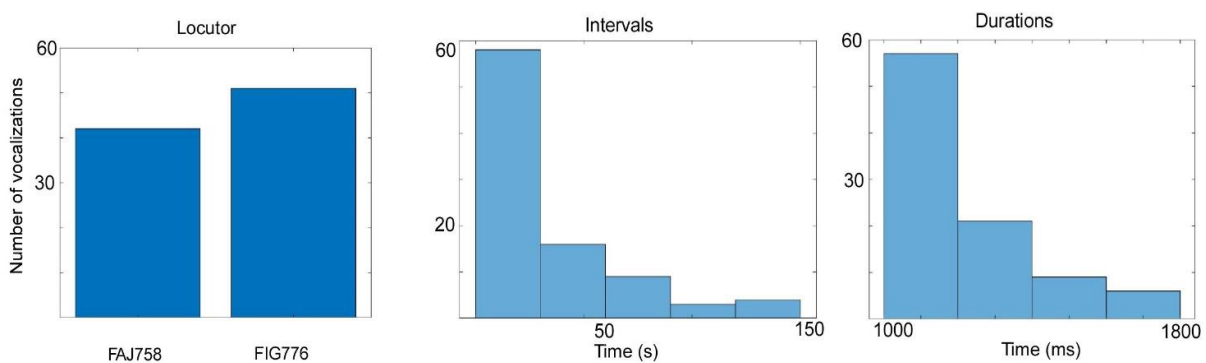


Figure 25. Long Grunts characterization. Left panel : Number of Long Grunts produced by FAJ758 and FIG776. Center panel : histogram of the intervals between two Long Grunts. Right panel : histogram of durations for Long Grunts

4.2.1.3. Repeated Common Grunt ($n = 54$ individual grunts)

Repeated Common Grunts varied very little in structure compared to Common Grunts. Their average duration was 500ms and they were spaced on average about 300ms apart (see the time intervals within a Repeated Grunts sequence in **Figure 28**). Repeated Grunts sequences were usually composed of 3 calls, up to 5 calls in a row. FIG776 appeared to produce more Repeated Grunts vocalizations than FAJ758 (see **Figure 27** left panel). The lowest frequency peak of Repeated Grunts produced by FAJ758 was 98Hz (± 13 Hz), and by FIG776 of 103Hz (± 17 Hz). The majority of Repeated Grunts were recorded in the morning, during the two hours prior to food distribution. The time intervals between two Repeated Grunts (see **Figure 27** center panel) takes into account the intervals between two sequences, which explains the long intervals.

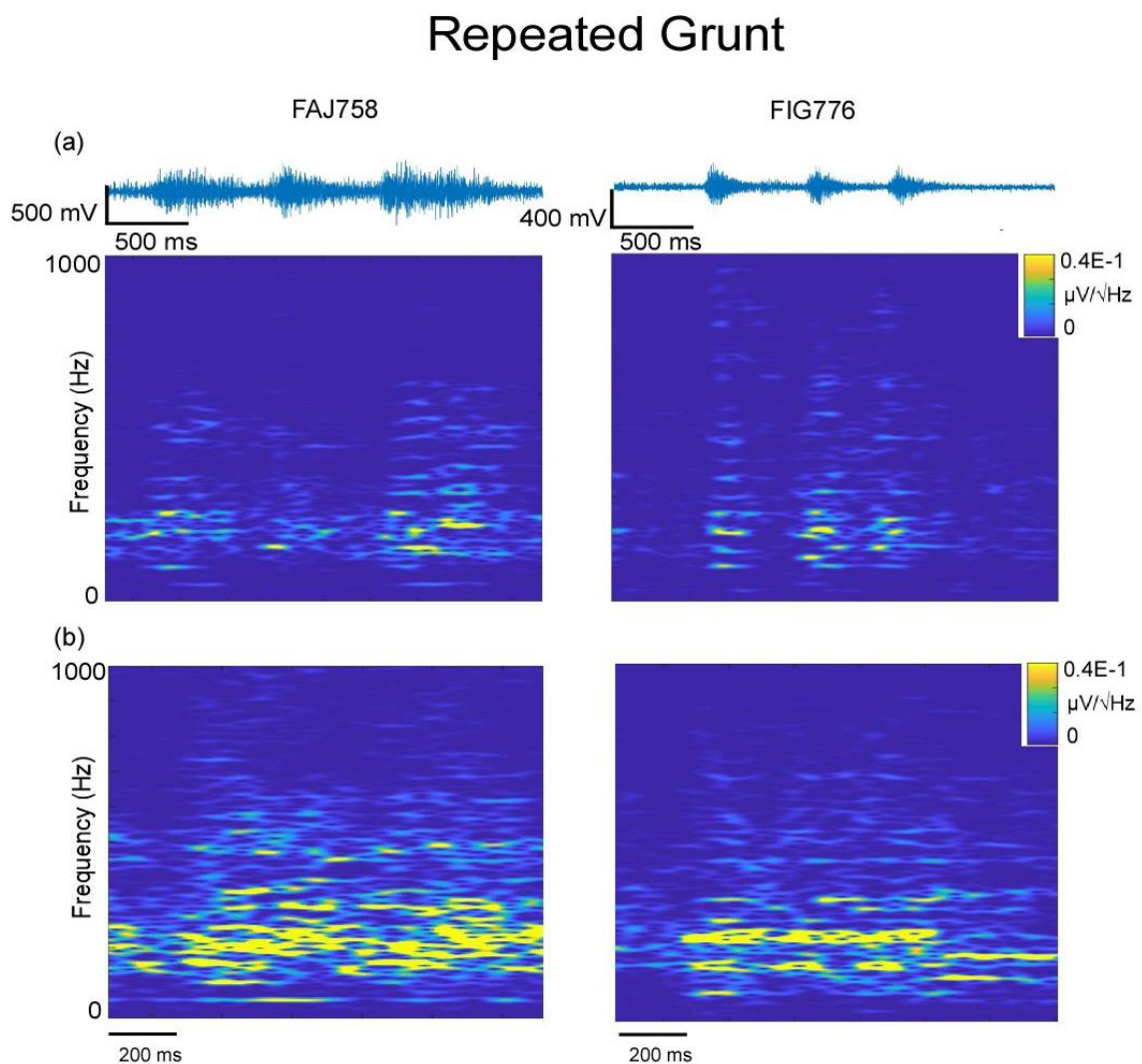


Figure 26. Repeated Grunt. (a) Acoustic waveforms and narrow band spectrograms of 3 samples of Repeated Grunts for FAJ758 and FIG776. (b) Narrow band spectrograms of the averaged Repeated Grunts for FAJ758 and FIG776. The spectrograms were generated in Matlab using the following parameters : 150ms window size, frequency range : 0-1000Hz, frequency steps : 300.

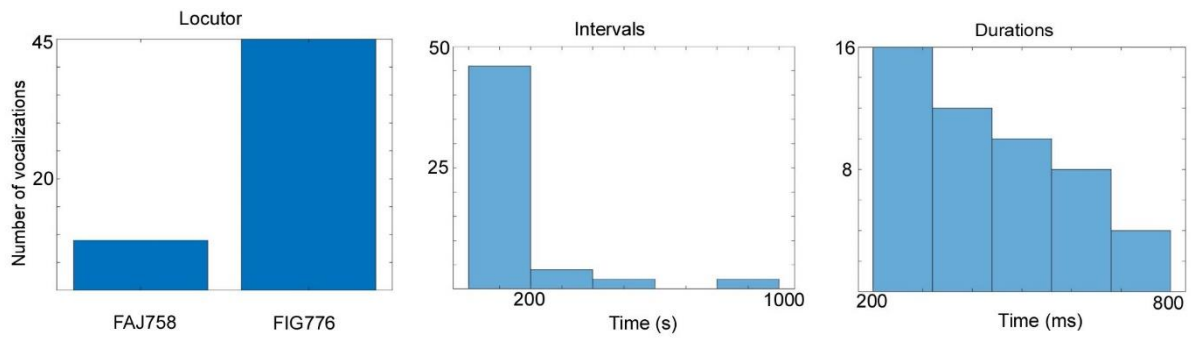


Figure 27. Repeated Grunt characterization. Left panel : Number of Repeated Grunts produced by FAJ758 and FIG776. Center panel : histogram of the intervals between two Repeated Grunts. Right panel : histogram of durations for Repeated Grunts.

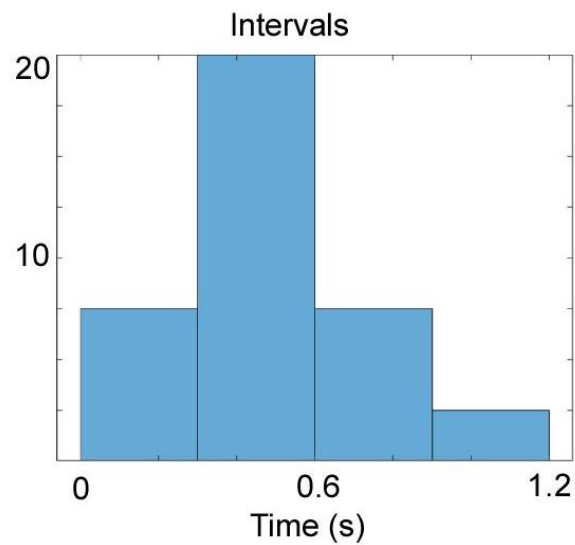


Figure 28. Time intervals within a Repeated Grunts sequence. The average intervals between two repeated grunts within a sequence was 300ms.

4.2.2. Trumpet (n=96)

We recorded 96 Trumpets, mostly produced by FIG776 (see **Figure 30** left panel). These very special calls resembled a rather loud trumpet sound and lasted on average 885ms. We recorded these vocalizations only in the morning, in the hour before the food distribution (like the Long Grunts). The Trumpets of FIG776 had sometimes been produced repeatedly and may testify to a great impatience in the animal because these calls were also followed by a consequent agitation (repeated displacements, bumps on the bars of the pen and the feeder, etc). The repeated series of Trumpets had three to five vocalizations in a row, separated by less than 500ms between them. FAJ758 Trumpet vocalizations had a lowest frequency peak of 132Hz (± 8 Hz), while that of FIG776 was 144Hz (± 11 Hz).

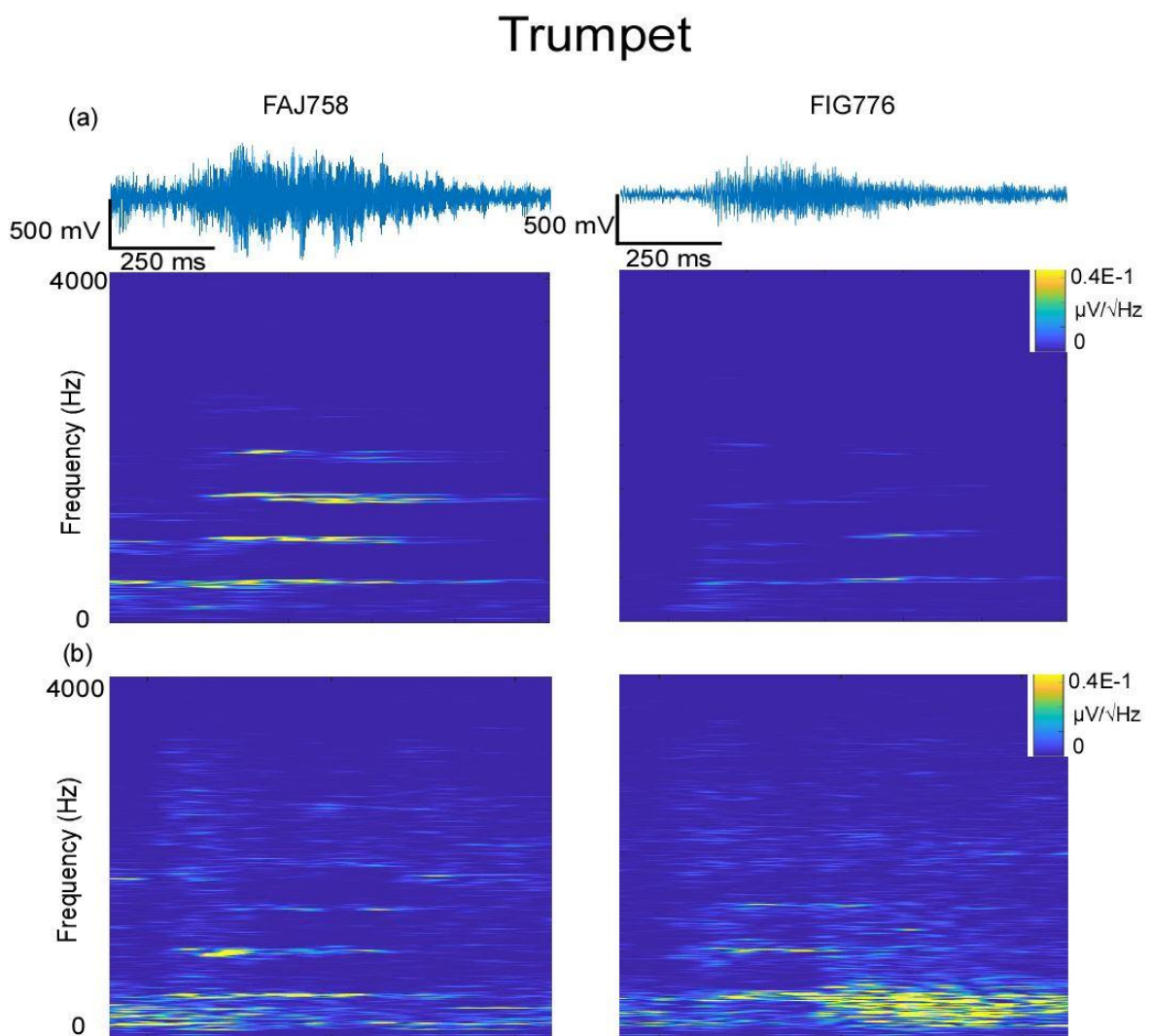


Figure 29. Trumpet. (a) Acoustic waveforms and narrow band spectrograms of a sample of Trumpet for FAJ758 and FIG776. (b) Narrow band spectrograms of the averaged Trumpets for FAJ758 and FIG776. The spectrograms were generated in Matlab using the following parameters : 150ms window size, frequency range : 0-4000Hz, frequency steps : 300.

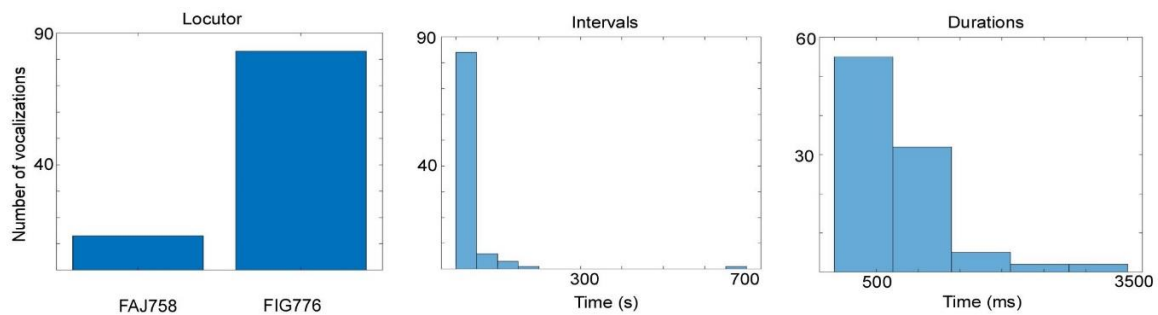


Figure 30. Trumpet characterization. Left panel : Number of Trumpets produced by FAJ758 and FIG776. Center panel : histogram of the intervals between two Trumpets. Right panel : histogram of durations for Trumpets.

4.2.3. Rattle (n = 16)

In the same way as the Trumpets and Long Grunts, we only recorded Rattles during the morning session, in the hour before the food distribution. Rattles were very long grunts with an average duration of 1.3sec (see **Figure 32** left panel). They differed acoustically from Long Grunts by the second half of the signal which was much guttural than that of a Long Grunt. The Rattle was a lower frequency call than the Long Grunt, the lowest frequency peak of FAJ758 for this type of vocalization was 68Hz (± 4 Hz) and for FIG776 of 76Hz (± 8 Hz). Contrary to what was recorded for Long Grunt or Trumpet, the Rattles were not followed by demonstrations of impatience but rather by periods of chewing or Common Grunts. Some Rattles were also followed by long periods of silence during which we could hear the zootechnicians working in the corridor. For this reason, we believed that Rattles could be akin to calling vocalizations to signify the will to be fed, and that chewing may be triggered by the salivary reflex.

Rattle

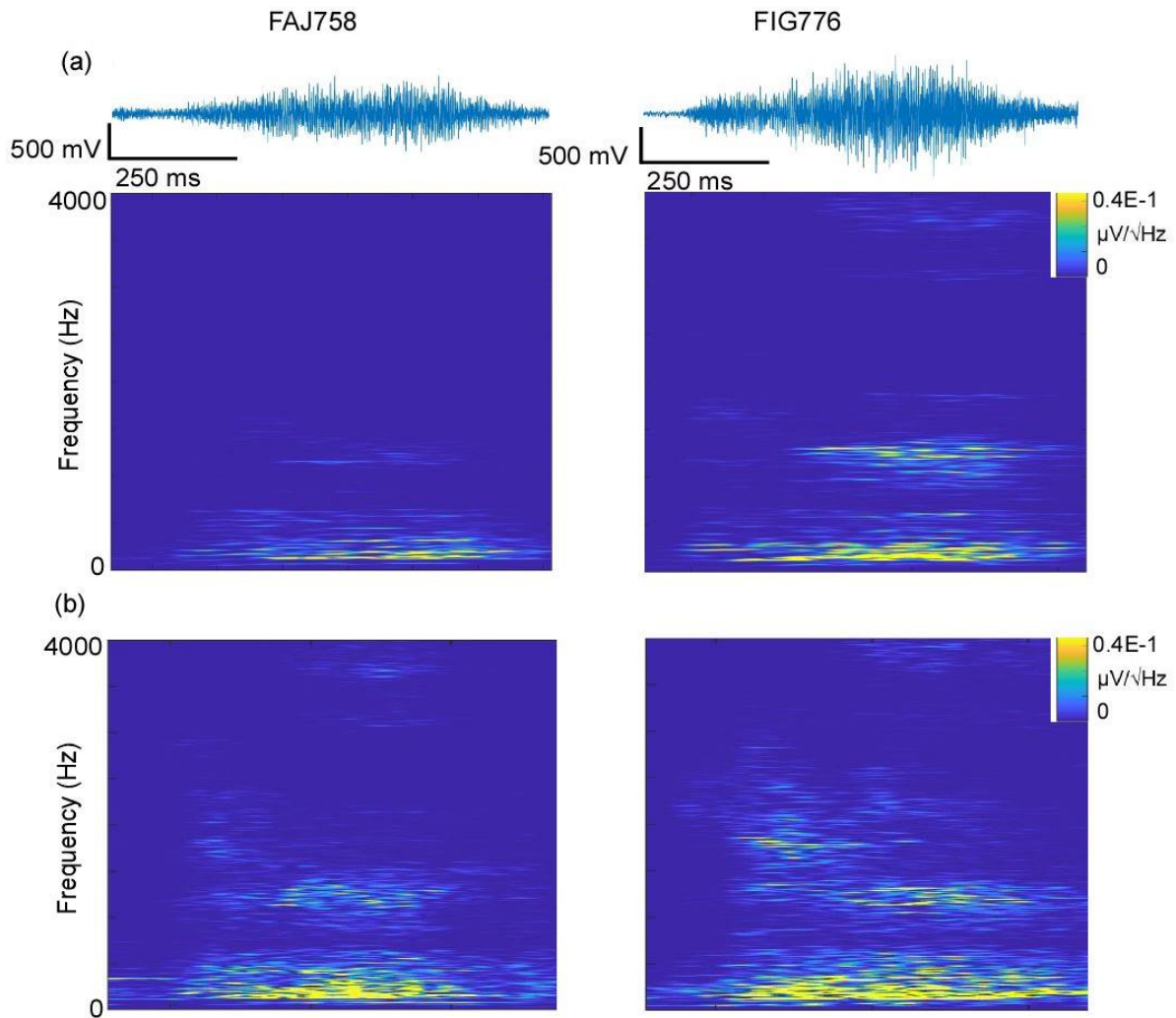


Figure 31. Rattle. (a) Acoustic waveforms and narrow band spectrograms of a sample of Rattle for FAJ758 and FIG776. (b) Narrow band spectrograms of the averaged Rattles for FAJ758 and FIG776. The spectrograms were generated in Matlab using the following parameters : 150ms window size, frequency range : 0-4000Hz, frequency steps : 300.

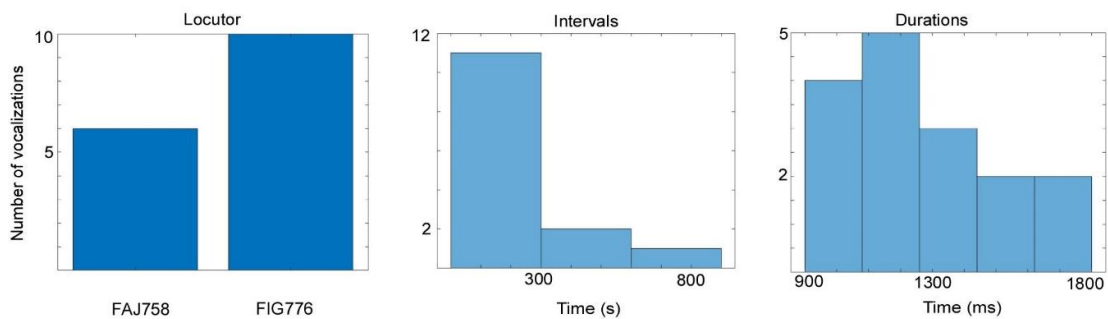


Figure 32. Rattle characterization. Left panel : Number of Rattles produced by FAJ758 and FIG776. Center panel : histogram of the intervals between two Rattles. Right panel : histogram of durations for Rattles.

4.2.4. Grunt-Squeal (n = 5)

We recorded very few Grunt Squeals (n =5), produced exclusively by FIG776 (see **Figure 34** left panel). These Grunt Squeals were preceded and followed by Common Grunts and often accompanied by sounds corresponding to rooting and foraging activities around the sleeping basket. The Grunt Squeals were recorded in the early morning, before the other vocalizations testifying the impatience of the animals (Long Grunts, Rattle and Trumpet). The lowest frequency peak of the FIG776 Grunt Squeal was 124Hz (± 22 Hz).

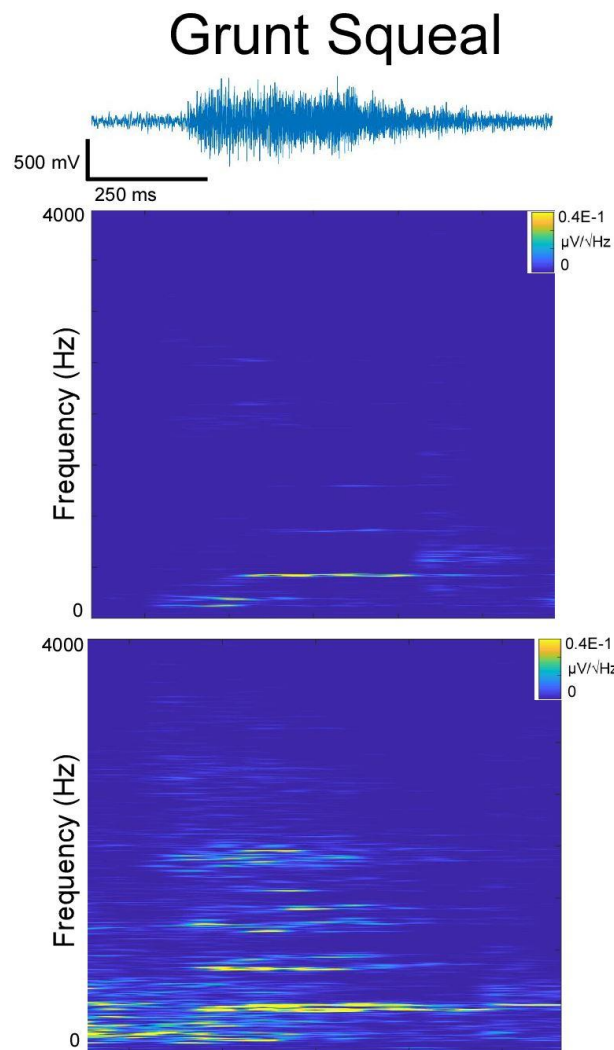


Figure 33. Grunt Squeal. Top panel : acoustic waveform of a sample of Grunt Squeal. Center panel : narrow band spectrogram of a sample of Grunt Squeal. Bottom panel : narrow band spectrogram of the averaged Grunt Squeals. The spectrogram were generated in Matlab using the following parameters : 150ms window size, frequency range : 0-4000Hz, frequency steps : 300.

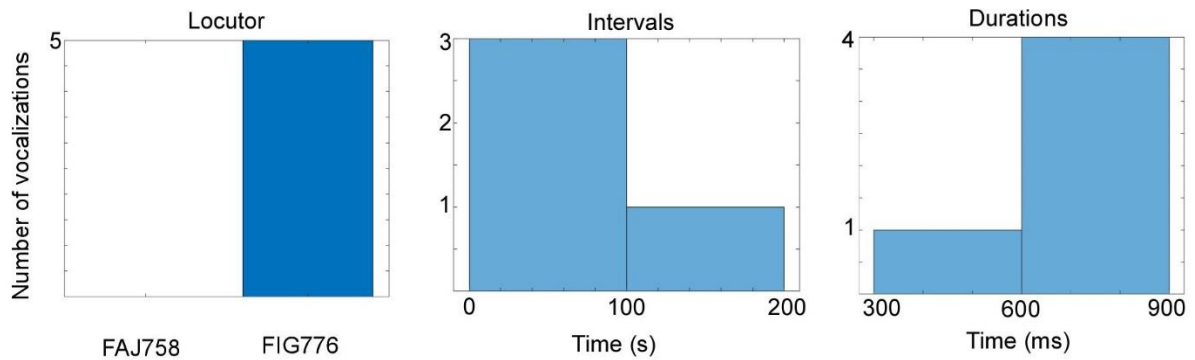


Figure 34. Grunt Squeal characterization. Left panel : Number of Grunt Squeals produced by FAJ758 and FIG776. Center panel : histogram of the intervals between two Grunt Squeals. Right panel : histogram of durations for Grunt Squeals.

4.2.5. Bark (n = 1)

We only recorded one Bark produced by FAJ758 (see **Figure 35** right panel). We could not assess acoustically the cause of this vocalization which in literature is synonymous with a state of surprise. It was directly preceded by a Grunt of FIG758 (see **Figure 35** orange rectangle) and followed 2 seconds later by a Trumpet of FIG758. The Bark had a fairly high amplitude of the order of 1V. The lowest frequency peak of the Bark of FAJ758 was 193Hz.

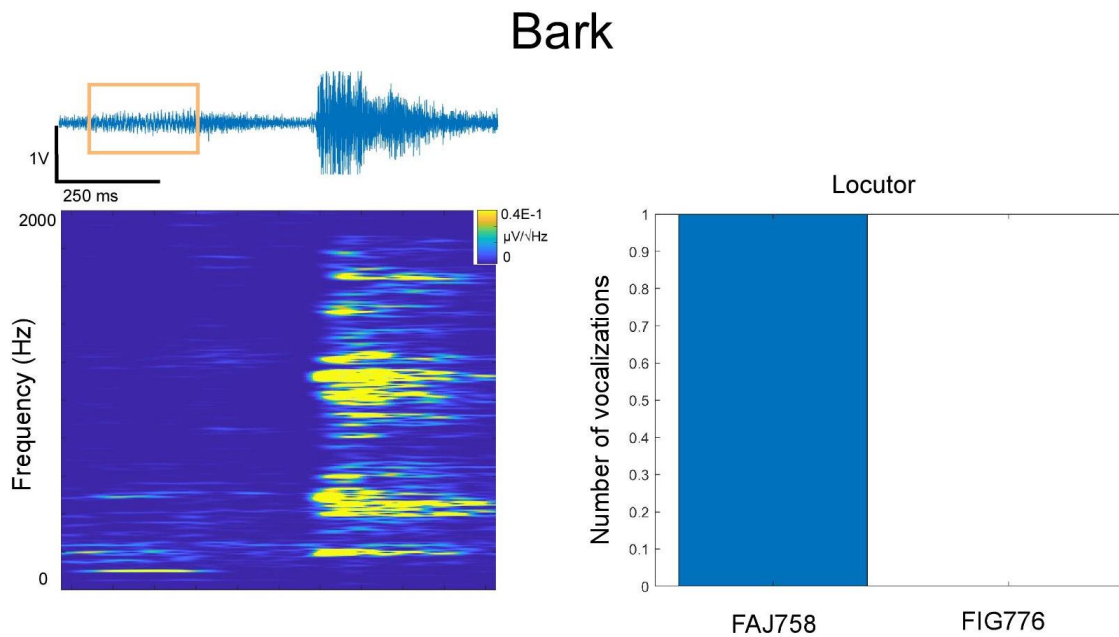


Figure 35. Bark. Left panel : narrow band spectrogram and acoustic waveform of the call Bark. The orange rectangle represent a Grunt produced by FIG776 just before the Bark of FAJ758. The spectrogram was generated in Matlab using the following parameters : 150ms window size, frequency range : 0-2000Hz, frequency steps : 300. Right panel : Number of Barks produced by FAJ758 and FIG776.

4.2.6. Blast (n = 421)

The Blast was a sound produced by the expulsion of air through the nose of the animal. Although not described in the literature as a vocalization, we had taken the step of treating it as such in view of the different production conditions that were its own. The Blast looked acoustically like the sound a human would produce by blowing heavily through the nose. These vocalizations were quite tenuous and we recorded very few in FIG776 (see **Figure 37** left panel). Their amplitude (about 50mV, see **Figure 36**) was on average ten times lesser than that of a Common Grunt. The duration of the Blasts was very variable, with an average of 500ms and sometimes almost a second (1.057sec for the longest Blast). Like the Grunts, some Blast were produced in a repeated way, with series of 3 to 6 Blasts. Within a series of repeated Blasts, the duration of the calls was shorter than that of a classic Blast (on average 340ms). The longest Blasts (those with a duration of more than 800ms) appeared to be accompanied by Common Grunts. Blasts were recorded throughout the day and were often accompanied by movements in the pen and chewing, even in the absence of food in the pen.

Blast

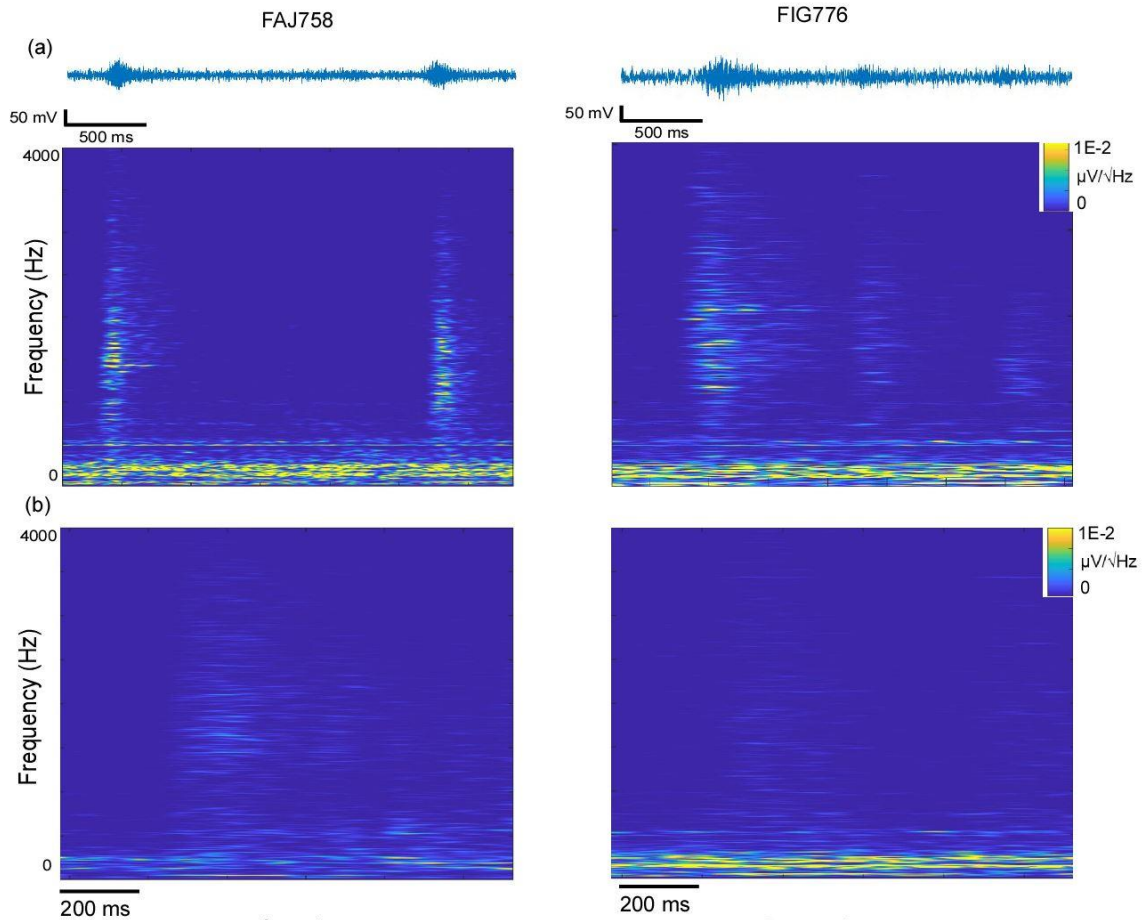


Figure 36. Blast. (a) Acoustic waveforms and narrow band spectrograms of 2 and 3 samples of Blasts for FAJ758 and FIG776 respectively. (b) Narrow band spectrograms of the averaged Blasts for FAJ758 and FIG776. The spectrograms were generated in Matlab using the following parameters : 150ms window size, frequency range : 0-4000Hz, frequency steps : 300.

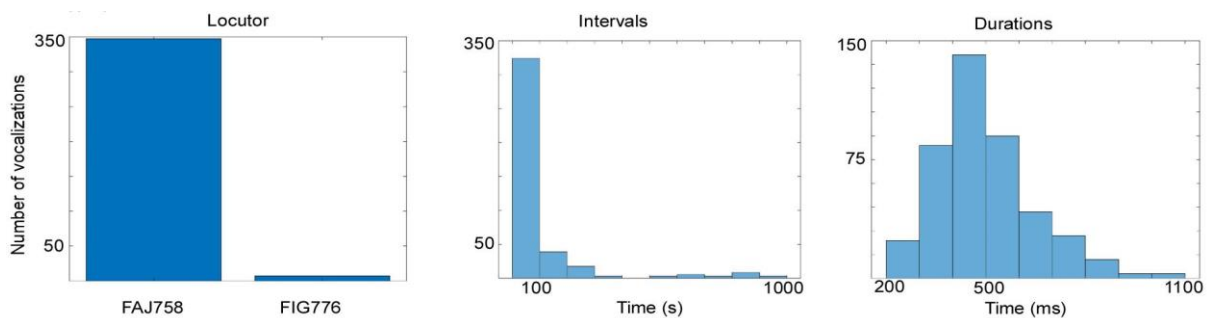


Figure 37. Blast characterization. Left panel : Number of Blasts produced by FAJ758 and FIG776. Center panel : histogram of the intervals between two Blasts. Right panel : histogram of durations for Blasts.

4.2.7. Vocal behavior of minipigs

During these 14 hours of recording, we noticed that the sequence of the morning was the one that contained the most different vocalizations. In the morning 949 vocalizations were recorded against 652 in the afternoon. Moreover, some vocalizations were not present at all in the afternoon. This was the case with Rattle, Grunt Squeal and Trumpet. Rattle and Trumpet vocalizations seemed very related to the expectation of food distribution, it may be normal that they were not present in the afternoon since there was no ration at that time. In **Figure 38**, we presented the percentages of vocalizations produced between morning and afternoon. As can be seen, only 2 types of vocalizations were recorded in the afternoon (PM) while 6 types of vocalizations were recorded in the morning (AM).

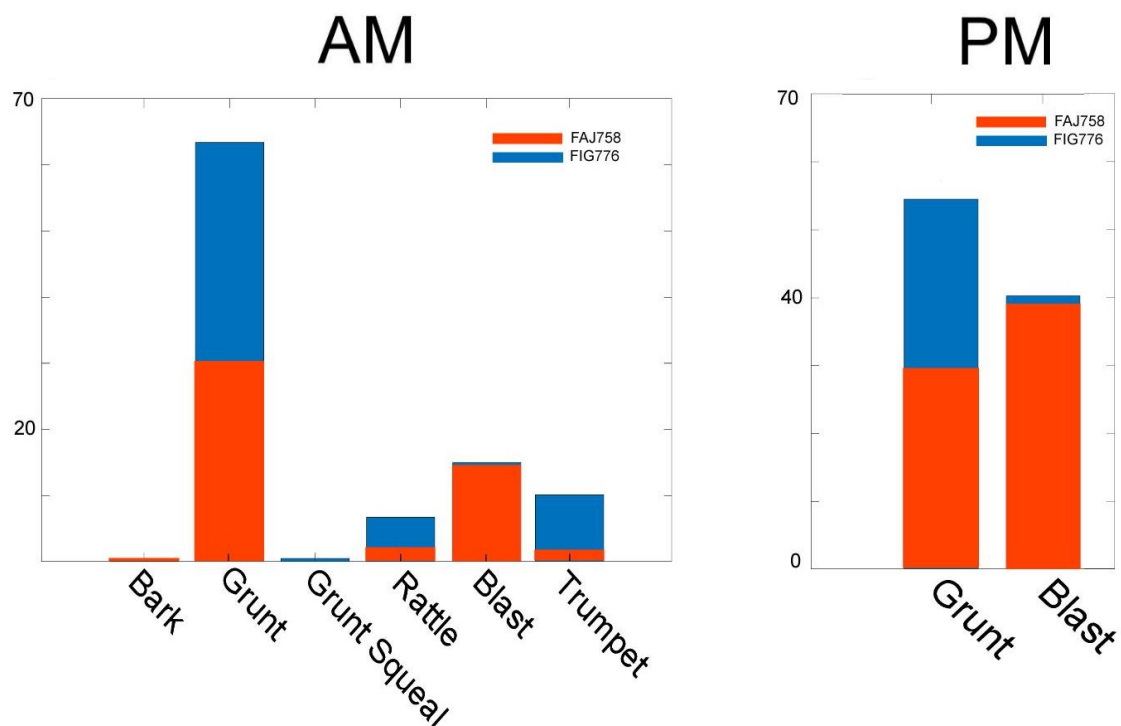


Figure 38. Proportion of vocalizations produced during the morning (AM) and the afternoon (PM). The six types of vocalizations were recorded during the morning but only two types were recorded on the afternoon. FAJ758 proportion of vocalizations are displayed in red and FIG776 in blue.

In addition, the number of some vocalizations recorded in the morning seemed to form a peak in the hours before food distribution. In **Figure 39**, the number of Grunts, Trumpets and Rattle increased before 9:40 (the time at which the daily ration was distributed, symbolized by the vertical red bar). After this moment, vocalizations became rarer and were of type Grunt and Blast, like what was recorded in the afternoon. It seemed therefore that the vocalizations Trumpets, Rattle and some Grunts were strongly linked to the emotion provided by the expectation of the daily ration. Blasts, on the other hand, did not have the same pattern of food-related production, and were produced throughout the day. Animals stopped producing them when they started to vocalize Trumpets or Rattles.

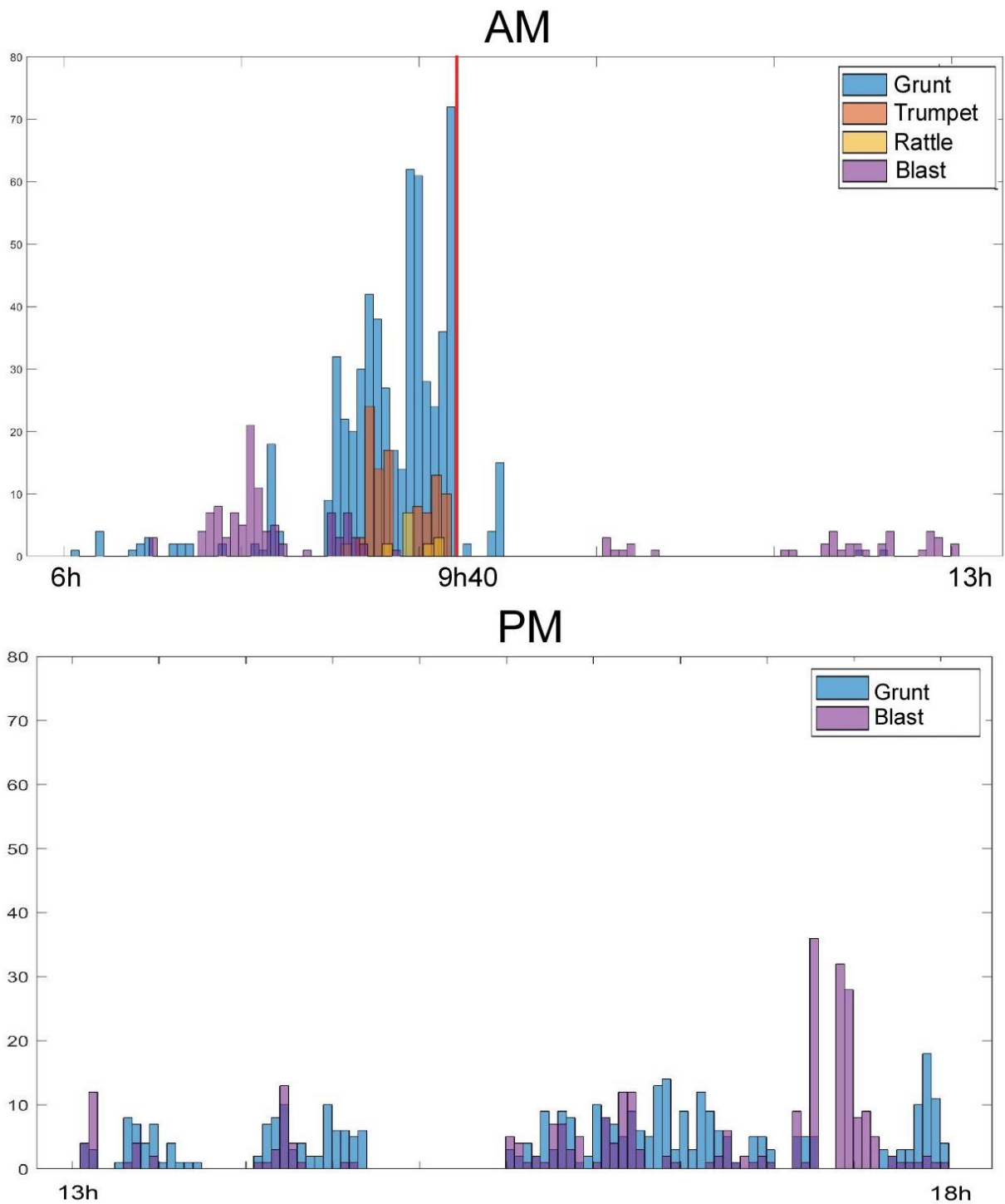


Figure 39. Histogram of vocalizations during all the day. Top panel : histogram of vocalizations during the morning (AM). Four types of vocalizations were represented : Grunts in blue (regardless of Grunt type), Trumpets in orange, Rattles in yellow and Blasts in purple. The red vertical bar corresponds to the time of distribution of the food ration (9h40 that day). Bottom panel : histogram of vocalizations during the afternoon (PM). The two types of

vocalizations represented are the only two recorded during the afternoon : Grunts in blue (regardless of Grunt type) and Blasts in purple.

Furthermore, we found that FAJ758 and FIG776 seemed to vocalize alternately. This ability of turn-taking in vocal expression symbolize social interaction. We annotated the vocalizations in which the two animals expressed themselves at the same time (that is to say vocalizing over each other) as Mixed vocalizations. The proportion of Mixed vocalizations was much lower than the proportion of separate vocalizations of FAJ785 and FIG776 (7% of Mixed versus 93% of disjointed vocalizations, see **Figure 40**)

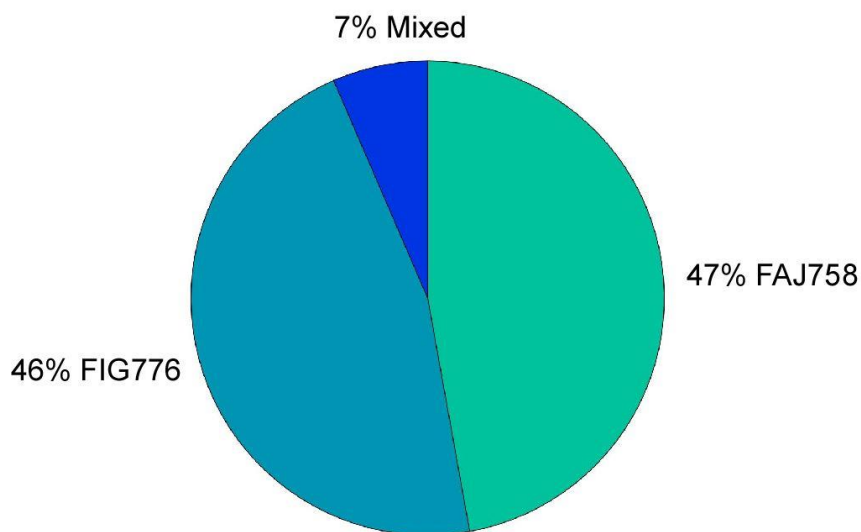


Figure 40. Pie chart of the proportion of Mixed calls (two locutors vocalizing at the same time) relatively to FAJ758 and FIG776 vocalizations. FAJ758 calls represented 47% of all vocalizations and FIG776 46%. Mixed calls accounted for 7% of the total recording.

In **Figure 41**, independently from the speaker, it appeared that Grunts were preceded by Grunts in 82.7% of cases, Blasts are preceded by Blasts in 78.17% of cases and Trumpets are preceded by Trumpets in 39.58% of cases. This result is influenced by the high number of Grunts compared to other calls, but also reveals patterns of calls production. Rattles, the vocalizations that seemed related to impatience for food distribution, are often preceded by Trumpets, also apparently related to anticipation. Trumpets appeared to be produced in sequences in 39.58% of cases, which did not necessarily mean that they were produced in a Repeated pattern, since animals could have alternated Trumpets alternately.

Previous Vocalization	Grunt	82.7	100	62.5	21.83	60.42
	Grunt Squeal	0.83				
	Rattle	2.33		12.5		
	Blast	4.99			78.17	
	Trumpet	8.99		25		39.58
		Grunt	Grunt Squeal	Rattle	Blast	Trumpet
		Vocalization				

Figure 41. General pattern of answers between one vocalization and the previous vocalization for both FAJ758 and FIG776. Blue rectangles represent percentages of times the current vocalization is preceded by the same type of vocalization (Grunt preceded by Grunt, Rattle preceded by Rattle, etc...). Light red rectangles represent percentages of times the current vocalization is preceded by another type of vocalization (Grunt preceded by Blast, Grunt preceded by Trumpet, etc...)

4.3. Discussion and perspectives

The vocalizations presented here were recorded from two minipigs FAJ758 and FIG776 separated in two pens. The audio recordings were performed with AudioMoth devices distributed in the stabulation pens.

We recorded 1277 vocalizations over a 14 hours session and sorted them into 6 call categories. The main characteristics of the 6 call types are shown below. Red values represent FAJ758 and blue values are those of FIG776. Percentages indicates the proportion of the call type in the whole recording session. Blank squares (as for example in Grunt Squeal Locutors) indicate that there was no vocalization of this type for the corresponding animal.

	Grunt	Trumpet	Rattle	Grunt Squeal	Bark	Blast
Number	738	96	16	5	1	421
Pitch	99Hz±12	132Hz±8	68Hz±4		193Hz	
	125Hz±19	144Hz±11	76Hz±8	124Hz±22		
Durations	607ms	885ms	1300ms	793ms	657ms	500ms
Percentages	63%	10.12%	1.68%	0.73%	0.1%	15%
	50.4%	13.5%	37.5%		100%	97.9%
Locutors						
	49.6%	86.5%	62.5%	100%		2.1%

Table 4. Summary table of the types of vocalizations recorded with their principal characteristics.

In order to record spontaneous minipig vocalizations, we chose not to intervene with our animals during the entire recording period. Thus, the vocalizations described and accounted for in the result part did not claim to account for the totality of the vocal repertoire of these animals. Some vocalizations of domestic pigs or wild boar described in the literature (Briefer et al., 2019; Garcia et al., 2016; Kiley, 1972; Tallet et al., 2013) such as Scream were not described nor recorded here. The scope of our study was intended to be descriptive and exploratory with regard to minipigs vocal utterances, with the aim of making simultaneous recordings of vocalizations and cortical activities.

We relied on audio cues and visual inspection of spectrograms to classify calls, which may induce errors as well in the classification itself but also in the locutor assessment. We did not assign call types based on the context but analyzed it afterwards to better understand the potential meaning of calls. Moreover, some of the call types were produced by a single locutor or only produced a couple of times. Generalizations to a more global minipig repertoire might be questionable.

However, the preliminary results summarized in this chapter allowed us to perceive globally the vocal behaviour of our animals. Other recording sessions on FAJ758 and FIG776 were performed, totalizing 4 days of 14h of vocalizations each. Classification and analysis of these 3 other recording sessions have to be completed to learn more about the different vocalizations of minipigs. In the long term, annotated data could allow machine learning algorithms to automatically sort these vocalizations by type and/or by speaker.

Moreover, in order to record vocalizations during social interactions in minipigs, we performed 7 days of recording in 5 other minipigs (aged from 3 months old to 13 months old) housed in the same pen. Analyzing these sessions may reveal other types of vocalizations related to grooming or playing for example, but the locutor would not be known due to group housing.

With the analysis of the vocalizations produced by FAJ758 and FIG776, we were able to familiarize with minipigs calls in order to study their cortical bases.

5. Cortical activity underlying vocal production in behaving minipigs

Animals communicate through multiple types of acoustic signaling (Z. Chen & Wiens, 2020), and many vertebrates, including birds and marine and terrestrial mammals, have the ability to produce vocalizations that often differ depending on the type of information they want to communicate (Stephan Brudzynski, 2010). Vocalizations, such as human speech and birds songs are motor processes requiring the coordination of various muscle groups and articulators. The coordination is made possible by the integration of the instructions coming from specific brain regions. Two types of vocal behaviors can be distinguished and proposed to stem from two different neural pathways (Hage, 2018; Hage & Nieder, 2016; U Jürgens, 2002; Mooney, 2020): Innate vocalizations, produced automatically as reflex in reaction to a stimulus or a situation (such as fear, pain, hunger, or surprise), are determined genetically and controlled by subcortical networks. By contrast, learned vocalizations characterized by single or sequences of stereotyped calls or more complex modulated sounds, are acquired by experience and controlled by cortical networks (Loh et al., 2017). Learned vocalizations imply volitional control, but innate vocalizations can be either automatic or controlled. In NHPs, automated innate vocalizations are produced by the brainstem vocal pattern-generating system, composed of the periaqueductal grey (PAG), parabrachial nucleus (PB), and ventrolateral pontine reticular formation (Lateral reg. form.) which are controlled among others by the anterior cingulate cortex (ACC) and the hypothalamus amygdala. On the other hand, innate controlled vocalizations other networks. These networks include the motor cortex in mammals (Fukushima et al., 2014; Okobi et al., 2019) and its analogue in birds (Chakraborty & Jarvis, 2015)(Mooney, 2020). In primates, production of learned vocalizations also activates the ventral premotor and inferior frontal cortices (Coudé et al., 2011; Gavrilov et al., 2017; Hage et al., 2013; Okubo et al., 2015; Roy et al., 2016), a region involved in complex sequence comprehension (Wilson et al., 2017). Both premotor and primary motor cortices are involved in the initiation of volitional calls. Additionally, in songbirds, interneurons in the high vocal center are active during all the vocal activity (Kozhevnikov & Fee, 2007). Although noticeable variations of anatomical pathways exist between humans and non-human primates (NHPs) or songbirds that may explain at least in part the unique ability of humans to speak (J. K. Rilling et al., 2008), the brain networks underlying vocal production show strong anatomical similarities between humans and monkeys (Hage, 2018; Michael Petrides et al., 2005). However, until now, very few neurophysiological data highlighting the cortical dynamics underlying vocal production have been reported in animal models other than NHPs and birds. Especially, no domestic species has yet been proposed to investigate vocal brain activity using electrophysiological approaches. A natural candidate model is the minipig and the pig, that are classified as domestic animals and are easier to handle and take care compared to wild species such as NHPs, and have recently started to attract attention in the field of neuroscience (Félix et al., 1999; Saikali et al., 2010; Simchick et al., 2019; Vrselja et al., 2019). In particular, minipigs have become a purpose bred for research. They are smaller than livestock animals bred for food production, yet physiologically in all other ways similar to agricultural pigs. For research lasting longer than 3 weeks, miniature swine are thus preferable both for handling ease and welfare considerations. Furthermore, miniature pigs have a convenient body size for

surgical procedures and given their anatomical similarities to humans, they are often used as preclinical models (Khoshnevis et al., 2017, 2020; Selek et al., 2014).

In the present study, we introduce a novel experimental paradigm to identify the cortical dynamics underlying vocal production in freely moving minipigs. A key problem to chronically implant neural probes in the pigs is the presence and development of frontal sinuses preventing safe access to neural structures with conventional craniotomy in adult animals (Gierthmuehlen et al., 2011; Torres-Martinez et al., 2019). These cavities indeed extend far caudally within the skull of adult animals from the frontal to the parietal bones. Performing a craniotomy in such condition leads to cross the sinuses and thus make a connection between the implanted zone and the nasal cavity, which ineluctably eventually leads to infections post-surgery. Here we first show that implantations of ECoG grids can be done using conventional craniotomy in minipigs younger than 5 months of age, a period when sinuses are not yet fully developed.

The cortical dynamics underlying vocalizations in minipigs has not been explored to date, and we addressed this gap by chronically implanting and recording from freely moving minipigs and analyzing the LFPs occurring during the vocal utterances of the animals. Our results show activation of the sensorimotor cortex around the onset of vocal production of grunts, the most common vocalization of pigs.

5.1. Methods

5.1.1. Animals

In this study, we considered minipigs of two different breeds over a period of four years. One Yucatan male (INRA, France) (YU254 minipig), and two Aachener females (Carfil Quality) (CH596 and GI2028 minipigs). The animals were housed when possible in groups or by pair with weekly renewed enrichment equipment and ad libitum water. Regular examinations of the minipigs were performed by a veterinarian to ensure a healthy condition and a socialization program was set up to ease human-animal interactions. At the end of this study, one of the implanted minipigs was rehabilitated in a pedagogic farm as its retirement period. Experiments were performed in compliance with European (2010-63-EU) and French (decree 2013-118 of rural code articles R214-87 to R214-126) regulations on animal experiments, following the approval of the local Grenoble ethical committee ComEth C2EA-12 and the French Ministry of Research (APAFIS#5221-2016042816336236.V3).

5.1.2. Socialization program

The Carfil minipigs underwent a socialization program to ease their manipulation by human experimenters. Part of my work was to set up the protocole from scratch and apply it in collaboration with the technician of the lab Cyril Zenga.

Human-pigs interactions in this study are of particular importance, because the proper course of post-surgical care as well as cortical recordings and rehoming procedure will depend on the socialization program. To date, scientific interest had mainly focused on the social interactions of pigs in farm conditions or in laboratory (Gielsing et al., 2011; Marino & Colvin, 2015). Recent studies have examined already some aspects of the interactions between pigs and humans (Bensoussan et al., 2019; Brajon, Laforest, Schmitt, et al., 2015), but the pigs' and especially minipigs' social behavior in interaction with humans still needs more investigations. Albiach-Serrano et al. (2012) have shown that farm pigs did not use human social cues (i.e., touching, pointing, gazing) to find food hidden in containers. However, group-living farm piglets were able to use human cues (pointing gesture, head orientation,) to find food after a great amount of training (Bensoussan et al., 2016; Nawroth et al., 2016). Moreover, juvenile domestic farm pigs were able to attribute attentive states to humans (Nawroth et al., 2013), and highly socialized domestic pigs show interspecific socio-communicative behaviors similar to those of dogs, like orientation towards the human face (Gerencsér et al., 2019).

The pig as a model species for preclinical and biomedical studies has been increasingly used for decades (Helke et al., 2016), and miniature breeds were developed to facilitate handling and housing (Bro et al., 2012; McAnulty et al., 2011). Along with that, the number of minipigs kept as pets has increased significantly (Marino & Colvin, 2015). Due to their intelligence and cognitive abilities, pigs can be kept as companion animals among humans. However, little is known about the education and socialization of minipigs required to live in an environment rich in human social contacts.

On many aspects, dogs' and pigs' socio-cognitive abilities present similitudes. For example, dogs and pigs are able to discriminate among conspecifics and show a preference for familiar animals over unfamiliar ones (McLeman et al., 2005; Molnar et al., 2009; Souza et al., 2006). Additionally, these two species are also capable to differentiate human individuals and recognize human faces (Brajon, Laforest, Bergeron, Tallet, & Devillers, 2015; Koba & Tanida, 2001; Nagasawa et al., 2011; Wondrak et al., 2018). Both dogs and pigs make use of visual, acoustic and olfactory cues to communicate with conspecifics and other species (Marino & Colvin, 2015; Miklosi, 2014). As opposed to the popular role of dogs as companion pets or work-related helpers (shepherd dogs, mountain rescue dogs, ec), pigs have been used as a livestock species solely until recently. As a consequence, the criterion of selection for the two species were completely different. For dogs, easy temperament and willingness to cooperate with humans were selected (Hare & Tomasello, 2005). For pigs, most of the selection is made upon growth and reproduction traits (Held et al., 2008). Regarding the differences and similarities between dogs and pigs, we decided to base our minipigs' socialization on a standardized social training for puppies (Vaterlaws-Whiteside & Hartmann, 2017). The program was carefully adapted taking into account some data collected on domestic pigs (American Mini Pig Association, Mini Pig Training Handbook), but also on farm pigs (Tallet et al., 2017).

The minipigs used in this study began the experimentation at the average age of 9 weeks. They arrived in groups of 2 to 3 individuals generally from the same litter (which we have

preferred in order to preserve the social structure of animals (Goumon et al., 2020)) or similar ages. Although very fearful at first, we found that among groups, one or two individual(s) tend to be more socially proactive towards humans. These animals were quickly identified in the first few days. Initially, we chose to target our interactions to these less fearful minipigs and to take advantage of the social transmission phenomenon on more shy minipigs (Tallet et al., 2018). Thus, even piglets that have been less manipulated in the first few weeks following their arrival tended to be attracted to humans after a few more days of socialization. When possible, we used older minipigs housed in adjacent pens to display social interactions with humans.

The protocole was performed everyday for about 45 minutes over a period of about two months. A recent study shown that human approach by piglets is favoured when the animals had a previous positive experience with the handler, even in the case in which the handler is passive and did not reinforce the animal (Brajon, Laforest, Bergeron, Tallet, Hötzel, et al., 2015). However, we have chosen to associate the human presence with soft contacts and the distribution of food, since piglets in this study tend to spend more time with the experimenter if they were previously gently handled and had food rewards. This choice appeared crucial to promote the manipulations imposed by post-surgical care that can be a source of great stress for the animals. The experimenter kept a calm voice to talk to the minipigs and encouraged every sign of interest from the animals. The experimenter wore the same clothing color and shape during the first month (white overalls) of the socialization program, as it could influence discrimination among other humans (Koba & Tanida, 2001).

At first the contacts were limited to positive physical contacts such as scratches and strokes (Brajon, Laforest, Bergeron, Tallet, Hötzel, et al., 2015; Tallet et al., 2014). Physical contacts with the experimenter were highly encouraged by high-value food and toys distribution (dried fruits, squishing ball, etc). The experimenter was also involved during play time as often as possible (play fetch, etc). When the litter was fully habituated to the experimenter's presence, the contacts were followed by physical restraints and lifts.

Once the animals were fully habituated to humans, we began a medical training protocole using positive reinforcement. Medical training was necessary to reduce the stress for both the minipig and the keepers during post-surgical treatment as well as medication. This protocole reduced the use of anesthetics or physical contentions necessary to post-surgical treatment. The animals learned to stand still on the treatment table and to take liquid medication from a syringe. They were also accustomed to undergo manipulations on the implanted area (on top of the skull). For this, we habituated the animal to be touched and scratched in this area, and applied products like cold water and body lotion. We also reinforced the immobility of the animal on the ground during such manipulations.

After the medical training, the animal undergo another habituation program during which it had to be habituated to the experimental recording protocole. The animal was placed in the recording pen (see **Section 5.1.6**) first in groups with its congeners then alone with the experimenter and finally alone for a few minutes. This habituation was repeated until the minipig showed no more freezing behaviors in the recording pen. The goal was for the minipig to be familiar with the recording pen, so that he did not feel any stress related to the discovery of this new environment during the cortical recordings. After the implantation, the animal was able to stand still during the installation of the recording deviced on top of its skull and was accustomed to be placed on the recording pen.

This whole program, reproduced and improved over the years since 2017, has allowed us to perform cortical and vocal recordings on freely moving animals, but also to replace some of our minipigs in educational farms as retirement.

5.1.3. Anatomical imaging (CT-scan and T1 MRI)

In minipigs, brain surgeries can lead to severe infections caused by the development of the frontal sinus. Indeed, the frontal sinus cavity extends from the frontal to the parietal bone.

We used CT-Scan to assess the development of the frontal sinuses in several minipigs at different ages between 3 and 12 months. CT images were acquired at the Grenoble Hospital, except for the 2 animals aged 5.5 and 12 months, for which they were provided by Ellegaard company. I analyzed DICOM data using InVesalius software (2007-2017, Center for Information Technology Renato Archer) and 3D reconstructed skull models with Blender (<https://www.blender.org/>).

Furthermore, for the implanted animals CH596 and GI2028, a CT-scan was acquired two weeks before implantation to assess the possibility of craniotomy and define the craniotomy over the skull as proposed previously for NHPs (X. Chen et al., 2017). In this case, the animal was pre-medicated with an IM injection of 1mg/kg Azaperone (Stresnil®, Elanco, Suresnes, France). After 15-20 minutes, the anesthesia was induced by intramuscular (IM) injection of 5mg/kg Tiletamine-Zolazepam (Zoletil® 100, Virbac, Carros, France). Additionally for CH596, a pre-surgical T1-weighted MRI (T1-MDEFT, 1-mm slice thickness, 0.43x0.43 mm² pixels, TE: 4 ms, TR: 2000 ms, Flip angle: 20°) was performed (to reconstruct the cortical surface) under a general anesthesia induced as for the CT scan and then further maintained under Isoflurane (Isoflo®, 2-2.5%). This MRI was acquired a few days after CT-scan, to allow the animal to fully recover from the anesthesia.

5.1.4. Surgery preparation using 3D modeling and printing

Chronically implanted devices in large animals require protection components to secure fragile electronics and connectors from hits, bites or even breaking. To do so, I developed customizable pieces adapted to the animal anatomy using 3D modeling following a procedure inspired from one previously proposed for NHPs (X. Chen et al., 2017). The CT-scan images were imported in the InVesalius software (2007-2017, Center for Information Technology Renato Archer) and segmented to obtain a model of the skull. The MR images were processed with 3D Slicer software (<http://www.slicer.org>) (Fedorov et al., 2012) to segment the brain and visualize the cortical gyrus and sulcus anatomy before implantation in order to make accurate anatomic assessment of the motor cortex for surgical planning. The 3D models obtained by CT-scan and MRI were then combined together using the Blender software (<https://www.blender.org/>) to model the full minipig's head. Based on this reconstruction, in collaboration with the veterinarian Mehrdad Khosh Nevis, we planned the coordinates of the

craniotomy according to the motor cortex location to access the implantation area (**Figure 42 (d)**).

Moreover, I designed using Blender software a customized metallic oval chamber (60x50mm) to be screwed on the skull during the implantation surgery (**Figure 42 (b)**). This chamber was adjusted to the minipig anatomy to closely fit its skull surface. Its role was to cover and protect the craniotomy area and house the connector of the implant. To ensure good resistance against possible damages, this chamber was 3D printed in biocompatible TA6V titanium (X3D, Lyon France). To close this chamber, a thick hood was 3D printed in transparent resin using a Form 2 printer (Formlabs, Sommerville, USA) (**Figure 42 (f)**). I designed this piece so that it could be easily removed by the experimenter for each recording session to connect the recording devices.

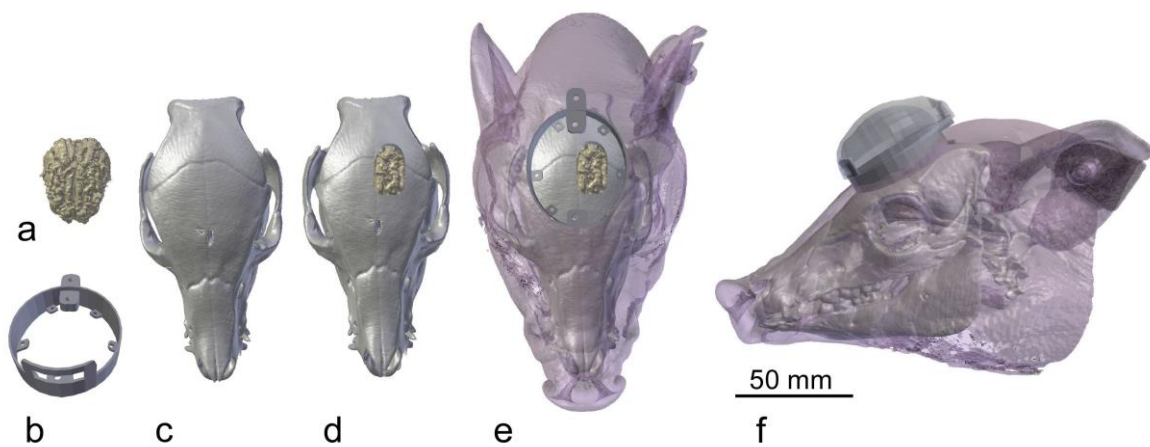


Figure 42. Surgery planning using personalized 3D modeling. (a) 3D modeling of a minipig's brain based on T1 MR images. (b) 3D representation of the protecting chamber. (c) 3D model of a minipig's skull based on a CT-Scan. (d) The brain model is aligned with the skull model and the craniotomy coordinates were planned. (e) Full 3D model with the protecting chamber and the skin of the animal to prepare the surgery (f) Lateral view of the full 3D model with the resin hood installed.

5.1.5. Implantation surgery

In the present study, one adult Yucatan (YU254) and two young Aachener minipigs (CH596 and GI2028) were chronically implanted with electrocorticographic (ECoG) grids. YU254 was implanted in 2015 before my thesis with a 64-channel clinical ECoG grid (PMT Corp. **Figure 43 (c),(d)**). The PMT grid was not modified so that the pigtailed could be tunneled below the skin toward the back of the animal.

During my PhD, I took part in the implantation of CH596 and GI2028. CH596 was implanted with a soft EcoG array made of a PDMS substrate and housing 32 recording contacts routed to a 36-pin omnetics connector (Fallegger et al., 2021) (see **Figure 43 (a),(b)**). GI2028 was implanted with the same implant as YU254, but the pigtailed of the PMT grid were cut and

reconnected to a 36-pin omnetics connector in order to connect the headstage directly on the head inside the titanium chamber. Thanks to the pre-implant CT in both CH596 and GI2028 and the MR imaging in CH596 and YU254, the ECoG implants were successfully positioned on the premotor and motor cortices in CH596, the temporal and part of the lateral frontal cortex in YU254, and the inferior frontal cortex along with the sensorimotor region in GI2028 (**Figure 43 (e),(f)**).

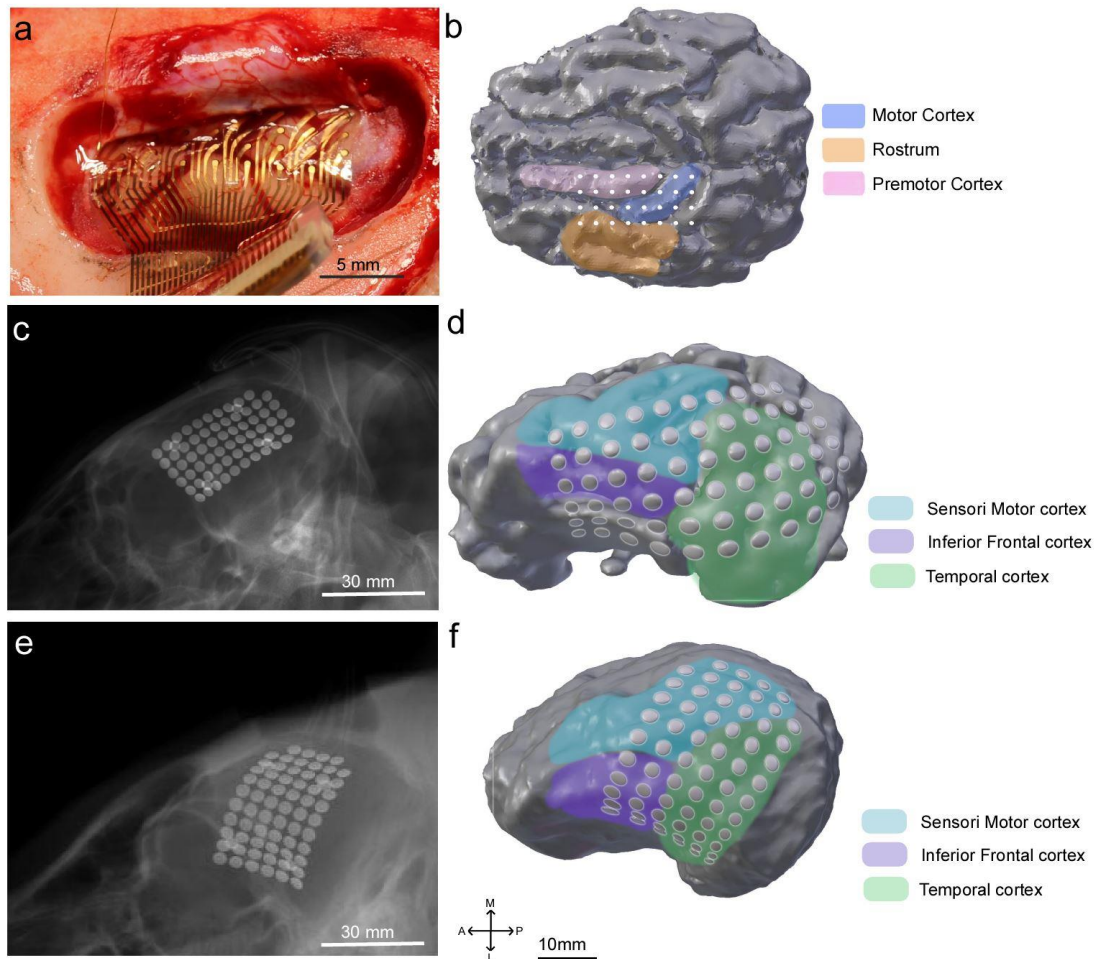


Figure 43. Electrode registration of soft ECoGs over the left hemisphere in three minipigs. (a) Flexible ECoG array placed surgically on the surface of the brain of CH596. (b), (d), (f) 3D reconstruction of CH596, YU254 and GI2028 brains respectively, with electrodes placement. (c), (e) X-ray projection of the head of YU254 and GI2028 respectively after implantation of clinical ECoG grids.

Each animal was initially premedicated and anesthetized using Stresnil and Zoletil as for CT and MRI imaging (see above). A trimmer was then used to shave the hair over the head from the eyes up to the back of the ear's roots. Then, the pig was placed in a stereotaxic frame (KOPF) over a warming blanket to prevent the peri-operative hypothermia. The surgery was performed by the veterinarian Mehrdad Khosh Nevis and Blaise Yvert and my role, along with Cyril Zenga, was to prepare the animal for the surgery (shaving, placement of catheter for IV

injections, placement of ECG electrodes, set up of the respiratory system) and to help maintain the sterility in the operating room.

The pig's head was typically fixed by the ear bars with a slight extension of the head. To continue the general anesthesia, mask or orotracheal intubation was performed and sedation was maintained by a continuous inhalation of isoflurane 2% (Khoshnevis et al., 2017, 2020; Selek et al., 2014; Torres-Martinez et al., 2019). Ketoprofen (3 mg/kg, Ketofen® CEVA) was administered IM to better maintain the anesthesia and improve postoperative analgesia. Before beginning the surgery, the skin incision site and extensive area surrounding it were disinfected by wiping skin with betadine scrub 4% and dermal 10% immediately prior to draping. Cardio-respiratory functions were monitored throughout the surgical procedure. Local analgesia was provided by subcutaneous (SC) injections of lidocaine (xylocaine adrenaline) before incising the skin according to the later position of titanium chamber on the skull. This positioning was based on the craniotomy coordinates which have been identified by the pre-operative CT and MRI reconstruction at D -14. An oval incision was done to remove the skin over the top of the skull. Using a periosteal elevator, the periosteum was retracted gently to the edge of the skull. The entire exposed area of the skull was well dried and cleaned. The craniotomy area was drawn over the left hemisphere of the skull based on the skull anatomical cues such as bregma, occipital crest, temporal crest, and Central tubercle of nuchal crest and according to the position of the motor cortex relative to bregma as identified from presurgical MRI and CT scan. Before craniotomy, the skull bone thickness (parietal and frontal bones) of craniotomy area was inferred from CT images and the 3D reconstructions I performed. The skull was drilled gently with electric surgical drill (Medtronic). During the craniotomy, the depth of drilled area was controlled several times by pushing gently on the craniotomy line. When the full thickness craniotomy has been reached, the bone flap was lifted away from the skull with forceps. After exposing the dura mater, its surface was dried and cleaned to ensure no further bleeding. Then the dura mater was cut with micro-dissecting scissors to reach the implantation area on the brain surface.

For the adult YU254 animal, for which the sinuses were already developed, the craniotomy was performed as a lateral dorso-ventral opening starting 10 mm posterior to bregma and 1.5 cm lateral to the midline. The clinical implant was inserted and then gently pushed rostrally below the dura to cover the temporal and part of the lateral frontal cortex. The implant pigtails were secured at the exit of the skull and then tunneled below the skin toward the back of the animal to exit the skin at the level of the forelimbs, a location that the animal could not reach using its nose or limbs. The craniotomy was closed and the skin sutured over the skull. A dedicated bag was taped on the back of the animal so that the pigtails exited the skin directly inside the bag, where they could eventually be connected to recording headstages. The transcutaneous exit area of the pigtails was disinfected every 2 or 3 days post-implantation with betadine to prevent infection.

For the two young Aachener animals, for which the sinuses were not yet well developed, the craniotomy extended from 5 mm posterior to 20 mm anterior to bregma and from 2 mm to 18 mm lateral of the midline. For CH596, the soft implant was positioned to cover the sensorimotor cortex and extended rostrally to this region. For G12028, the craniotomy was slightly widened posteriorly to let the ECoG grid be inserted and gently pushed below the dura in the antero-posterior with an approximate angle of 30 degrees with respect to the midline to reach the inferior frontal cortex in its anterior end and still cover part of the sensorimotor region in its posterior end (**Figure 43 (f)**). After the implantation, unilateral duraplasty was performed using

an onlay, suture-free, 3-dimensional-collagen matrix graft (*DuraGen*®, Integra LifeSciences). To close the craniotomy, the bone flap was thinned and placed back on the Duragen, and then fixed on the surrounding skull using titanium strips and screws. For both Aachener animals, the titanium chamber was then fixed on the skull using self-drilling titanium screws. Then, its interior space was filled with bone cement (CMW1 + Gentamycin®, DEPUY) to seal the craniotomy and surrounding area. At the end of the surgery, the chamber was closed by a 3D printed hood. The detailed surgery procedure for CH596 is illustrated in **Figure 44**. After surgery, the animal was monitored in a recovery room, pain relief was supplied with Ketofen. Prophylactic antibiotics (Kesium® CEVA) and anti-inflammatory agent (Metacam® Boehringer Ingelheim) were administered for 7 days post-operative.

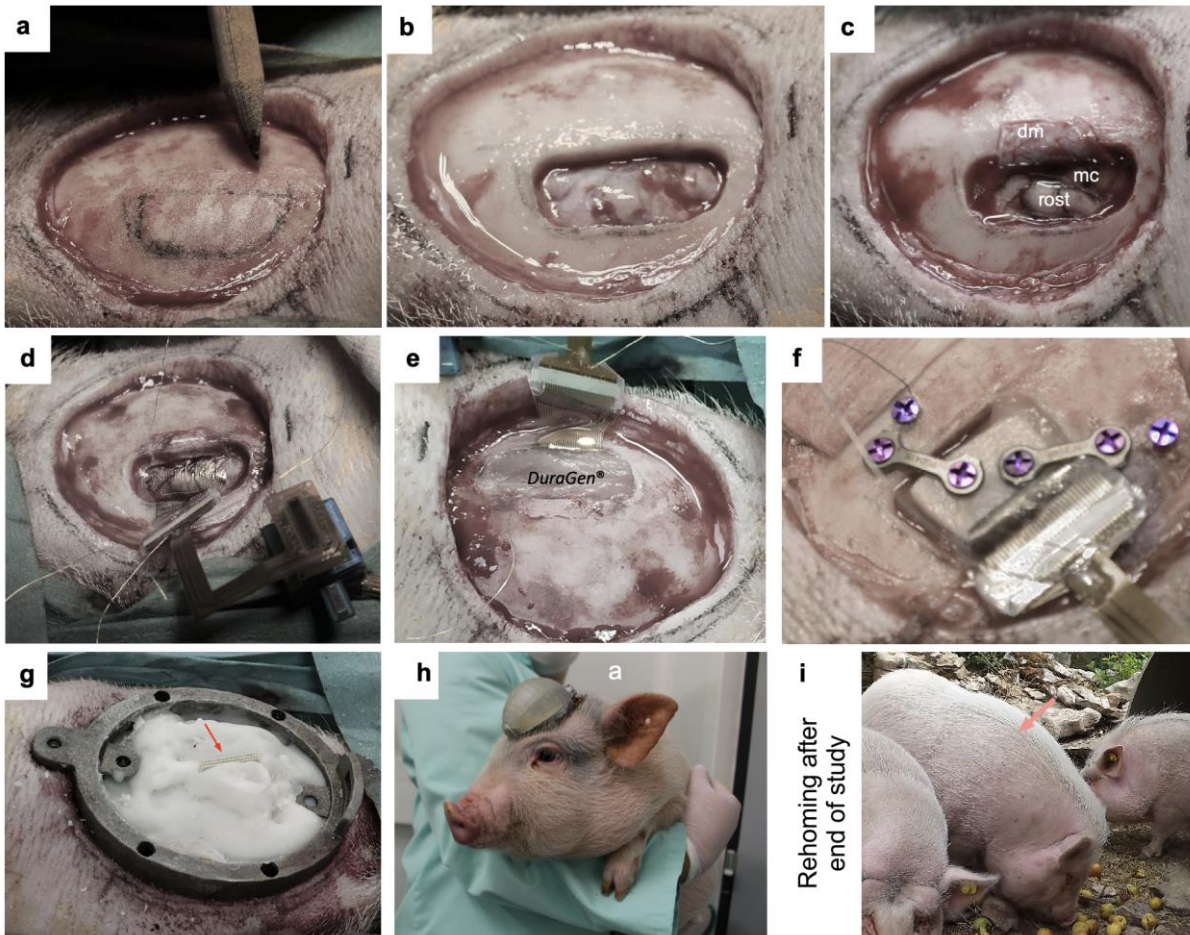


Figure 44. Surgical procedure for the implantation process of a soft ECoG over premotor and motor cortices in CH596. (a) The craniotomy area was drawn over the left hemisphere of the skull based on CT-scan. (b) The bone flap was lifted away from the skull. (c) The dura mater was cut with micro-dissecting scissors. (d) The implant was positioned to cover the premotor and motor cortices. (e) Duraplasty was performed. (f) the bone flap was placed back and fixed on the skull using titanium strips and screws. (g). The titanium chamber was fixed on the skull and the interior space of the chamber was filled with bone cement. The cemented connector is indicated by the red arrow. (h) Implanted animal several days after surgery with protective cap closing the chamber. (i) Explanted animal CH596 (middle pointed by arrow) rehomed with congeners in a farm after ending its investigation. All panels refer to animal CH596 except panel f corresponding to animal BA638 (the same approach was used for CH596 but no picture of this step was taken during the surgery).

There was no post-operative wound infection and the skin repair has been processed normally around the titanium chamber. Care and disinfection were necessary to avoid infection around the chamber. In post-implantation period, the minipigs were kept 9 months at the most to perform several recordings. During this period, there was no evidence of the infection or nervous symptoms following the surgical procedure.

5.1.6. Simultaneous electrophysiological, audio and video recordings

Neural activity was recorded using the wireless W2100 system (MultichannelSystems, Reutlingen, Germany). In the first year of my thesis, I helped for the conception and building of a 2m x 2m x 2m recording pen that was sound-attenuated using several layers of acoustic foam (

Figure 45(a),(b)). Four wireless receivers were fixed on the roof of the pen and connected to 2 recording bases located outside the pen. Five microphones (Pro45, Audio-Technica Inc, USA) were positioned in the pen, one at each corner 1m from the floor and one on the ceiling in the center of the pen, where a camera (UI-3140CP-C-HQ Rev.2, IDS Imaging, Obersulm, Germany) was also positioned to monitor the animal behavior along the recordings. During a typical experimental recording, the protecting hood was detached and wireless HS32 headstages (MultichannelSystems, Reutlingen, Germany) were connected to the implant. CH596 implant required one headstage (ECoG 32 channels), GI2028 and YU254 required two headstages each (ECoG 64 channels). For CH596 and GI2028, a protecting cap was designed in Blender software (**Figure 44(d)**) and 3D printed in thick resin to protect the headstages and batteries during the recording process. The recording hood was thicker and larger than the normal hood, it was designed to be fixed on the protecting chamber (see

Figure 45(c)). Since no recording pen was built during the preliminary recordings of YU254 in 2015, the animal was placed in a hammock.

CH596 and GI2028 were held in the arms or let to move and behave freely separately in the pen under the supervision of an experimenter ensuring that the animal did not rub its head against the floor or the walls. Also, the experimenter was present to arouse more vocalizations. Cortical, audio and video data were acquired the MCS experimenter software or inhouse Pulsio software. Neural data was acquired at a 20kHz sampling rate after 1-5000 Hz bandpass filtering and 16-bits AD conversion at the headstage level. Acquisition in YU254 was performed at 2kHz. Audio data was also acquired at 20kHz after amplification by a sound card (OctoMic II, RME-Audio, Haimhausen, Germany). Video was acquired at 50Hz, synchronized with the neural and audio data.

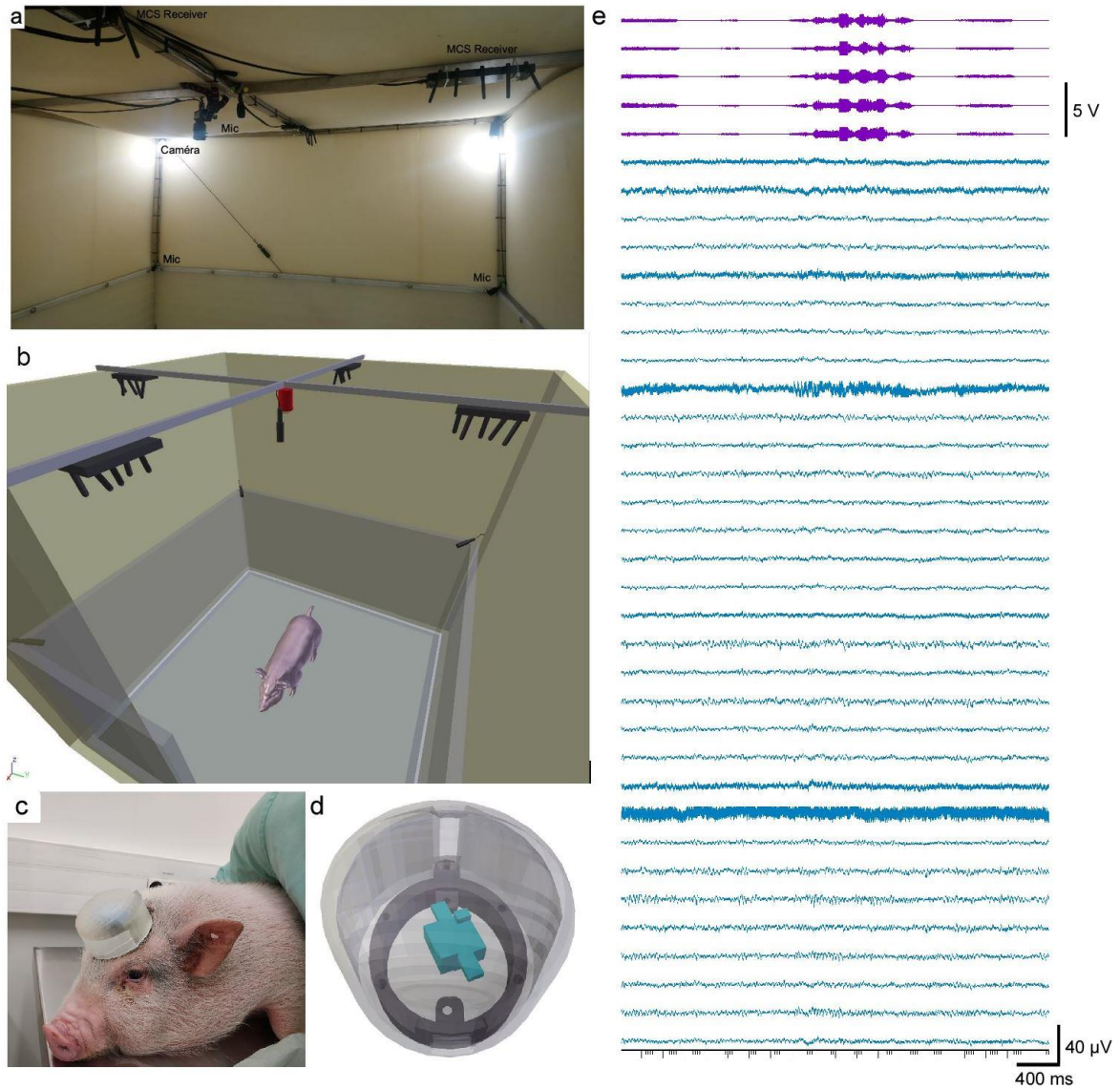


Figure 45. Setup for both vocalizations and cortical data recordings in freely moving minipigs. (a) Roof of the recording pen with the recording setup. (b) 3D representation of the recording pen, roof view from the door. (c) The recording cap is screwed to the protecting chamber during recording sessions to protect the wireless devices. (d) 3D modeling of the recording cap with a representation of a wireless headstage (in blue). (e) Raw recordings of vocalizations (purple lines) and cortical data (blue lines) visualized with Spike2.

5.1.7. Audio data processing

Among the various vocalizations, our study was focused on grunts because they were the far most preponderant ones. The onset time and duration of all vocalizations were extracted from the ongoing audio signals using a custom script under the spike2 software (CED Corp., Cambridge, UK). These times were further used to compute evoked potentials responses time-locked to vocal production onsets.

5.1.8. Neural data processing

Cortical data was low-pass filtered below 10Hz and downsampled at 200Hz and evoked potentials were computed by averaging single trials locked to the onset of vocalizations and correcting the baseline with respect to the [-3, -2] s interval preceding the vocalization onset. To assess the statistical significance of these averages, we first built a distribution of bootstrap averages (Blaise Yvert et al., 2002). If N vocalizations were recorded, N trials were drawn with replacement from the original set of N trials, and averaged and baseline-corrected. This procedure was repeated 1000 times. We further assessed significant vocalization-induced cortical activations using the following procedure. A rest period void of vocal production was considered and used to select N resting trials, which were in turn averaged and baseline corrected with the same parameters as the signal. The standard deviations corresponding to both the vocalization and the resting averages were also computed and a Welch t-test was performed to compare both distribution at every time point of the average potential. A threshold was set at 0.05 and all time points for which the P-value of the Welch test was below this threshold were considered to correspond to statistically significant activity. This procedure was further retained to build spatiotemporal maps of cortical activity using our previously developed NeuroMap software (freely available at <https://sites.google.com/site/neuromapsoftware/>) (Abdoun et al., 2011). For animal G12028 only, cortical data were common average referenced.

5.2. Results

5.2.1. Evolution of the frontal sinuses over the motor cortex after 6 months

Before this study and according to the several pre-implant CT acquisitions in different ages of Aachener and Göttingen minipigs, it was observed that before 5 months of age, the sinuses

have not yet extended too caudally and the motor cortex could be accessible through a direct craniotomy (see **Figure 46**). Thanks to this acquired information, the Aachener minipigs were implanted at approximately 4.5 months of age. After the implantation, the sinuses developed by circumventing the implanted area, following the external border of the protecting chamber (see **Figure 47**). This avoided infections of the implanted zone, preserving the health of the animal and allowing to rehome them when possible.

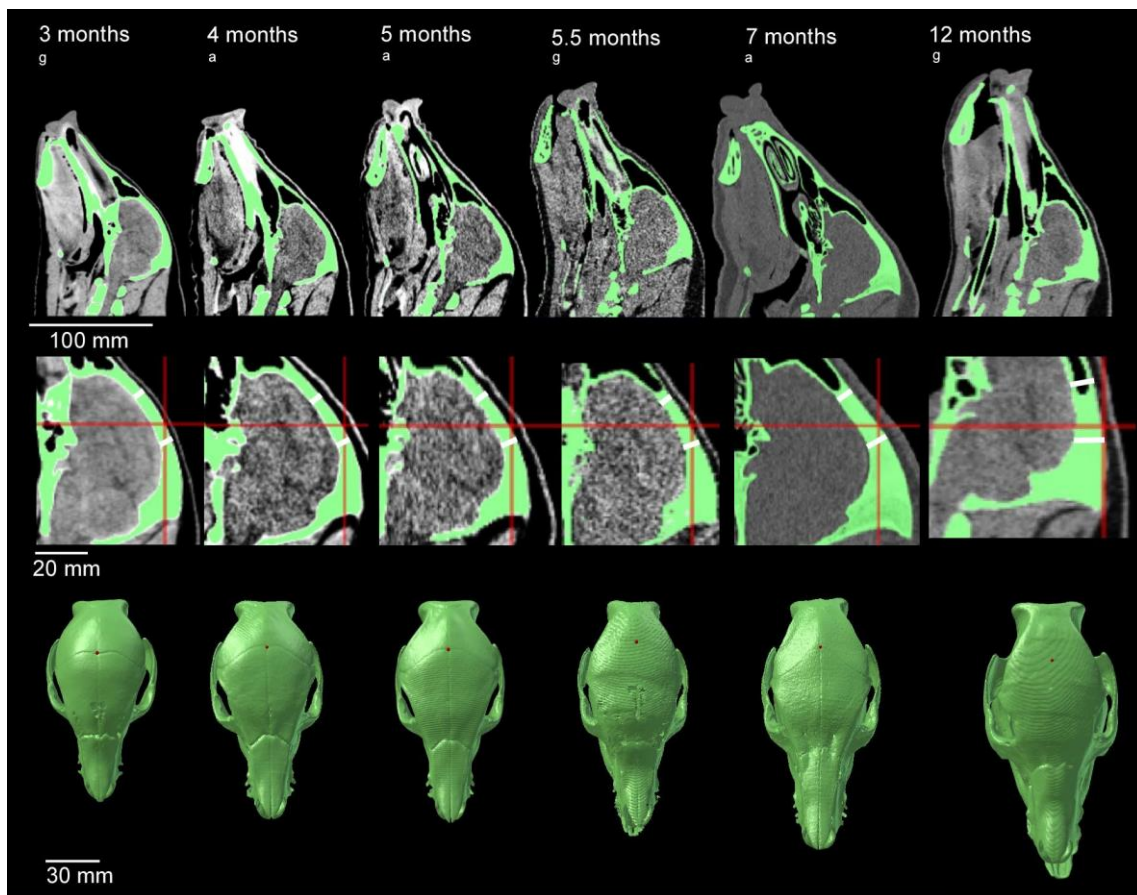


Figure 46. Development of frontal sinus in minipigs between 3 and 12 months of age. Top row: Mid-sagittal CT images of the whole head at various ages. Middle row: close-up of the brain area, with a representation of a typical craniotomy over the motor cortex (white lines). Bregma is represented by the red cross. Bottom row: 3D reconstructions of the skulls. Bregma is represented by the red dot. a=Aachener minipigs, g=Göttingen minipigs

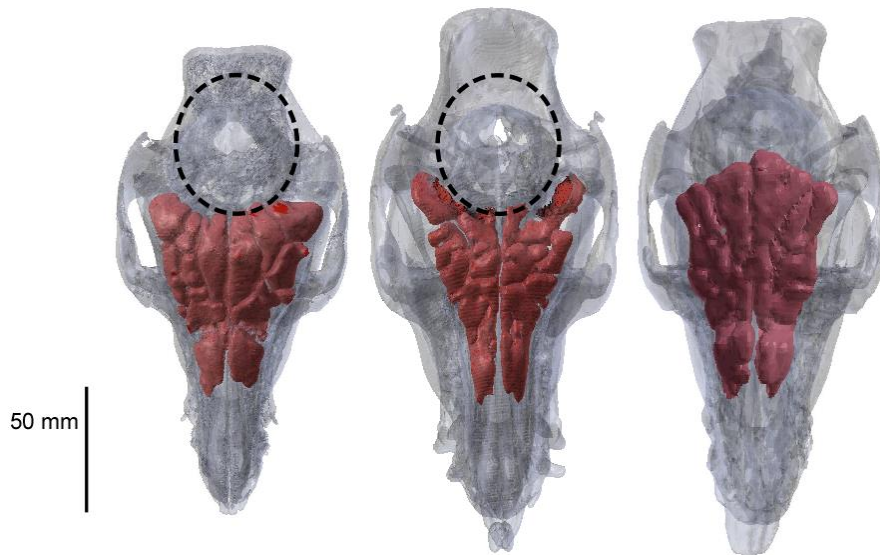


Figure 47. Evolution of sinus following implantation. From left to right : 5 ½ months Ellegaard minipig after implantation at 4 months, 9 months Aarchener minipig after implantation at 7 months, 1 year Ellegaard minipig without implantation. The sinusal cavities are represented in red.

5.2.2. Vocalizations

During a recording session, the animals CH596 and GI2028 were placed in the recording pen and their vocalizations were recorded with 5 microphones. Part of my role was to stay in the recording pen with the animal during the recording session to trigger vocalization and ensure the animal was not trying to remove the recording devices. Minipig YU254, who was implanted and recorded before the beginning of my thesis, was placed in a hammock. YU254 did not undergo a socialization program and his placement in the hammock was necessary to connect the wireless system.

5.2.2.1. YU254 vocalizations

The recording session lasted approximately 15 minutes during which YU254 produced 112 Grunts. One sample of these vocalizations is shown in **Figure 48(a)**. The lowest frequency peak of Grunts produced by YU254 was 130 ± 12 Hz. The average duration of the calls was 599ms and the maximum duration was 1.6sec. As can be seen in **Figure 48(a)** on bottom histogram, the vocalizations were globally fairly close together (the median delay between two vocalizations was 3.43sec). YU254 tended to produce calls repeatedly, which was also described as common when producing Grunt-type calls in Marthe Kiley's analysis (Kiley, 1972b). Additionally, the Grunts in YU254 seemed to be associated with increase

inconfort due to his placement in the hammock. Moreover, the Grunts were sometimes followed by Screams which were not analyzed here due to the fact that they were systematically accompanied by a lot of artefacts with squeals due to movements of the animal.

Because of these special recording conditions, the hammock placement was subsequently abandoned in favour of freely moving recordings in a pen (see methods page 89).

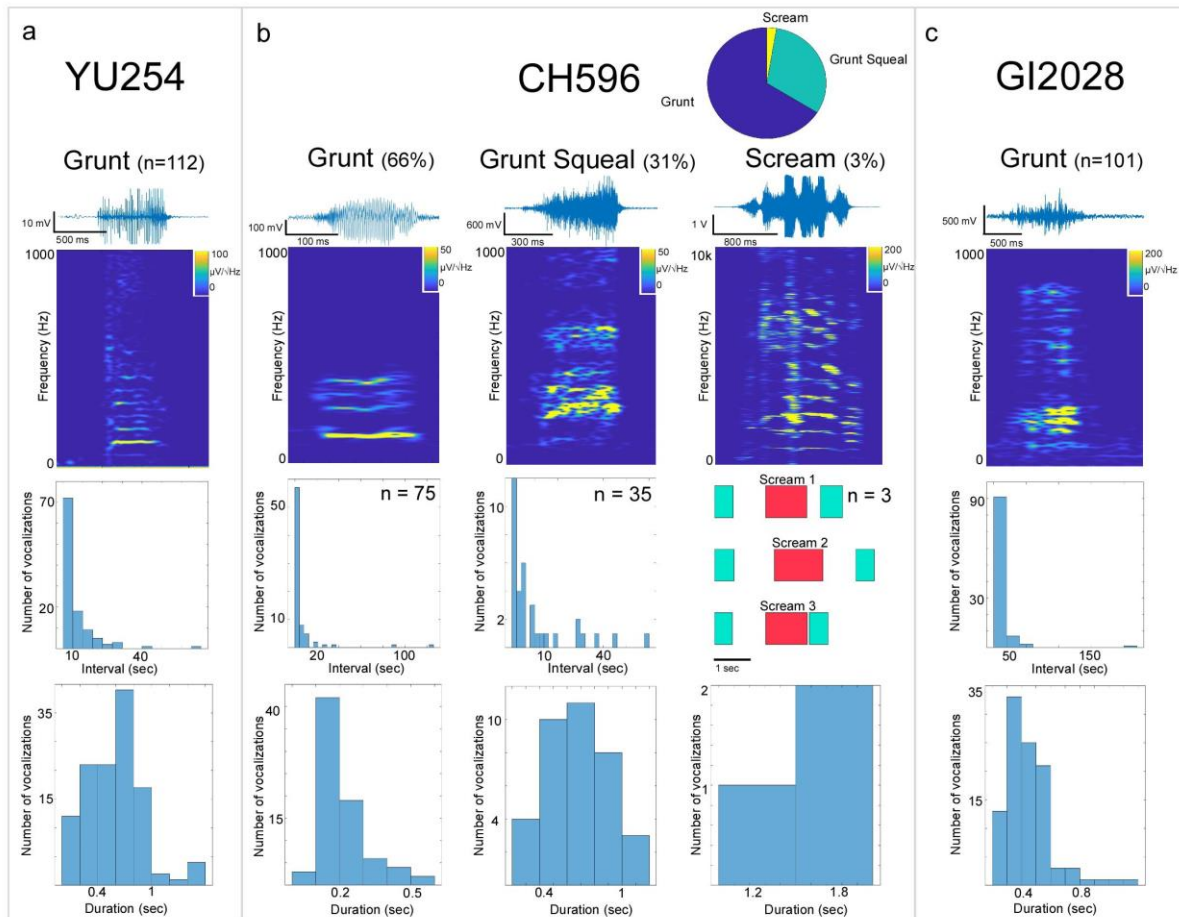


Figure 48. Characterization of vocalizations for all the animals. For each panel, a trace of an example of each type of vocalization is represented with its spectrogram (parameters identical to the parameters used in Chapter 4). The middle histogram represents the intervals between two vocalizations of the same type, except for Scream vocalizations in panel CH596, which displays the patterns of production of Screams 1, 2 and 3 (red rectangles) surrounded by Grunt Squeals (blue rectangles). The bottom histogram shows the durations of the vocalizations. (a) Vocalizations of YU254. (b) Vocalizations of CH596. (c) Vocalizations of GI2028.

5.2.2.2. CH596 vocalizations

CH596 minipig was placed in the recording pen with a familiar experimenter that participated to the socialization program (see Socialization program page 81). The human presence was necessary to trigger various vocalizations on the part of CH596. The recording session lasted about 15 minutes during which we recorded 3 different types of vocalizations. Most commonly, CH596 produced Grunts ($n = 75$). In addition, CH596 produced 35 Grunt Squeals and 3 Screams when we held her in our arms and moved into the box while holding it. A sample of each vocalization is shown in **Figure 48(b)**.

Grunts ($n = 75$)

The Grunts produced by CH596 lasted on average 206ms and a maximum of 592ms. The longer Grunts were often followed by the other two types of vocalizations mentioned below. The lowest frequency peak of CH596 was 132 ± 8 Hz. The median time between two Grunt vocalizations was 1.8sec.

Grunt Squeal ($n = 35$)

The Grunt Squeals produced by CH596 lasted an average of 686ms and a maximum of 1.09sec. These vocalizations had higher frequency components than conventional Grunts and the lowest frequency peak was 140 ± 9 Hz. These calls were usually preceded by several Grunts. In the Grunt part of the Grunt Squeal vocalization, the amplitude was about 300mV (triple the amplitude of a classic Grunt) and in the Squeal part the amplitude reached 600mV. The Grunt part of the Grunt Squeal generally did not last as long as a classic Grunt (average duration = 120ms compared to 206ms for a classic Grunt). The Squeal part lasted about 600ms (on average 597ms). We also noticed that the amplitude of these calls tended to increase towards the end of the sound. Grunt Squeals were frequently produced in close proximity over time, as shown in **Figure 48(b)** (middle histogram). The average time between two Grunt Squeal vocalizations was 4 seconds.

Screams ($n = 3$)

Screams vocalizations produced by CH596 were rare, we only recorded three of them. These vocalizations were systematically preceded and followed by one or more Grunt Squeals and had an average duration of 1.54sec and a maximum of 1.81sec. The production pattern of the Screams is shown in **Figure 48(b)** middle right picture. As can be seen, the intervals between the previous and subsequent Screams (red rectangles) and Grunt Squeals (blue rectangles) were quite short (average 955ms). Thus, the Screams were never isolated and were produced when the animal had already expressed vocalizations with high emotional valence like the Grunt Squeal. The Screams were extremely loud, their amplitude reached 1V (about 2 times more than the Grunt Squeals) and vary constantly over time. The frequency components of

Screams were very high, with some activity bands located beyond 6000Hz. The lowest frequency band was very variable, on average 885 ± 27 Hz. We triggered Screams vocalizations by holding the animal in the arms and tilting down as if to lay her on the ground or tilting up as if to turn her over on her back. We think that height changes were stressful for the animal, but not the fact of being carried in the arms. A sudden change in height may have induced the production of Screams in the animal CH596.

5.2.2.3. GI2028 vocalizations

GI2028 was placed in the recording pen with a familiar experimenter. GI2028 produced 101 Grunts during a recording session of about 20 minutes. These vocalizations lasted on average 347ms and at maximum 1.02sec. On average, the lowest frequency peak of the Grunts of GI2028 was 112 ± 8 Hz, which was slightly lower than the two previous animals (130Hz and 132Hz for YU254 and CH596 respectively). A sample of one Grunt is shown in **Figure 48(c)**. The delays between the different vocalizations of the animal were relatively short, with a median delay between two calls of 4.87sec.

In addition, GI2028 produced two sequences of repeated short Grunts very close in time (first series: 3 vocalizations of 230 ± 20 ms every 350 to 400ms each; second series: 5 vocalizations of 200 to 300ms every 350 to 400ms each). This type of vocalizations reflected the situation in which we conducted the recording. The experimenter present in the box with GI2028 was standing behind the animal and leaned to touch her back or to pretend to catch her and restrict her movements by holding her at the back of the front legs. Repeated Grunts could therefore reflect an anticipation of the negative stimulus of restriction of the animal's movements. In Marthe Kiley's analysis, this type of Repeated Grunt were produced during frustrating situations. The recording process for GI2028 might elicit a frustration due to the separation from her congeners.

Locutor	YU254		CH596		GI2028
	Grunt	Grunt	Grunt Squeal	Scream	Grunt
Number	112	75	35	3	101
Pitch	130 ± 12 Hz	132 ± 8 Hz	140 ± 9 Hz ± 27	885 Hz	112 ± 8 Hz
Durations	599 ms	206 ms	686 ms	1540 ms	347 ms
Percentages	100%	66%	31%	3%	100%

Table 5. Summary table of the vocalizations produced by the 3 animals.

5.2.3. Vocal production activates motor and premotor regions

Figure 49 shows that grunts vocalizations triggered three different types of activity recorded over motor and premotor regions of the cortex in minipig CH596

The first activity **McP1** is a positive peak occurring in the posterior part of the implant, covering the motor and sensori motor cortices (**Figure 49(c)**). McP1 had an average amplitude of 11 μ V and occurred on average 120ms after grunt onset (see **Figure 49 (d)**).

The second activity **PMcN1** is a negative peak occurring on average 41ms before vocalization onset and had an amplitude of -6 μ V (see **Figure 49 (e)**). **PMcN1** was recorded on the premotor cortex in the frontal part of the implant.

The third activity **PMcN2** is a negative peak occurring about 780ms before vocalization onset and peaking over the premotor cortex. This peak had an average amplitude of -8 μ V (see **Figure 49 (f)**) and was recorded significantly by the frontal half of the implant.

The electrodes recording **McP1** and **PMcN2** were distinct, but some of the electrodes recording **PMcN1** were common with those recording **PMcN2** (for example electrode 4 in **Figure 48**).

Figure 50 maps the dynamics of the 3 components over the cortical anatomy.

CH596

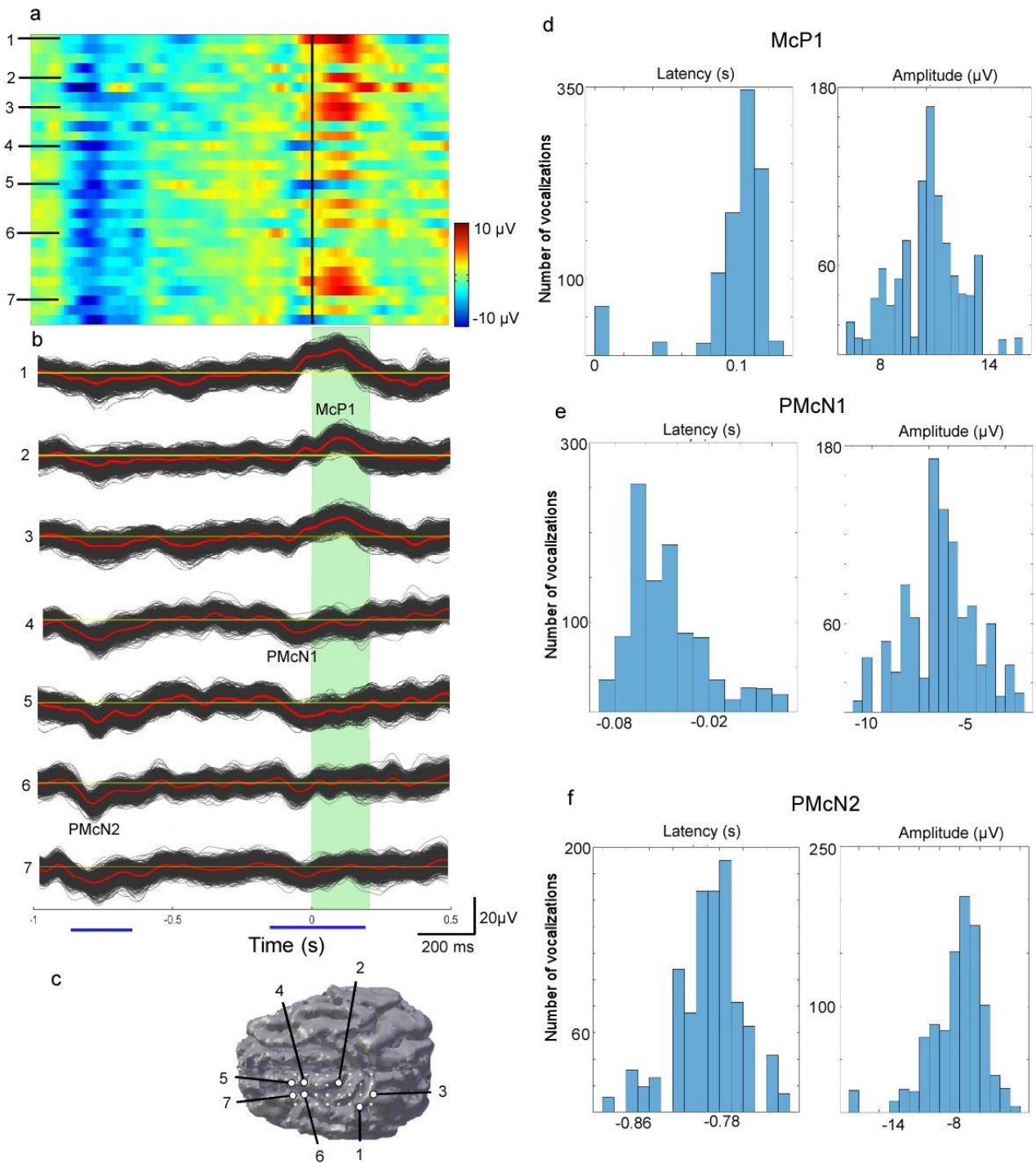


Figure 49. Cortical activity recorded during Grunt vocalizations in CH596. (a) spatiotemporal activity of different electrodes (one electrode is represented as one line, the vertical black line represents vocalization onset). Seven electrodes were selected and the bootstrap ($n = 1000$) evoked potentials are represented in (b). The horizontal blue bars represent the timings at which spatiotemporal mapping is illustrated on **Figure 50** (c) electrodes mapping over the left hemisphere in CH596. The 7 selected electrodes are displayed in white. (

d),(e),(f) Characterization of peaks McP1, PMcN1 and PMcN2 from bootstrap averages. Left panels : Latencies of the peaks in seconds. Right panels : Amplitudes of the peaks in μV .

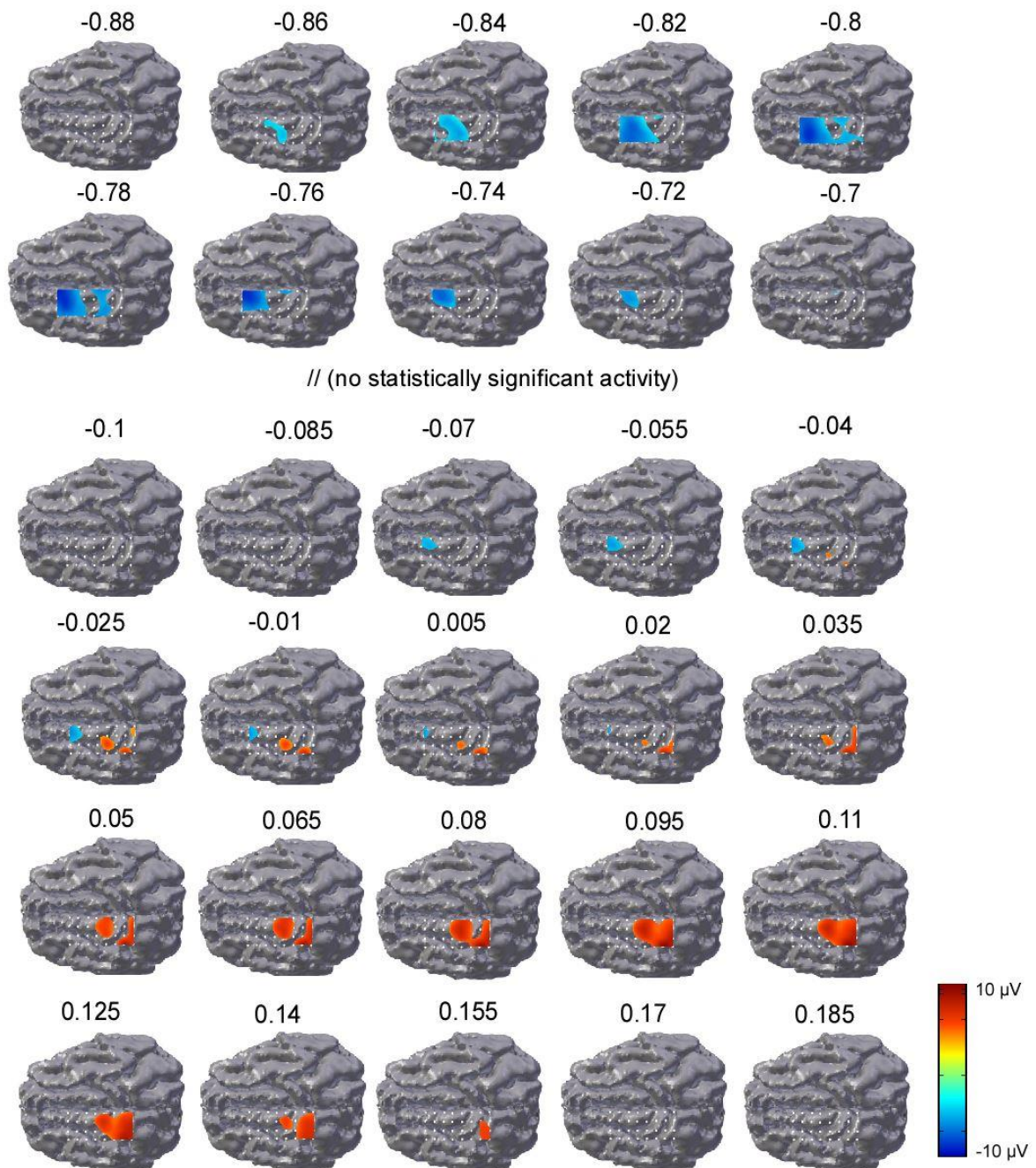


Figure 50. Spatiotemporal mapping of the cortical activity in CH596. The timings are those indicated by the blue horizontal bars in **Figure 49**.

5.2.4. Vocal production activates temporal gyrus, inferior frontal gyrus and sensori motor cortex

The cortical activity of YU254 was recorded simultaneously with its vocalizations during one session of approximately 15min. The implant covered a large part of the left hemisphere. We observed two different patterns of activity located on two different areas of the cortex.

The first activity **TempN1** was located on the temporal gyrus and recorded by one electrode, located latero-ventrally to the rostrum (**Figure 51 (c)**). **TempN1** was a slow negative peak occurring after the onset of the vocalizations. Its average latency was of 667ms after vocalization onset and its average amplitude was $-22\mu\text{V}$ (see **Figure 51 (d)**). **TempN1** started on average 200ms after vocalization onset. Before that, the activity recorded by electrode 1 was positive (see **Figure 52**). After the end of **TempN1** (667 ms after grunt onset on average), the activity recorded by electrode1 was positive as well.

Moreover, the second activity **FrontLatP1** was recorded on the lateral frontal gyrus of YU254 (**Figure 51 (c)**). **FrontLatP1** was a positive peak occurring 28ms after vocalization onset with an average amplitude of $13\mu\text{V}$ (see **Figure 51 (e)**). Before vocalization onset, the activity recorded in the inferior frontal gyrus by electrode 2 and 3 was negative. After the end of **FrontInfP1** (577 ms after grunt onset on average), the activity was negative as well (see **Figure 52**).

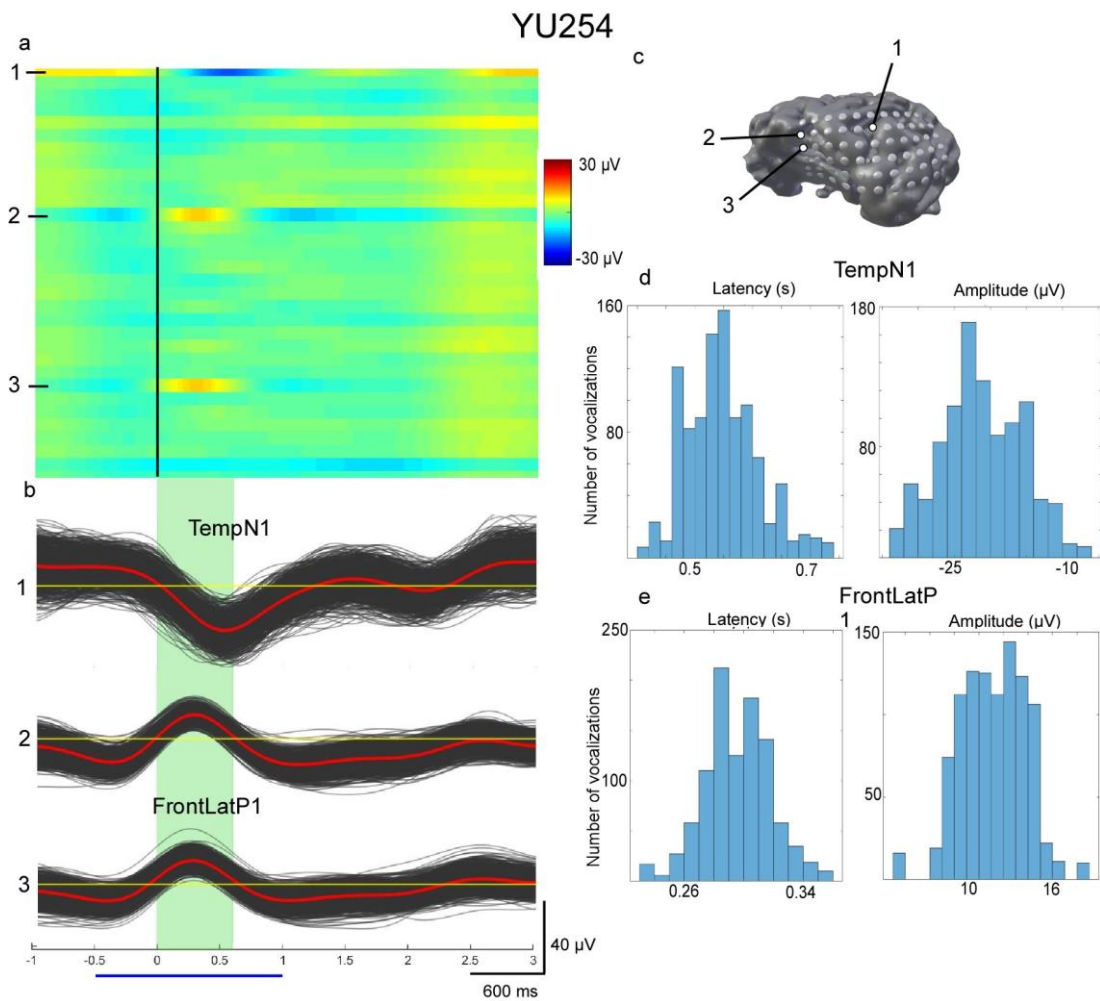


Figure 51. Cortical activity recorded during Grunt vocalizations in YU254. (a) spatiotemporal representation of the activity. (one electrode is represented as one line, the vertical black line represents vocalization onset). Three electrodes were selected and the bootstrap ($n = 1000$) evoked potentials are represented in (b). The horizontal blue bar represent the timings at which spatiotemporal mapping is illustrated on **Figure 52**. (c) electrodes mapping over the left hemisphere in YU254. The 3 selected electrodes are displayed in white. (d),(e) Characterization of peaks TempN1 and FrontLatP1 from bootstrap averages. Left panels : Latencies of the peaks in seconds. Right panels : Amplitudes of the peaks in μV .

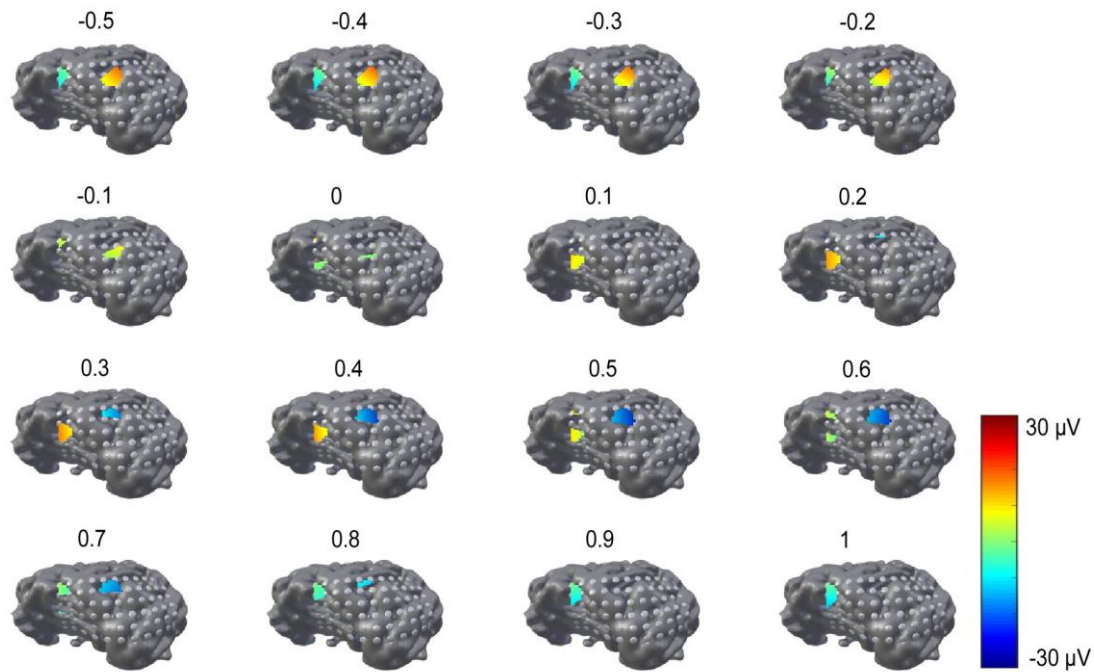


Figure 52. Spatiotemporal mapping of the cortical activity in YU254. The timings are those indicated by the blue horizontal bars in **Figure 51**.

In animal GI2028, we recorded cortical activity with a wide implant covering a large area of the left hemisphere. Two different regions of the brain showed activities occurring during Grunt vocalization.

In the sensorimotor area, covered among others by electrodes 1 and 2, we recorded a positive peak **SensMotP1** occurring on average 240ms after vocalization onset with an amplitude of 48μV (see **Figure 53 (d)**).

In the inferior frontal gyrus, covered among others by electrodes 3 and 4, we recorded another positive peak **FrontInfP2** occurring on average 250ms after grunts onsets with an amplitude of 38μV (see **Figure 53 (e)**).

Similarly, to what was recorded in YU254, after the end of both **SensMotP1** and **FrontInfP2**, electrodes 1, 2, 3 and 4 recorded slow negative oscillations. As can be seen on **Figure 54**, we noted a sort of rebound effect after positive peaks of activity.

GI2028

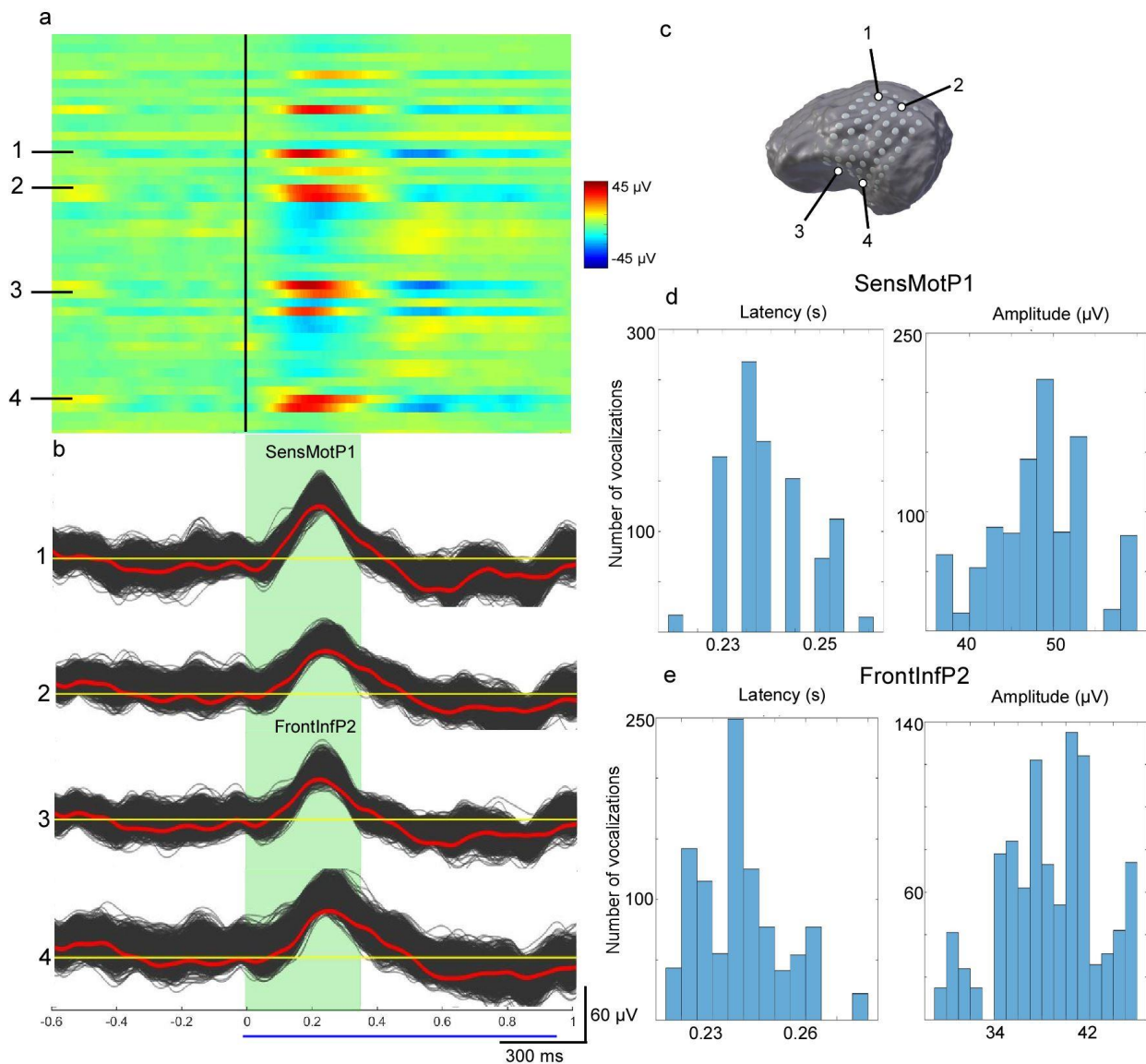


Figure 53. Cortical activity synchronized with Grunt vocalizations of GI2028. (a) spatiotemporal representation of the activity. (one electrode is represented as one line, the vertical black line represents vocalization onset). Four electrodes were selected and the bootstrap ($n = 1000$) evoked potentials are represented in (b). The horizontal blue bar represent the timings at which spatiotemporal mapping is illustrated on **Figure 54**. (c) electrodes mapping over the left hemisphere in GI2028. The 4 selected electrodes are displayed in white. (d), (e) Characterization of peaks SensMotP1 and FrontInfP2 from bootstrap averages. Left panels : Latencies of the peaks in seconds. Right panels : Amplitudes of the peaks in μV .

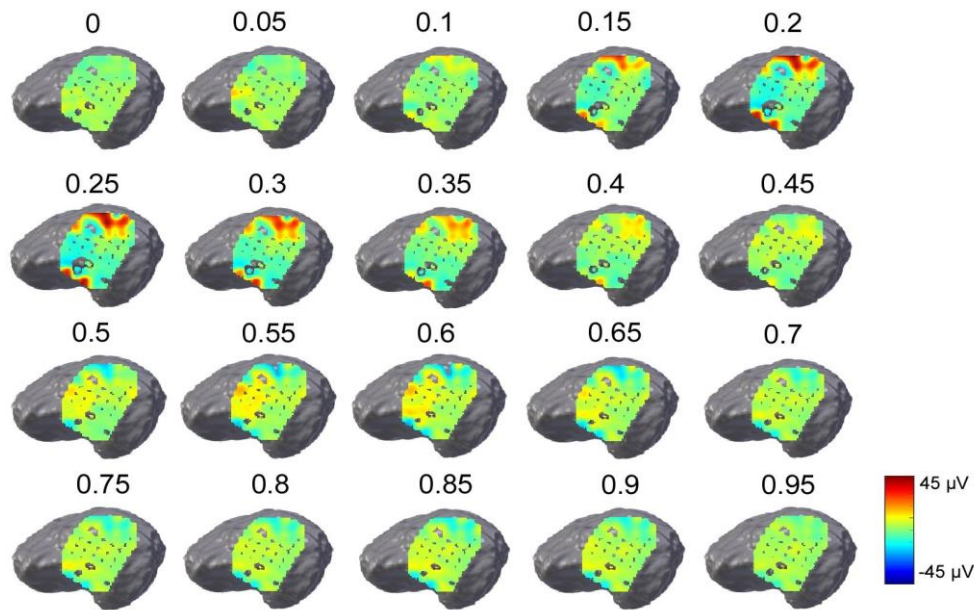


Figure 54. Spatiotemporal mapping of the cortical activity of GI2028. The timings are those indicated by the blue horizontal bar in **Figure 53**.

5.3. Discussion and perspectives

In this chapter we explored the cortical dynamics in relation with vocal behavior in three different minipigs. Since no previous investigations were available on minipigs, the animals were implanted in different areas of the brain to cover various locations. We identified three areas of interest with activities correlated to vocal production : the motor, sensorimotor and premotor cortex, the inferior frontal gyrus and the temporal gyrus.

Vocal production activated motor and premotor cortices in CH596. Results shown that two different areas in the motor and premotor cortices elicited two different types of activities. The first activity, a negative peak **PMcN2**, was located in the premotor cortex and had a latency of about 780ms before vocalization onset. After that, another short negative peak **PMcN1** in the premotor cortex was recorded about 45ms before vocalization onset. Additionally, in the motor cortex, a positive peak **McP1** occurred during the vocalization itself.

Production of vocalizations activated also lateral and inferior frontal cortex, along with sensori motor regions in YU254 and GI2028.

YU254 recording sites in the lateral frontal area **FrontLatP1** had a positive peak occurring during vocalizations, preceded and followed by slow negative oscillations. One recording site located latero-ventrally to the rostrum showed a negative peak **TempN1** occurring during Grunts.

In minipig GI2028, a **SensMotP1** and **FrontInfP2** activities were recorded, with positive peaks occurring during the Grunts. The recording sites were located over the inferior frontal cortex and the sensorimotor area.

The regions activated by vocalizations in minipigs show similarities with those related to voluntary vocal production in NHPs (ventral prefrontal cortex, ventral premotor cortex and motor cortex).

The findings of the present chapter have implications for the use of minipigs as a preclinical model for neuroscience studies, since we presented a way to perform chronic brain recordings overcoming the sinus problematic. However, assessing whether the minipigs vocalizations are indeed controlled cortically still requires investigations. We can consider a protocol in which the animal learns to vocalize in response to a stimulus to compare spontaneous and triggered vocalizations. A playback protocol is currently being tested, during which the animal will hear different types of sounds to assess which type could elicit the more responses.

A consistent feature observed in the three animals was the time-locked positive potential occurring during Grunt vocalizations. Despite the various locations of recording of this activity, the consistency of this response opens new perspectives of investigation. However, the electrodes placement over the 3D reconstructed brains of the animals was quite imprecise, which can lead to errors in the interpretation of the results. Additional studies have to be made to replicate the results obtained in these 3 animals and analyze further the activities of the left hemisphere in minipigs. To do so, a large dense surface probe is being designed to cover all the areas of interest. A denser probe than those used in this chapter might allow a more precise visualization of cortical dynamics and relations between the different areas of interest, according to the size of the cortical columns in minipigs (Ritter et al., 2021).

Moreover, one of the future aims will be to perform single unit recordings in freely moving minipigs in the cortical areas identified in this chapter. This could be achieved by the implantation of surface graphene probes similar to those used in rats in **Chapter 3**. Single unit recordings might also be achieved with the implantation of soft intracortical arrays.

Finally, another goal would be to perform long term recordings, with sessions of several hours. The recording could be performed in the stabulation pen to better take into account the normal behavior of the animal. Such studies might allow to record other types of vocalizations like those shown in **Chapter 4**. Very long term recordings in the stabulation pen might induce less stress and be more representative of the animal's global vocal productions.

6. General conclusion and perspectives

The goal of this thesis was to initiate an investigation of the cortical bases of vocalizations in minipigs. Since little is known about minipigs as preclinical models, we proceeded in an exploratory way to set the bases for future investigations. In parallel, we performed preliminary recordings with novel graphene-based cortical arrays on rats auditory cortex in response to pure tones. The results shown that both LFP and spike-like activities could be recorded from the surface of the brain and were correlated to auditory perception. This study allowed the decoding of pure tone frequencies from sharp events recorded on the surface of A1.

Toward understanding vocal networks in minipigs, we first built a new setup to record both vocal and cortical activities in freely moving and behaving animals, along with the development of a methodology to perform cortical implantation and analysis in these animals. We then investigated the cortical activity correlated to vocal production.

Secondly, we explored minipigs' vocal repertoire since it was not described in the literature. To do so, we sorted and analyzed vocalizations produced by freely moving minipigs in their housing pens. We reported 6 different types of vocalizations and characterized them in order to establish a base of the vocal repertoire of minipigs for future investigations.

Finally, we built a new setup for simultaneous cortical and vocal recordings in minipigs. In parallel, we developed a methodology to chronically implant subdural probes over the left hemisphere in this model. The results from 3 animals showed that several cortical areas presented activities correlated to vocal production: motor, premotor and sensorimotor cortices, along with the lateral frontal cortex and the inferior frontal cortex. In one animal, we identified a first activity before the vocalization onset over the premotor cortex and then a subsequent activity during the vocalization itself over the motor cortex. Then, in two other animals, we found activity over the lateral inferior frontal cortex starting around 400 ms before until more than 1 second after vocal onset, in the middle of which the temporal cortex was also activated. The identification of these areas was the first step to underpin the cortical dynamics underlying vocalizations in minipigs. Further experiments will now be required to confirm a whole activation scheme in all these areas in the same animals.

Also, as a perspective, the experimental setup has to be improved and further developed in several ways.

First, the detection of precise vocalization onset could be improved using statistical models. Since low frequency LFP were correlated to Grunt's onsets, the sorting of vocal productions with respect to noise might be facilitated or even automated. The sorting process was highly time consuming and such an automation might be more precise than manual annotation.

Additionally, the implantation of wide dense μ Electrode arrays over a large portion of the left hemisphere might allow a more precise analysis of the dynamics within and between cortical areas. Increasing the number of recording sites and the total covered surface of the hemisphere would permit investigations on other cortical areas such as frontal, motor/premotor and auditory cortices at a finer grain. How minipigs' cortical dynamics might defer for

vocalizations produced in response to vocalizations of peers compared to self-vocalizations would for instance be an interesting route of investigation.

At this stage, we only analyzed LFPs in our minipigs. Using intracortical probes to capture the spiking activity in the areas probed by ECoG would definitely bring additional detailed insight into the local ensemble dynamics underlying vocal production in these areas.

Additionally, a protocole allowing to assess the voluntary aspect of the production of vocalizations in minipigs is necessary. To do so, minipigs need to undergo a reinforcement program during which they will learn to produce vocalizations in response to an external stimulus (sound or visual clues, conspecifics vocalizations, etc...). The differences of cortical activity elicited by triggered and spontaneous vocalizations might provide insights into the cortical network involved in volitional vocal productions in minipigs.

Finally, we hypothesize that very long term sessions of several hours or even days in the housing environment might allow the recording of many more various vocalizations than short recordings with an experimenter. To perform that, the recording setup could be modified to allow such more ecological recordings. Recording larger datasets over long sessions would require to use machine learning techniques to automatically classify the vocalizations, and to decode the call type based on cortical activity as a proxy for speech BCIs in humans.

8. References

- Abdoun, O., Joucla, S., Mazzocco, C., & Yvert, B. (2011). NeuroMap: A Spline-Based Interactive Open-Source Software for Spatiotemporal Mapping of 2D and 3D MEA Data. *Frontiers in Neuroinformatics*, *4*, 119. <https://doi.org/10.3389/fninf.2010.00119>
- Ackermann, H., Hage, S. R., & Ziegler, W. (2014). Brain mechanisms of acoustic communication in humans and nonhuman primates: An evolutionary perspective. *The Behavioral and Brain Sciences*, *37*(6), 529–546. <https://doi.org/10.1017/S0140525X13003099>
- Aitken, P. G. (1981). Cortical control of conditioned and spontaneous vocal behavior in rhesus monkeys. *Brain and Language*, *13*(1), 171–184. [https://doi.org/10.1016/0093-934X\(81\)90137-1](https://doi.org/10.1016/0093-934X(81)90137-1)
- Albiach-Serrano, A., Bräuer, J., Cacchione, T., Zickert, N., & Amici, F. (2012). The effect of domestication and ontogeny in swine cognition (*Sus scrofa scrofa* and *S. s. Domestica*). *Applied Animal Behaviour Science*, *141*(1), 25–35. <https://doi.org/10.1016/j.applanim.2012.07.005>
- Algers, B. (1993). Nursing in Pigs: Communicating Needs and Distributing Resources'l. *Journal of Animal Science*, *71*, 2826–2831. <https://doi.org/10.2527/1993.71102826x>
- Allison, T., McCarthy, G., Luby, M., Puce, A., & Spencer, D. D. (1996). Localization of functional regions of human mesial cortex by somatosensory evoked potential recording and by cortical stimulation. *Electroencephalography and Clinical Neurophysiology*, *100*(2), 126–140. [https://doi.org/10.1016/0013-4694\(95\)00226-x](https://doi.org/10.1016/0013-4694(95)00226-x)
- Amiez, C., Sallet, J., Hopkins, W. D., Meguerditchian, A., Hadj-Bouziane, F., Ben Hamed, S., Wilson, C. R. E., Procyk, E., & Petrides, M. (2019). Sulcal organization in the medial frontal cortex provides insights into primate brain evolution. *Nature Communications*, *10*(1), 3437. <https://doi.org/10.1038/s41467-019-11347-x>

- Andics, A., Gábor, A., Gácsi, M., Faragó, T., Szabó, D., & Miklósi, Á. (2016). Neural mechanisms for lexical processing in dogs. *Science*, 353(6303), 1030. <https://doi.org/10.1126/science.aaf3777>
- Andics, A., Gácsi, M., Faragó, T., Kis, A., & Miklósi, A. (2014). Voice-Sensitive Regions in the Dog and Human Brain Are Revealed by Comparative fMRI. *Current Biology*, 24, 574–578.
- Appleby, M. C., Weary, D. M., Taylor, A. A., & Illmann, G. (1999). Vocal communication in pigs: Who are nursing piglets screaming at? *Ethology*, 105(10), 881–892. <https://doi.org/10.1046/j.1439-0310.1999.00459.x>
- Arnold, K., & Zuberbuhler, K. (2006). Semantic combinations in primate calls. *Nature Brief Communications*, June 2006, 1–2. <https://doi.org/10.1038/441303a>
- Arnold, K., & Zuberbuhler, K. (2017). Meaningful call combinations in a non-human primate. *Current Biology*, October, 1–3. <https://doi.org/10.1016/j.cub.2008.01.040>
- Arroyo, S., Lesser, R. P., Gordon, B., Uematsu, S., Jackson, D., & Webber, R. (1993). Functional significance of the mu rhythm of human cortex: An electrophysiologic study with subdural electrodes. *Electroencephalography and Clinical Neurophysiology*, 87(3), 76–87. [https://doi.org/10.1016/0013-4694\(93\)90114-B](https://doi.org/10.1016/0013-4694(93)90114-B)
- Aubin, T., Jouventin, P., & Charrier, I. (2015). Mother Vocal Recognition in Antarctic Fur Seal *Arctocephalus gazella* Pups: A Two-Step Process. *PLoS ONE*, September. <https://doi.org/10.1371/journal.pone.0134513>
- Babiloni, F., Cincotti, F., Carducci, F., Rossini, P. M., & Babiloni, C. (2001). Spatial enhancement of EEG data by surface Laplacian estimation: The use of magnetic resonance imaging-based head models. *Clinical Neurophysiology*, 112(5), 724–727. [https://doi.org/10.1016/S1388-2457\(01\)00494-1](https://doi.org/10.1016/S1388-2457(01)00494-1)

- Belin, P., Bodin, C., & Aglieri, V. (2018). A “voice patch” system in the primate brain for processing vocal information? *International Conference on Auditory Cortex 2017*, 366, 65–74. <https://doi.org/10.1016/j.heares.2018.04.010>
- Bensoussan, S., Cornil, M., Meunier-Salaün, M.-C., & Tallet, C. (2016). Piglets Learn to Use Combined Human-Given Visual and Auditory Signals to Find a Hidden Reward in an Object Choice Task. *PLOS ONE*, 11(10), e0164988. <https://doi.org/10.1371/journal.pone.0164988>
- Bensoussan, S., Tigeot, R., Lemasson, A., Meunier-Salaün, M.-C., & Tallet, C. (2019). Domestic piglets (*Sus scrofa domestica*) are attentive to human voice and able to discriminate some prosodic features. *Applied Animal Behaviour Science*, 210, 38–45. <https://doi.org/10.1016/j.applanim.2018.10.009>
- Binder, J. R., Frost, J. A., Hammeke, T. A., Cox, R. W., Rao, S. M., & Prieto, T. (1997). Human Brain Language Areas Identified by Functional Magnetic Resonance Imaging. *Journal of Neuroscience*, 17(1), 353–362. <https://doi.org/10.1523/JNEUROSCI.17-01-00353.1997>
- Bonnet, S., Bêche, J. F., Gharbi, S., Abdoun, O., Bocquetlet, F., Joucla, S., Agache, V., Sauter, F., Pham, P., Dupont, F., Matonti, F., Hoffart, L., Roux, S., Djilas, M., Kolomiets, B., Caplette, R., Chavane, F., Picaud, S., Yvert, B., & Guillemaud, R. (2012). NeuroPXI: A real-time multi-electrode array system for recording, processing and stimulation of neural networks and the control of high-resolution neural implants for rehabilitation. *Irbm*, 33(2), 55–60. <https://doi.org/10.1016/j.irbm.2012.01.013>
- Bradbury, J., & Vehrencamp, S. (2011). *Principles of animal communication*.
- Brajon, S., Laforest, J.-P., Bergeron, R., Tallet, C., & Devillers, N. (2015). The perception of humans by piglets: Recognition of familiar handlers and generalisation to unfamiliar humans. *Animal Cognition*, 18(6), 1299–1316. <https://doi.org/10.1007/s10071-015-0900-2>

- Brajon, S., Laforest, J.-P., Bergeron, R., Tallet, C., Hötzel, M.-J., & Devillers, N. (2015). Persistency of the piglet's reactivity to the handler following a previous positive or negative experience. *Applied Animal Behaviour Science*, *162*, 9–19. <https://doi.org/10.1016/j.applanim.2014.11.009>
- Brajon, S., Laforest, J.-P., Schmitt, O., & Devillers, N. (2015). The Way Humans Behave Modulates the Emotional State of Piglets. *PLOS ONE*, *10*(8), 1–17. <https://doi.org/10.1371/journal.pone.0133408>
- Bro, A., Sørensen, J. C., Nielsen, M. S., Rosendahl, F., Deding, D., Ettrup, K. S., Jensen, K. N., Jørgensen, R. L., & Glud, A. N. (2012). *The Göttingen minipig in translational neuroscience*. 8–9.
- Brudzynski, Stephan. (2010). *Handbook of Mammalian Vocalization* (Stefan Brudzynski, Ed.). Academic Press. [https://doi.org/10.1016/s1569-7339\(10\)70001-1](https://doi.org/10.1016/s1569-7339(10)70001-1)
- Burle, B., Spieser, L., Roger, C., Casini, L., Hasbroucq, T., & Vidal, F. (2015). Spatial and temporal resolutions of EEG: Is it really black and white? A scalp current density view. *International Journal of Psychophysiology: Official Journal of the International Organization of Psychophysiology*, *97*(3), 210–220. PubMed. <https://doi.org/10.1016/j.ijpsycho.2015.05.004>
- Buxhoeveden, D., Switala, A. E., Litaker, M., Roy, E., & Casanova, M. F. (2001). Lateralization of minicolumns in human planum temporale is Absent in Nonhuman Primate Cortex. *Brain Behav Evol*, *57*(6), 349–358.
- Castermans, T., Duvinage, M., Cheron, G., & Dutoit, T. (2014). About the cortical origin of the low-delta and high-gamma rhythms observed in EEG signals during treadmill walking. *Neuroscience Letters*, *561*, 166–170. <https://doi.org/10.1016/j.neulet.2013.12.059>
- Catani, M., Jones, D. K., & ffytche, D. H. (2005). Perisylvian language networks of the human brain. *Annals of Neurology*, *57*(1), 8–16. <https://doi.org/10.1002/ana.20319>

- Catchpole, C. K., & Slater, P. J. B. (2003). *Bird Song: Biological Themes and Variations*. Cambridge University Press. <https://books.google.fr/books?id=sB24pLg4gywC>
- Chakraborty, M., & Jarvis, E. D. (2015). Brain evolution by brain pathway duplication. *Philosophical Transactions of the Royal Society B: Biological Sciences*. <https://doi.org/10.1098/rstb.2015.0056>
- Chapman, R. F. (Ed.). (1998). Chemoreception. In *The Insects: Structure and Function* (4th ed., pp. 636–654). Cambridge University Press; Cambridge Core. <https://doi.org/10.1017/CBO9780511818202.025>
- Chen, X., Possel, J. K., Wacongne, C., van Ham, A. F., Klink, P. C., & Roelfsema, P. R. (2017). 3D printing and modelling of customized implants and surgical guides for non-human primates. *Journal of Neuroscience Methods*, 286, 38–55. <https://doi.org/10.1016/j.jneumeth.2017.05.013>
- Chen, Z., & Wiens, J. J. (2020). The origins of acoustic communication in vertebrates. *Nature Communications*, 11(1), 1–8. <https://doi.org/10.1038/s41467-020-14356-3>
- Cheney, D. L., & Seyfarth, R. M. (2018). Flexible usage and social function in primate vocalizations. *PNAS*, 1–6. <https://doi.org/10.1073/pnas.1717572115>
- Cochin, S., Barthelemy, C., Roux, S., & Martineau, J. (1999). Observation and execution of movement: Similarities demonstrated by quantified electroencephalography. *European Journal of Neuroscience*, 11(5), 1839–1842. <https://doi.org/10.1046/j.1460-9568.1999.00598.x>
- Coudé, G., Ferrari, P. F., Rodà, F., Maranesi, M., Borelli, E., Veroni, V., Monti, F., Rozzi, S., & Fogassi, L. (2011). Neurons controlling voluntary vocalization in the macaque ventral premotor cortex. *PLoS ONE*, 6(11), 1–10. <https://doi.org/10.1371/journal.pone.0026822>

- da Silva Cordeiro, A. F., de Alencar Nääs, I., Oliveira, S. R. M., Violaro, F., de Almeida, A. C. M., & Neves, D. P. (2013). Understanding vocalization might help to assess stressful conditions in piglets. *Animals*, 3(3), 923–934. <https://doi.org/10.3390/ani3030923>
- Darwin, C. (1877). *L'expression des émotions chez l'homme et les animaux*. sn. <https://books.google.fr/books?id=ElkFQbJnArAC>
- David, S. V., & Shamma, S. A. (2013). Integration over multiple timescales in primary auditory cortex. *The Journal of Neuroscience: The Official Journal of the Society for Neuroscience*, 33(49), 19154–19166. <https://doi.org/10.1523/JNEUROSCI.2270-13.2013>
- Déaux, E. C., Allen, A. P., Clarke, J. A., & Charrier, I. (2016). Concatenation of ' alert ' and ' identity ' segments in dingoes ' alarm calls. *Nature Publishing Group, February*, 1–9. <https://doi.org/10.1038/srep30556>
- Deiber, M. P., Wise, S. P., Honda, M., Catalan, M. J., Grafman, J., & Hallett, M. (1997). Frontal and parietal networks for conditional motor learning: A positron emission tomography study. *Journal of Neurophysiology*, 78(2), 977–991. <https://doi.org/10.1152/jn.1997.78.2.977>
- Diamond, I. T., & Neff, W. D. (1957). Ablation of temporal cortex and discrimination of auditory patterns. *Journal of Neurophysiology*, 20(3), 300–315. <https://doi.org/10.1152/jn.1957.20.3.300>
- Dingle, H., & Caldwell, R. L. (1969). The Aggressive and Territorial Behaviour of the Mantis Shrimp *Gonodactylus bredini* Manning (Crustacea: Stomatopoda). *Behaviour*, 33(1/2), 115–136. JSTOR.
- Dujardin, E., & Jürgens, U. (2005). Afferents of vocalization-controlling periaqueductal regions in the squirrel monkey. *Brain Research*, 1034(1), 114–131. <https://doi.org/10.1016/j.brainres.2004.11.048>

- Dujardin, E., & Jürgens, U. (2006). Call type-specific differences in vocalization-related afferents to the periaqueductal gray of squirrel monkeys (*Saimiri sciureus*). *Behavioural Brain Research*, *168*(1), 23–36. <https://doi.org/10.1016/j.bbr.2005.10.006>
- Ehret, G. (1987). Left hemisphere advantage in the mouse brain for recognizing ultrasonic communication calls. *Nature*, *325*(6101), 249–251. <https://doi.org/10.1038/325249a0>
- Engesser, S., Crane, J. M. S., Savage, J. L., Russell, A. F., & Townsend, S. W. (2015). Experimental Evidence for Phonemic Contrasts in a Nonhuman Vocal System. *PLOS Biology*, *13*(6), e1002171. <https://doi.org/10.1371/journal.pbio.1002171>
- Engineer, C. T., Perez, C. a., Chen, Y. H., Carraway, R. S., Reed, A. C., Shetake, J. a., Jakkamsetti, V., Chang, K. Q., & Kilgard, M. P. (2008). Cortical activity patterns predict speech discrimination ability. *Nature Neuroscience*, *11*(5), 603–608. <https://doi.org/10.1038/nn.2109>
- Erné, S. N., Scheer, H. J., Hoke, M., Pantew, C., & Lütkenhöner, B. (1987). Brainstem auditory evoked magnetic fields in response to stimulation with brief tone pulses. *The International Journal of Neuroscience*, *37*(3–4), 115–125. <https://doi.org/10.3109/00207458708987142>
- Fallegger, F., Schiavone, G., Pirondini, E., Wagner, F. B., Vachicouras, N., Serex, L., Zegarek, G., May, A., Constanthin, P., Palma, M., Khoshnevis, M., Van Roost, D., Yvert, B., Courtine, G., Schaller, K., Bloch, J., & Lacour, S. P. (2021). MRI-Compatible and Conformal Electrocorticography Grids for Translational Research. *Advanced Science*, *n/a*(n/a), 2003761. <https://doi.org/10.1002/advs.202003761>
- Fedorov, A., Beichel, R., Kalpathy-Cramer, J., Finet, J., Fillion-Robin, J. C., Pujol, S., Bauer, C., Jennings, D., Fennessy, F., Sonka, M., Buatti, J., Aylward, S., Miller, J. V., Pieper, S., & Kikinis, R. (2012). 3D Slicer as an image computing platform for the Quantitative Imaging Network. *Magnetic Resonance Imaging*, *30*(9), 1323–1341. <https://doi.org/10.1016/j.mri.2012.05.001>

- Félix, B., Léger, M. E., Albe-Fessard, D., Marcilloux, J. C., Rampin, O., Laplace, J. P., Duclos, A., Fort, F., Gougis, S., Costa, M., & Duclos, N. (1999). Stereotaxic atlas of the pig brain. *Brain Research Bulletin*, *49*(1–2), 1–138. [https://doi.org/10.1016/S0361-9230\(99\)00012-X](https://doi.org/10.1016/S0361-9230(99)00012-X)
- Ferrari, P. F., Roda, F., Maranesi, M., Borelli, E., Coude, G., Veroni, V., Monti, F., Rozzi, S., & Fogassi, L. (2011). Neurons Controlling Voluntary Vocalization in the Macaque Ventral Premotor Cortex. *PLoS ONE*, *6*(2783), 1–10. <https://doi.org/10.1371/journal.pone.0026822>
- Fitch, R. H., Brown, C. P., & Tallal, P. (1993). Left hemisphere specialization for auditory temporal processing in rats. *Annals of the New York Academy of Sciences*, *682*, 346–347. <https://doi.org/10.1111/j.1749-6632.1993.tb22989.x>
- Fitch, T., & Hauser, M. D. (2004). Computational constraints on syntactic processing in nonhuman primates. *Science*, *303*(5656), 377–380.
- Fraser, D. (1975). Vocalizations of Isolated Piglets. I. Sources of Variation and Relationships Among Measures Vocalizations of Isolated Piglets. I. Sources of. *Animal Studies Repository*, *1*, 387–394.
- Friederici, A. D. (2009). Pathways to language: Fiber tracts in the human brain. *Trends in Cognitive Sciences*, *13*(4), 175–181. <https://doi.org/10.1016/j.tics.2009.01.001>
- Fukushima, M., Saunders, R. C., Fujii, N., Averbeck, B. B., & Mishkin, M. (2014). Modeling vocalization with ECoG cortical activity recorded during vocal production in the macaque monkey. *2014 36th Annual International Conference of the IEEE Engineering in Medicine and Biology Society, EMBC 2014*, 6794–6797. <https://doi.org/10.1109/EMBC.2014.6945188>
- Garcia, M., Gingras, B., Bowling, D. L., Herbst, C. T., Boeckle, M., Locatelli, Y., & Fitch, W. T. (2016). Structural Classification of Wild Boar (*Sus scrofa*) Vocalizations. *Ethology*, *122*(4), 329–342. <https://doi.org/10.1111/eth.12472>

- Gardner, B. T., & Gardner, R. A. (1975). Evidence for sentence constituents in the early utterances of child and chimpanzee. *Journal of Experimental Psychology: General*, *104*(3), 244–267. <https://doi.org/10.1037/0096-3445.104.3.244>
- Gardner, R. A., & Gardner, B. T. (1969). Teaching Sign Language to a Chimpanzee. *Science*, *165*(3894), 664–672.
- Gaudin, E. P. (1968). On the Middle Ear of Birds. *Acta Oto-Laryngologica*, *65*(1–6), 316–326.
- Gavrilov, N., Hage, S. R., & Nieder, A. (2017). Functional Specialization of the Primate Frontal Lobe during Cognitive Control of Vocalizations. *Cell Reports*, *21*(9), 2393–2406. <https://doi.org/10.1016/j.celrep.2017.10.107>
- Gemba, H., Kyuhou, S., Matsuzaki, R., & Amino, Y. (1999). Cortical field potentials associated with audio-initiated vocalization in monkeys. *Neuroscience Letters*, *272*(1), 49–52. [https://doi.org/10.1016/s0304-3940\(99\)00570-4](https://doi.org/10.1016/s0304-3940(99)00570-4)
- Gerencsér, L., Pérez Fraga, P., Lovas, M., Újváry, D., & Andics, A. (2019). Comparing interspecific socio-communicative skills of socialized juvenile dogs and miniature pigs. *Animal Cognition*, *22*(6), 917–929. <https://doi.org/10.1007/s10071-019-01284-z>
- Gevins, A., Smith, M. E., McEvoy, L., & Yu, D. (1997). High-resolution EEG mapping of cortical activation related to working memory: Effects of task difficulty, type of processing, and practice. *Cerebral Cortex (New York, N.Y. : 1991)*, *7*(4), 374–385. <https://doi.org/10.1093/cercor/7.4.374>
- Gielsing, E. T., Nordquist, R. E., & van der Staay, F. J. (2011). Assessing learning and memory in pigs. *Animal Cognition*, *14*(2), 151–173. <https://doi.org/10.1007/s10071-010-0364-3>
- Gierthmuehlen, M., Ball, T., Henle, C., Wang, X., Rickert, J., Raab, M., Freiman, T., Stieglitz, T., & Kaminsky, J. (2011). Evaluation of μ ECoG electrode arrays in the minipig: Experimental procedure and neurosurgical approach. *Journal of Neuroscience Methods*, *202*(1), 77–86. <https://doi.org/10.1016/j.jneumeth.2011.08.021>

- Goumon, S., Illmann, G., Leszkowová, I., Dostálová, A., & Cantor, M. (2020). Dyadic affiliative preferences in a stable group of domestic pigs. *Applied Animal Behaviour Science*, 230. <https://doi.org/10.1016/j.applanim.2020.105045>
- Gower, D. B. (1972). 16-Unsaturated C19 steroids a review of their chemistry, biochemistry and possible physiological role. *Journal of Steroid Biochemistry*, 3(1), 45–103. [https://doi.org/10.1016/0022-4731\(72\)90011-8](https://doi.org/10.1016/0022-4731(72)90011-8)
- Green, H. D., & Walker, A. E. (1938). THE EFFECTS OF ABLATION OF THE CORTICAL MOTOR FACE AREA IN MONKEYS. *Journal of Neurophysiology*, 1(3), 262–280. <https://doi.org/10.1152/jn.1938.1.3.262>
- Grinnell, A. (2004). Rebound excitation (Off-responses) following non-neural suppression in the cochleas of echolocating bats. *Journal of Comparative Physiology*, 82, 179–194.
- Hackett, T. a. (2015). Anatomical organization of the auditory cortex. *Handbook of Clinical Neurology*, 129, 27–53. <https://doi.org/10.1016/B978-0-444-62630-1.00002-0>
- Hage, S. R. (2018). Dual neural network model of speech and language evolution: New insights on flexibility of vocal production systems and involvement of frontal cortex. *Current Opinion in Behavioral Sciences*, 21, 80–87. <https://doi.org/10.1016/j.cobeha.2018.02.010>
- Hage, S. R., Gavrillov, N., & Nieder, A. (2013). Cognitive control of distinct vocalizations in rhesus monkeys. *Journal of Cognitive Neuroscience*. https://doi.org/10.1162/jocn_a_00428
- Hage, S. R., & Jürgens, U. (2006). On the Role of the Pontine Brainstem in Vocal Pattern Generation: A Telemetric Single-Unit Recording Study in the Squirrel Monkey. *Journal of Neuroscience*, 26(26), 7105–7115. <https://doi.org/10.1523/JNEUROSCI.1024-06.2006>

- Hage, S. R., & Nieder, A. (2016). Dual Neural Network Model for the Evolution of Speech and Language. In *Trends in Neurosciences*. <https://doi.org/10.1016/j.tins.2016.10.006>
- Hämäläinen, M., Hari, R., Ilmoniemi, R. J., Knuutila, J., & Lounasmaa, O. V. (1993). Magnetoencephalography—Theory, instrumentation, and applications to noninvasive studies of the working human brain. *Reviews of Modern Physics*, 65(2), 413–497. <https://doi.org/10.1103/RevModPhys.65.413>
- Hare, B., & Tomasello, M. (2005). Human-like social skills in dogs? *Trends in Cognitive Sciences*, 9(9), 439–444. <https://doi.org/10.1016/j.tics.2005.07.003>
- Hari, R., Pelizzone, M., Mäkelä, J., Hällström, J., Leinonen, L., & Lounasmaa, O. V. (1987). Neuromagnetic Responses of the Human Auditory Cortex to On-and Offsets of Noise Bursts. *Audiology: Official Organ of the International Society of Audiology*, 26, 31–43.
- Harvey, E. N. (1952). Bioluminescence. *Journal of Chemical Education*, 29(9), 474. <https://doi.org/10.1021/ed029p474.2>
- Hast, M. H., Fischer, J. M., Wetzell, A. B., & Thompson, V. E. (1974). Cortical motor representation of the laryngeal muscles in *Macaca mulatta*. *Brain Research*, 73(2), 229–240. [https://doi.org/10.1016/0006-8993\(74\)91046-4](https://doi.org/10.1016/0006-8993(74)91046-4)
- Hauser, M., Chomsky, N., & Tecumseh Fitch, W. (2002). The faculty of language: What is it, who has it, and how did it evolve? *Science*.
- Hayes, K., & Hayes, C. (1951). The intellectual development of a home-raised chimpanzee. *Proceedings of the American Philosophical Society*, 95(2), 105–109.
- Heelan, C., Lee, J., O'Shea, R., Lynch, L., Brandman, D. M., Truccolo, W., & Nurmikko, A. V. (2019). Decoding speech from spike-based neural population recordings in secondary auditory cortex of non-human primates. *Communications Biology*, 2(1), 466. <https://doi.org/10.1038/s42003-019-0707-9>

- Hefner, H. E., & Heffner, R. S. (1986). Effect of unilateral and bilateral auditory cortex lesions on the discrimination of vocalizations by Japanese macaques. *Journal of Neurophysiology*, *56*(3), 683–701.
- Held, S., Cooper, J., & Mendl, M. (2008). Advances in the Study of Cognition, Behavioural Priorities and Emotions. In *The Welfare of Pigs* (pp. 47–94). https://doi.org/10.1007/978-1-4020-8909-1_3
- Helke, K. L., Nelson, K. N., Sargeant, A. M., Jacob, B., McKeag, S., Haruna, J., Vemireddi, V., Greeley, M., Brocksmith, D., Navratil, N., Stricker-Krongrad, A., & Hollinger, C. (2016). Pigs in Toxicology: Breed Differences in Metabolism and Background Findings. *Toxicologic Pathology*, *44*(4), 575–590. <https://doi.org/10.1177/0192623316639389>
- Henry, K. R. (1985). ON and OFF components of the auditory brainstem response have different frequency- and intensity-specific properties. *Hearing Research*, *18*(3), 245–251. [https://doi.org/10.1016/0378-5955\(85\)90041-3](https://doi.org/10.1016/0378-5955(85)90041-3)
- Hickok, G., & Poeppel, D. (2004). Dorsal and ventral streams: A framework for understanding aspects of the functional anatomy of language. *Cognition*, *92*(1–2), 67–99. <https://doi.org/10.1016/j.cognition.2003.10.011>
- Hickok, G., & Poeppel, D. (2007). *The cortical organization of speech processing*. *8*(May), 393–402. <https://doi.org/10.1038/nrn2113>
- Higham, J. P., & Hebets, E. A. (2013). An introduction to multimodal communication. *Behav Ecol Sociobiol*, *67*(September 2013), 1381–1388. <https://doi.org/10.1007/s00265-013-1590-x>
- Hölldobler, B., & Wilson, E. (2004). The multiple recruitment systems of the african weaver ant *Oecophylla longinoda* (Latreille) (Hymenoptera: Formicidae). *Behavioral Ecology and Sociobiology*, *3*, 19–60.

- Howard, S. R., Avarguès-Weber, A., Garcia, J. E., Greentree, A. D., & Dyer, A. G. (2019). Symbolic representation of numerosity by honeybees (*Apis mellifera*): Matching characters to small quantities. *Proceedings of the Royal Society B: Biological Sciences*, 286(1904), 20190238. <https://doi.org/10.1098/rspb.2019.0238>
- Hughes, J. R. (2008). Gamma, fast, and ultrafast waves of the brain: Their relationships with epilepsy and behavior. *Epilepsy & Behavior: E&B*, 13(1), 25–31. <https://doi.org/10.1016/j.yebeh.2008.01.011>
- Irestedt, M., Jonsson, K., Fjeldsa, J., Christidis, L., & Ericson, P. G. (2009). An unexpectedly long history of sexual selection in birds-of-paradise. *BioMed Central*, May 2014. <https://doi.org/10.1186/1471-2148-9-235>
- Jelsing, J., Hay-Schmidt, A., Dyrby, T., Hemmingsen, R., Uylings, H. B. M., & Pakkenberg, B. (2006). The prefrontal cortex in the Göttingen minipig brain defined by neural projection criteria and cytoarchitecture. *Brain Research Bulletin*, 70(4–6), 322–336. <https://doi.org/10.1016/j.brainresbull.2006.06.009>
- Jensen, P., & Algers, B. (1984). An ethogram of piglet vocalizations during suckling. *Applied Animal Ethology*, 11, 237–248.
- Jensen, P., & Redbo, I. (1987). Behaviour during Nest Leaving in Free-Ranging Domestic Pigs. *Applied Animal Behaviour Science*, 18, 355–362.
- Jiang, X. (2018). *Prefrontal Cortex: Role in Language Communication during Social Interaction*.
- Jobsis, F. (1977). Noninvasive, infrared monitoring of cerebral and myocardial oxygen sufficiency and circulatory parameters. *Science*, 198(4323), 1264. <https://doi.org/10.1126/science.929199>

- Jones, R. B., & Nowell, N. W. (1973). The coagulating glands as a source of aversive and aggression-inhibiting pheromone(s) in the male albino mouse. *Physiology & Behavior*, 11(4), 455–462. [https://doi.org/10.1016/0031-9384\(73\)90031-0](https://doi.org/10.1016/0031-9384(73)90031-0)
- Jürgens, U. (2002). Neural pathways underlying vocal control. *Neuroscience & Biobehavioral Reviews*, 26(2), 235–258. [https://doi.org/10.1016/S0149-7634\(01\)00068-9](https://doi.org/10.1016/S0149-7634(01)00068-9)
- Jürgens, U. (2009). The Neural Control of Vocalization in Mammals: A Review. *Journal of Voice*, 23(1), 1–10. <https://doi.org/10.1016/j.jvoice.2007.07.005>
- Jürgens, U., & Pratt, R. (1979). Role of the periaqueductal grey in vocal expression of emotion. *Brain Research*, 167(2), 367–378. [https://doi.org/10.1016/0006-8993\(79\)90830-8](https://doi.org/10.1016/0006-8993(79)90830-8)
- Jürgens, Uwe. (2000). Localization of a pontine vocalization-controlling area. *The Journal of the Acoustical Society of America*, 108(4), 1393–1396. <https://doi.org/10.1121/1.1289204>
- Jürgens, Uwe. (2002). Neural pathways underlying vocal control. *Neuroscience and Biobehavioral Reviews*, 26(2), 235–258. [https://doi.org/10.1016/s0149-7634\(01\)00068-9](https://doi.org/10.1016/s0149-7634(01)00068-9)
- Kalatsky, V. a., Polley, D. B., Merzenich, M. M., Schreiner, C. E., & Stryker, M. P. (2005). Fine functional organization of auditory cortex revealed by Fourier optical imaging. *Proceedings of the National Academy of Sciences of the United States of America*, 102(37), 13325–13330. <https://doi.org/10.1073/pnas.0505592102>
- Kern, M., Ball, T., Mutschler, I., Aertsen, A., & Schulze-Bonhage, A. (2009). *Signal quality of simultaneously recorded invasive and non-invasive EEG*.
- Khazipov, R., Zaynutdinova, D., Ogievetsky, E., Valeeva, G., Mitrukhnina, O., Manent, J.-B., & Represa, A. (2015). Atlas of the Postnatal Rat Brain in Stereotaxic Coordinates. *Frontiers in Neuroanatomy*, 9(December), 161. <https://doi.org/10.3389/fnana.2015.00161>

- Khodagholi, D., Gelinias, J. N., Thesen, T., Doyle, W., Devinsky, O., Malliaras, G. G., & Buzsáki, G. (2015). NeuroGrid: Recording action potentials from the surface of the brain. *Nature Neuroscience*, *18*(2), 310–315. PubMed. <https://doi.org/10.1038/nn.3905>
- Khoshnevis, M., Carozzo, C., Bonnefont-Rebeix, C., Belluco, S., Leveneur, O., Chuzel, T., Pillet-Michelland, E., Dreyfus, M., Roger, T., Berger, F., & Ponce, F. (2017). Development of induced glioblastoma by implantation of a human xenograft in Yucatan minipig as a large animal model. *Journal of Neuroscience Methods*, *282*, 61–68. <https://doi.org/10.1016/j.jneumeth.2017.03.007>
- Khoshnevis, M., Carozzo, C., Brown, R., Bardiès, M., Bonnefont-Rebeix, C., Belluco, S., Nennig, C., Marcon, L., Tillement, O., Gehan, H., Louis, C., Zahi, I., Buronfosse, T., Roger, T., & Ponce, F. (2020). Feasibility of intratumoral ¹⁶⁵Holmium siloxane delivery to induced U87 glioblastoma in a large animal model, the Yucatan minipig. *PLoS ONE*, *15*(6), 1–19. <https://doi.org/10.1371/journal.pone.0234772>
- Kiley, M. (1972). The Vocalizations of Ungulates , their Causation and Function. *Z. Tierpsychol.*, *31*, 171–222.
- King, S. L., & Janik, V. M. (2013). Bottlenose dolphins can use learned vocal labels to address each other. *PNAS*, *May*. <https://doi.org/10.1073/pnas.1304459110>
- Kirzinger, A., & Jürgens, U. (1982). Cortical lesion effects and vocalization in the squirrel monkey. *Brain Research*, *233*(2), 299–315. [https://doi.org/10.1016/0006-8993\(82\)91204-5](https://doi.org/10.1016/0006-8993(82)91204-5)
- Kluender, K., Diehl, R., & Killeen, P. (1987). Japanese quail can learn phonetic categories. *Science*, *237*(4819), 1195–1197. <https://doi.org/10.1126/science.3629235>
- Koba, Y., & Tanida, H. (2001). How do miniature pigs discriminate between people?: Discrimination between people wearing coveralls of the same colour. *Applied Animal Behaviour Science*, *73*(1), 45–58. [https://doi.org/10.1016/S0168-1591\(01\)00106-X](https://doi.org/10.1016/S0168-1591(01)00106-X)

- Kopp-Scheinflug, C., Sinclair, J. L., & Linden, J. F. (2018). When Sound Stops: Offset Responses in the Auditory System. *Special Issue: Time in the Brain*, 41(10), 712–728. <https://doi.org/10.1016/j.tins.2018.08.009>
- Kozhevnikov, A. A., & Fee, M. S. (2007). Singing-related activity of identified HVC neurons in the zebra finch. *Journal of Neurophysiology*, 97(6), 4271–4283. <https://doi.org/10.1152/jn.00952.2006>
- Kuhl, P. K., & Miller, J. D. (1975). Speech perception by the chinchilla: Voiced-voiceless distinction in alveolar plosive consonants. *Science (New York, N.Y.)*, 190(4209), 69–72. <https://doi.org/10.1126/science.1166301>
- Laidre, M. E., & Johnstone, R. A. (2013). Animal signals. *Current Biology*, 23(18), R829–R833. <https://doi.org/10.1016/j.cub.2013.07.070>
- Lane, F. W. (1960). *Kingdom of the Octopus: The Life History of the Cephalopoda*. Sheridan House. <https://books.google.fr/books?id=UPgLAQAIAAJ>
- Larson, C. R., & Kistler, M. K. (1984). Periaqueductal gray neuronal activity associated with laryngeal EMG and vocalization in the awake monkey. *Neuroscience Letters*, 46(3), 261–266. [https://doi.org/10.1016/0304-3940\(84\)90109-5](https://doi.org/10.1016/0304-3940(84)90109-5)
- Leliveld, L. M. C., Döpjan, S., Tuchscherer, A., & Puppe, B. (2020). Hemispheric Specialization for Processing the Communicative and Emotional Content of Vocal Communication in a Social Mammal, the Domestic Pig. *Frontiers in Behavioral Neuroscience*, 14, 217. <https://doi.org/10.3389/fnbeh.2020.596758>
- Liégeois-Chauvel, C., Musolino, A., Badier, J. M., Marquis, P., & Chauvel, P. (1994). Evoked potentials recorded from the auditory cortex in man: Evaluation and topography of the middle latency components. *Electroencephalography and Clinical Neurophysiology*, 92(3), 204–214. [https://doi.org/10.1016/0168-5597\(94\)90064-7](https://doi.org/10.1016/0168-5597(94)90064-7)

- Lind, M. N., Moustgaard, A., Jelsing, J., Vajta, G., Cumming, P., & Hansen, A. K. (2007). The use of pigs in neuroscience: Modeling brain disorders. *Neuroscience and Biobehavioral Reviews*, 31, 728–751. <https://doi.org/10.1016/j.neubiorev.2007.02.003>
- Logothetis, N. K., Pauls, J., Augath, M., Trinath, T., & Oeltermann, A. (2001). Neurophysiological investigation of the basis of the fMRI signal. *Nature*, 412(6843), 150–157. <https://doi.org/10.1038/35084005>
- Loh, K. K., Petrides, M., Hopkins, W. D., Procyk, E., & Amiez, C. (2017). Cognitive control of vocalizations in the primate ventrolateral-dorsomedial frontal (VLF-DMF) brain network. *Neuroscience and Biobehavioral Reviews*, 82, 32–44. <https://doi.org/10.1016/j.neubiorev.2016.12.001>
- Loh, K. K., Procyk, E., Neveu, R., Lamberton, F., Hopkins, W. D., Petrides, M., & Amiez, C. (2020). Cognitive control of orofacial motor and vocal responses in the ventrolateral and dorsomedial human frontal cortex. *Proceedings of the National Academy of Sciences*, 117(9), 4994–5005. <https://doi.org/10.1073/pnas.1916459117>
- Lorenzo, D., Velluti, J. C., Crispino, L., & Velluti, R. (1977). Cerebellar sensory functions: Rat auditory evoked potentials. *Experimental Neurology*, 55(3, Part 1), 629–636. [https://doi.org/10.1016/0014-4886\(77\)90289-8](https://doi.org/10.1016/0014-4886(77)90289-8)
- Ludlow, C. L., Rosenberg, J., Fair, C., Buck, D., Schesselman, S., & Salazar, A. (1986). Brain lesions associated with nonfluent aphasia fifteen years following penetrating head injury. *Brain: A Journal of Neurology*, 109 (Pt 1), 55–80. <https://doi.org/10.1093/brain/109.1.55>
- Lütke, L., Häusler, U., & Jürgens, U. (2000). Neuronal activity in the medulla oblongata during vocalization. A single-unit recording study in the squirrel monkey. *Behavioural Brain Research*, 116(2), 197–210. [https://doi.org/10.1016/s0166-4328\(00\)00272-2](https://doi.org/10.1016/s0166-4328(00)00272-2)
- Mäkelä, J. P., Hämäläinen, M., Hari, R., & McEvoy, L. (1994). Whole-head mapping of middle-latency auditory evoked magnetic fields. *Electroencephalography and Clinical*

Neurophysiology/Evoked Potentials Section, 92(5), 414–421.
[https://doi.org/10.1016/0168-5597\(94\)90018-3](https://doi.org/10.1016/0168-5597(94)90018-3)

Manteuffel, G., Puppe, B., & Schön, P. C. (2004). Vocalization of farm animals as a measure of welfare. *Annual Review of Neuroscience*, 88, 163–182.
<https://doi.org/10.1016/j.applanim.2004.02.012>

Marchant, J. N., Whittaker, X., & Broom, D. M. (2001). Vocalisations of the adult female domestic pig during a standard human approach test and their relationships with behavioural and heart rate measures. *Applied Animal Behaviour Science*, 72(1), 23–39.

Marino, L., & Colvin, C. M. (2015). Thinking pigs: A comparative review of cognition, emotion, and personality in *Sus domesticus*. *International Journal of Comparative Psychology*, 28.

Marler, P., & Tamura, M. (1964). Culturally transmitted patterns of vocal behavior in sparrows. *Science (New York, N.Y.)*, 146(3650), 1483–1486.
<https://doi.org/10.1126/science.146.3650.1483>

Mathevon, N., Casey, C., Reichmuth, C., & Charrier, I. (2017). Northern Elephant Seals Memorize the Rhythm and Timbre of Their Rivals' Voices. *Current Biology*, 27(15), 2352–2356.e2. <https://doi.org/10.1016/j.cub.2017.06.035>

McAnulty, P. A., Dayan, A. D., Ganderup, N. C., & Hastings, K. L. (2011). *The Minipig in Biomedical Research*. Taylor & Francis. https://books.google.fr/books?id=-a1-yy9_4MIC

McCormick, D. A., McGinley, M. J., & Salkoff, D. B. (2015). Brain state dependent activity in the cortex and thalamus. *Current Opinion in Neurobiology*, 31, 133–140.
<https://doi.org/10.1016/j.conb.2014.10.003>

- McLeman, M. A., Mendl, M., Jones, R. B., White, R., & Wathes, C. M. (2005). Discrimination of conspecifics by juvenile domestic pigs, *Sus scrofa*. *Animal Behaviour*, *70*(2), 451–461. <https://doi.org/10.1016/j.anbehav.2004.11.013>
- McCloughlin, M. P., Stewart, R., & McElligott, A. G. (2019). Automated bioacoustics: Methods in ecology and conservation and their potential for animal welfare monitoring. *Journal of the Royal Society, Interface*, *16*(155), 20190225. <https://doi.org/10.1098/rsif.2019.0225>
- Meeren, H. K. M., van Cappellen van Walsum, A. M., van Luijckelaar, E. L. J. M., & Coenen, A. M. L. (2001). Auditory evoked potentials from auditory cortex, medial geniculate nucleus, and inferior colliculus during sleep–wake states and spike-wave discharges in the WAG/Rij rat. *Brain Research*, *898*(2), 321–331. [https://doi.org/10.1016/S0006-8993\(01\)02209-0](https://doi.org/10.1016/S0006-8993(01)02209-0)
- Mesgarani, N., David, S. V., Fritz, J. B., & Shamma, S. A. (2008). Phoneme representation and classification in primary auditory cortex. *J Acoust Soc Am*, *123*(2), 899–909. <https://doi.org/10.1121/1.2816572>
- Miklosi, A. (2014). *Dog Behaviour, Evolution, and Cognition*. OUP Oxford. <https://books.google.fr/books?id=L3CWBQAAQBAJ>
- Møller, A. P. (1988). False Alarm Calls as a Means of Resource Usurpation in the Great Tit *Parus major*. *Ethology*, *79*(1), 25–30. <https://doi.org/10.1111/j.1439-0310.1988.tb00697.x>
- Molnar, C., Pongracz, P., Faragó, T., Antal, D., & Miklosi, A. (2009). Dogs discriminate between barks: The effect of context and identity of the caller. *Behavioural Processes*, *82*, 198–201. <https://doi.org/10.1016/j.beproc.2009.06.011>
- Mooney, R. (2020). The neurobiology of innate and learned vocalizations in rodents and songbirds. *Current Opinion in Neurobiology*, *64*, 24–31. <https://doi.org/10.1016/j.conb.2020.01.004>

- Moura, D. J., Silva, W. T., Naas, I. A., & Tol, Y. A. (2008). Real time computer stress monitoring of piglets using vocalization analysis. *Computers and Electronics in Agriculture*, 4, 11–18. <https://doi.org/10.1016/j.compag.2008.05.008>
- Nagasawa, M., Murai, K., Mogi, K., & Kikusui, T. (2011). Dogs can discriminate human smiling faces from blank expressions. *Animal Cognition*, 14(4), 525–533. <https://doi.org/10.1007/s10071-011-0386-5>
- Nawroth, C., Ebersbach, M., & von Borell, E. (2013). Are juvenile domestic pigs (*Sus scrofa domestica*) sensitive to the attentive states of humans?—The impact of impulsivity on choice behaviour. *Behavioural Processes*, 96, 53–58. <https://doi.org/10.1016/j.beproc.2013.03.002>
- Nawroth, C., Ebersbach, M., & von Borell, E. (2016). Are domestic pigs (*Sus scrofa domestica*) able to use complex human-given cues to find a hidden reward? *Animal Welfare (South Mimms, England)*, 25, 185–190. <https://doi.org/10.7120/09627286.25.2.185>
- Newport, E. L., & Aslin, R. N. (2004). Learning at a distance I. Statistical learning of non-adjacent dependencies. *Cognitive Psychology*, 48(2), 127–162. [https://doi.org/10.1016/s0010-0285\(03\)00128-2](https://doi.org/10.1016/s0010-0285(03)00128-2)
- Newport, E. L., Hauser, M. D., Spaepen, G., & Aslin, R. N. (2004). Learning at a distance II. Statistical learning of non-adjacent dependencies in a non-human primate. *Cognitive Psychology*, 49(2), 85–117. <https://doi.org/10.1016/j.cogpsych.2003.12.002>
- Norris, T. F. (2012). *The Ecology and Acoustic Behavior of Minke Whales in the Hawaiian and other Pacific Islands*.
- Norris, T., Martin, S., Thomas, L., Yack, T., Oswald, J. N., Nosal, E.-M., & Janik, V. (2012). Acoustic Ecology and Behavior of Minke Whales in the Hawaiian and Marianas Islands: Localization, Abundance Estimation, and Characterization of Minke Whale “Boings”. In A. N. Popper & A. Hawkins (Eds.), *The Effects of Noise on Aquatic Life* (pp. 149–153). Springer New York.

- Okobi, D. E., Banerjee, A., Matheson, A. M. M., Phelps, S. M., & Long, M. A. (2019). Motor cortical control of vocal interaction in neotropical singing mice. *Science*, 363(6430), 983–988. <https://doi.org/10.1126/science.aau9480>
- Okubo, T. S., Mackevicius, E. L., Payne, H. L., Lynch, G. F., & Fee, M. S. (2015). Growth and splitting of neural sequences in songbird vocal development. *Nature*, 528(7582), 352–357. <https://doi.org/10.1038/nature15741>
- Onishi, S., & Davis, H. (1968). Effects of duration and rise time of tone bursts on evoked V potentials. *The Journal of the Acoustical Society of America*, 44(2), 582–591. <https://doi.org/10.1121/1.1911124>
- Palva, S., & Palva, J. M. (2007). New vistas for alpha-frequency band oscillations. *Trends in Neurosciences*, 30(4), 150–158. <https://doi.org/10.1016/j.tins.2007.02.001>
- Perdeck, A. C. (1958). The Isolating Value of Specific Song Patterns in Two Sibling Species of Grasshoppers (*Chorthippus brunneus* Thunb. And *C. biguttulus* L.). *Behaviour*, 12(1/2), 1–75. JSTOR.
- Petrides, M., & Pandya, D. N. (2002). Comparative cytoarchitectonic analysis of the human and the macaque ventrolateral prefrontal cortex and corticocortical connection patterns in the monkey. *The European Journal of Neuroscience*, 16(2), 291–310. <https://doi.org/10.1046/j.1460-9568.2001.02090.x>
- Petrides, Michael, Cadoret, G., & Mackey, S. (2005). Orofacial somatomotor responses in the macaque monkey homologue of Broca's area. *Nature*, 435(7046), 1235–1238. <https://doi.org/10.1038/nature03628>
- Phillips, D. P., & Hall, S. E. (1990). Response timing constraints on the cortical representation of sound time structure. *The Journal of the Acoustical Society of America*, 88(3), 1403–1411. <https://doi.org/10.1121/1.399718>

- Picton, T. W., Hillyard, S. A., Krausz, H. I., & Galambos, R. (1974). Human auditory evoked potentials. I: Evaluation of components. *Electroencephalography and Clinical Neurophysiology*, 36, 179–190. [https://doi.org/10.1016/0013-4694\(74\)90155-2](https://doi.org/10.1016/0013-4694(74)90155-2)
- Plakke, B., Diltz, M. D., & Romanski, L. M. (2013). Coding of vocalizations by single neurons in ventrolateral prefrontal cortex. *Hearing Research*, 305, 135–143. <https://doi.org/10.1016/j.heares.2013.07.011>
- Plourde, G. (2006). Auditory evoked potentials. *Monitoring Consciousness*, 20(1), 129–139. <https://doi.org/10.1016/j.bpa.2005.07.012>
- Poblano, A., Peñaloza, Y., Arch, E., & Morales, J. (1996). Brainstem auditory evoked responses in rats. Effects of the development, stimulation rate and electrode placement. *Acta otorrinolaringologica espanola*, 47(3), 193–198.
- Polikov, V. S., Tresco, P. A., & Reichert, W. M. (2005). Response of brain tissue to chronically implanted neural electrodes. *Journal of Neuroscience Methods*, 148(1), 1–18. <https://doi.org/10.1016/j.jneumeth.2005.08.015>
- Puppe, B., Scho, P., Dupjan, S., Tuchscherer, A., & Manteuffel, G. (2008). Differential vocal responses to physical and mental stressors in domestic pigs (*Sus scrofa*). *Applied Animal Behaviour Science*, 114, 105–115. <https://doi.org/10.1016/j.applanim.2007.12.005>
- Qin, L., Chimoto, S., Sakai, M., Wang, J., & Sato, Y. (2007). Comparison Between Offset and Onset Responses of Primary Auditory Cortex on–off Neurons in Awake Cats. *Journal of Neurophysiology*, 97(5), 3421–3431. <https://doi.org/10.1152/jn.00184.2007>
- Randall, J. A. (1997). Species-specific footdrumming in kangaroo rats: *Dipodomys ingens*, *D. deserti*, *D. spectabilis*. *Animal Behaviour*, 54(5), 1167–1175. <https://doi.org/10.1006/anbe.1997.0560>

- Ray, S., & Maunsell, J. H. R. (2011). Different origins of gamma rhythm and high-gamma activity in macaque visual cortex. *PLoS Biology*, 9(4), e1000610. <https://doi.org/10.1371/journal.pbio.1000610>
- Reed, P., Howell, P., Sackin, S., Pizzimenti, L., & Rosen, S. (2003). Speech perception in rats: Use of duration and rise time cues in labeling of affricate/fricative sounds. *Journal of the Experimental Analysis of Behavior*, 80(2), 205–215. <https://doi.org/10.1901/jeab.2003.80-205>
- Rijntjes, M., Weiller, C., Bormann, T., & Musso, M. (2012). The dual loop model: Its relation to language and other modalities. *Frontiers in Evolutionary Neuroscience*, 4, 9. <https://doi.org/10.3389/fnevo.2012.00009>
- Rilling, J. (2014). Comparative primate neurobiology and the evolution of the brain language systems. *Current Opinion in Neurobiology*, 28, 10–14.
- Rilling, J. K., Glasser, M. F., Preuss, T. M., Ma, X., Zhao, T., Hu, X., & Behrens, T. E. J. (2008). The evolution of the arcuate fasciculus revealed with comparative DTI. *Nature Neuroscience*, 11(4), 426–428. <https://doi.org/10.1038/nn2072>
- Ritter, C., Maier, E., Schneeweiß, U., Wölk, T., Simonnet, J., Malkawi, S., Eigen, L., Tunckol, E., Purkart, L., & Brecht, M. (2021). An isomorphic three-dimensional cortical model of the pig rostrum. *Journal of Comparative Neurology*, 529(8), 2070–2090. <https://doi.org/10.1002/cne.25073>
- Romanski, L. M. (2007). Representation and Integration of Auditory and Visual Stimuli in the Primate Ventral Lateral Prefrontal Cortex. *Cerebral Cortex*, 17(suppl_1), i61–i69. <https://doi.org/10.1093/cercor/bhm099>
- Rosowski, J. (2003). The Middle and External Ears of Terrestrial Vertebrates as Mechanical and Acoustic Transducers. *Biology and Engineering*.

- Roussel, P., Godais, G. L., Bocquelet, F., Palma, M., Hongjie, J., Zhang, S., Giraud, A.-L., Mégevand, P., Miller, K., Gehrig, J., Kell, C., Kahane, P., Chabardés, S., & Yvert, B. (2020). Observation and assessment of acoustic contamination of electrophysiological brain signals during speech production and sound perception. *Journal of Neural Engineering*, 17(5), 056028. <https://doi.org/10.1088/1741-2552/abb25e>
- Roy, S., Zhao, L., & Wang, X. (2016). Distinct Neural Activities in Premotor Cortex during Natural Vocal Behaviors in a New World Primate, the Common Marmoset (*Callithrix jacchus*). *Journal of Neuroscience*, 36(48), 12168–12179. <https://doi.org/10.1523/JNEUROSCI.1646-16.2016>
- Rutkowski, R. G., Miasnikov, A. a., & Weinberger, N. M. (2003). Characterisation of multiple physiological fields within the anatomical core of rat auditory cortex. *Hearing Research*, 181(1–2), 116–130. [https://doi.org/10.1016/S0378-5955\(03\)00182-5](https://doi.org/10.1016/S0378-5955(03)00182-5)
- Ruxton, G. D., & Schaefer, H. M. (2011). Resolving current disagreements and ambiguities in the terminology of animal communication. *Journal of Evolutionary Biology*, 24, 2574–2585. <https://doi.org/10.1111/j.1420-9101.2011.02386.x>
- Saez, I., Lin, J., Stolk, A., Chang, E., Parvizi, J., Schalk, G., Knight, R. T., & Hsu, M. (2018). Encoding of Multiple Reward-Related Computations in Transient and Sustained High-Frequency Activity in Human OFC. *Current Biology*, 28(18), 2889-2899.e3. <https://doi.org/10.1016/j.cub.2018.07.045>
- Saikali, S., Meurice, P., Sauleau, P., Eliat, P., Bellaud, P., Randuineau, G., Vérin, M., & Malbert, C. (2010). A three-dimensional digital segmented and deformable brain atlas of the domestic pig. *Journal of Neuroscience Methods*, 192, 102–109. <https://doi.org/10.1016/j.jneumeth.2010.07.041>
- Sally, S. L., & Kelly, J. B. (1988). Organization of auditory cortex in the albino rat: Sound frequency. *Journal of Neurophysiology*, 59(5), 1627–1638.

- Sauleau, P., Lapouble, E., Val-Laillet, D., & Malbert, C.-H. (2009). The pig model in brain imaging and neurosurgery. *Animal*, 3(08), 1138–1151. <https://doi.org/10.1017/S1751731109004649>
- Savage-rumbaugh, S., & Lewin, R. (1996). *Kanzi: The Ape at the Brink of the Human Mind* (Vol. 17, Issue 1).
- Schenker, N., Buxhoeveden, D., Blackmon, W., Amunts, K., Zilles, K., & Semendeferi, K. (2008). A Comparative quantitative analysis of cytoarchitecture and minicolumnar organization in Broca's area in humans and great apes. *The Journal of Comparative Neurology*, 510(1), 117–128.
- Schenker, N., Hopkins, W. D., Spocter, M., Garrison, A., Stimpson, C., Erwin, J., Hof, P., & Scherwood, C. (2010). Broca's area homologue in chimpanzees (*Pan troglodytes*): Probabilistic Mapping, Asymmetry, and Comparison to Humans. *Cerebral Cortex*, 20(3), 730–742.
- Schmidt, V. (2015). *Comparative anatomy of the pig brain—An integrative magnetic resonance imaging (MRI) study of the porcine brain with special emphasis on the external morphology of the cerebral cortex.*
- Schön, P. C., Puppe, B., & Manteuffel, G. (2004). Automated recording of stress vocalization as a tool to document impaired welfare in pigs. *Animal Welfare*, November.
- Seager, M. A., Johnson, L. D., Chabot, E. S., Asaka, Y., & Berry, S. D. (2002). *Oscillatory brain states and learning: Impact of hippocampal theta-contingent training*. 5.
- Selek, L., Seigneuret, E., Nogue, G., Wion, D., Nissou, M. F., Salon, C., Seurin, M. J., Carozzo, C., Ponce, F., Roger, T., & Berger, F. (2014). Imaging and histological characterization of a human brain xenograft in pig: The first induced glioma model in a large animal. *Journal of Neuroscience Methods*, 221, 159–165. <https://doi.org/10.1016/j.jneumeth.2013.10.002>

- Seyfarth, B. Y. R. M., Cheney, D. L., & Marler, P. (1980). Vervet Monkey Alarm Calls: Semantic Communication in a Free-Ranging Primate. *Anim. Behav.*, 1970, 1070–1094.
- Shaw, N. A. (1988). The auditory evoked potential in the rat—A review. *Progress in Neurobiology*, 31(1), 19–45. [https://doi.org/10.1016/0301-0082\(88\)90021-4](https://doi.org/10.1016/0301-0082(88)90021-4)
- Signoret, J.-P., Du Mesnil du Buisson, F., & Busnel, R.-G. (1960). *Rôle d'un signal acoustique de verrat dans le comportement réactionnel de la truie en oestrus* (pp. 1355–1357) [Compte-Rendus de l'Académie des Sciences 250].
- Simchick, G., Shen, A., Campbell, B., Park, H. J., West, F. D., & Zhao, Q. (2019). Pig Brains Have Homologous Resting-State Networks with Human Brains. *Brain Connectivity*, 9(7), 566–579. <https://doi.org/10.1089/brain.2019.0673>
- Simonyan, K. (2014). The laryngeal motor cortex: Its organization and connectivity. *Current Opinion in Neurobiology*, 28, 15–21.
- Simpson, G., & Knight, R. (1993). Multiple brain systems generating the rat auditory evoked potential. I. Characterization of the auditory cortex response. *Brain Research*, 602, 240–250.
- Smith, W. K. (1945). The functional significance of the rostral cingulate cortex as revealed by its responses to electrical excitation. *Journal of Neurophysiology*, 8(4), 241–255. <https://doi.org/10.1152/jn.1945.8.4.241>
- Souza, A. S., Jansen, J., Tempelman, R. J., Mendl, M., & Zanella, A. J. (2006). A novel method for testing social recognition in young pigs and the modulating effects of relocation. *Applied Animal Behaviour Science*, 99(1), 77–87. <https://doi.org/10.1016/j.applanim.2005.09.008>
- Steinschneider, M., Schroeder, C. E., Arezzo, J. C., & Vaughan, H. G. J. (1994). Speech-evoked activity in primary auditory cortex: Effects of voice onset time.

Electroencephalography and Clinical Neurophysiology, 92(1), 30–43.

[https://doi.org/10.1016/0168-5597\(94\)90005-1](https://doi.org/10.1016/0168-5597(94)90005-1)

Steinschneider, Mitchell, Fishman, Y. I., & Arezzo, J. C. (2003). Representation of the voice onset time (VOT) speech parameter in population responses within primary auditory cortex of the awake monkey. *The Journal of the Acoustical Society of America*, 114(1), 307–321. <https://doi.org/10.1121/1.1582449>

Steriade, M. (2006). Grouping of brain rhythms in corticothalamic systems. *Neuroscience*, 137(4).

Takahashi, H., Nakao, M., & Kaga, K. (2004). Cortical mapping of auditory-evoked offset responses in rats. *NeuroReport*, 15(10). https://journals.lww.com/neuroreport/Fulltext/2004/07190/Cortical_mapping_of_auditory_evoked_offset.7.aspx

Tallet, C., Brajon, S., Devillers, N., & Lensink, J. (2017). *Pig-human interactions: Creating a positive perception of humans to ensure pig welfare.*

Tallet, C., Leribillard, O., Rault, J. L., & Meunier-Salaün, M.-C. (2018). Transmission sociale du comportement d'approche de l'homme chez le porc (*Sus scrofa domesticus*). 48. *Colloque de la Société Française pour l'Étude du Comportement Animal (Sfeca)*, np. <https://hal.archives-ouvertes.fr/hal-01824186>

Tallet, C., Linhart, P., Policht, R., Hammerschmidt, K., & Kratinova, P. (2013). Encoding of Situations in the Vocal Repertoire of Piglets (*Sus scrofa*): A Comparison of Discrete and Graded Classifications. *PLoS ONE*, 8(8). <https://doi.org/10.1371/journal.pone.0071841>

Tallet, C., Sy, K., Prunier, A., Nowak, R., Boissy, A., & Boivin, X. (2014). Behavioural and physiological reactions of piglets to gentle tactile interactions vary according to their previous experience with humans. *Livestock Science*, 167, 331–341. <https://doi.org/10.1016/j.livsci.2014.06.025>

- Thorson, I. L., Liénard, J., & David, S. V. (2015). The Essential Complexity of Auditory Receptive Fields. *PLoS Computational Biology*, 11(12), e1004628. <https://doi.org/10.1371/journal.pcbi.1004628>
- Tinbergen, N. (1959). Comparative Studies of the Behaviour of Gulls (Laridae): A Progress Report. *Behaviour*, 15(1/2), 1–70. JSTOR.
- Torres-Martinez, N., Cretallaz, C., Ratel, D., Mailley, P., Gaude, C., Costecalde, T., Hebert, C., Bergonzo, P., Scorsone, E., Mazellier, J.-P., Divoux, J.-L., & Sauter-Starace, F. (2019). Evaluation of chronically implanted subdural boron doped diamond/CNT recording electrodes in miniature swine brain. *Bioelectrochemistry*, 129, 79–89. <https://doi.org/10.1016/j.bioelechem.2019.05.007>
- van Deursen, J. A., Vuurman, E. F. P. M., Verhey, F. R. J., van Kranen-Mastenbroek, V. H. J. M., & Riedel, W. J. (2008). Increased EEG gamma band activity in Alzheimer's disease and mild cognitive impairment. *Journal of Neural Transmission*, 115(9), 1301–1311. <https://doi.org/10.1007/s00702-008-0083-y>
- Vaterlaws-Whiteside, H., & Hartmann, A. (2017). Improving Puppy Behavior using a new Standardized Socialization Program. *Applied Animal Behaviour Science*, 197. <https://doi.org/10.1016/j.applanim.2017.08.003>
- Vergara, R. C., Jaramillo-Riveri, S., Luarte, A., Moënné-Loccoz, C., Fuentes, R., Couve, A., & Maldonado, P. E. (2019). The Energy Homeostasis Principle: Neuronal Energy Regulation Drives Local Network Dynamics Generating Behavior. *Frontiers in Computational Neuroscience*, 13, 49–49. PubMed. <https://doi.org/10.3389/fncom.2019.00049>
- Volkov, I. O., & Galazjuk, A. V. (1991). Formation of spike response to sound tones in cat auditory cortex neurons: Interaction of excitatory and inhibitory effects. *Neuroscience*, 43(2–3), 307–321. [https://doi.org/10.1016/0306-4522\(91\)90295-y](https://doi.org/10.1016/0306-4522(91)90295-y)

- Vršelja, Z., Daniele, S. G., Silbereis, J., Talpo, F., Morozov, Y. M., Sousa, A. M. M., Tanaka, B. S., Skarica, M., Pletikos, M., Kaur, N., Zhuang, Z. W., Liu, Z., Alkawadri, R., Sinusas, A. J., Latham, S. R., Waxman, S. G., & Sestan, N. (2019). Restoration of brain circulation and cellular functions hours post-mortem. *Nature*, *568*(7752), 336–343. <https://doi.org/10.1038/s41586-019-1099-1>
- Wang, Y., Saito, T., Hosokawa, T., Kurasaki, M., & Saito, K. (2001). Changes in Middle Latency Auditory-Evoked Potentials of the Rat Exposed to Styrene. *Journal of Health Science*, *47*(2), 175–183. <https://doi.org/10.1248/jhs.47.175>
- Weary, M., & Fraser, D. (1995). Calling by domestic piglets: Reliable signals of need? *Anim. Behav.*, *50*, 1047–1055.
- Whittemore, C., & Kyriazakis, I. (2006). *Whittemore's science and practice of pig production*.
- Wild, B., Rodden, F. A., Grodd, W., & Ruch, W. (2003). Neural correlates of laughter and humour. *Brain: A Journal of Neurology*, *126*(Pt 10), 2121–2138. <https://doi.org/10.1093/brain/awg226>
- Wilson, B., Marslen-Wilson, W. D., & Petkov, C. I. (2017). Conserved Sequence Processing in Primate Frontal Cortex. *Trends in Neurosciences*, *40*(2), 72–82. <https://doi.org/10.1016/j.tins.2016.11.004>
- Wondrak, M., Conzelmann, E., Veit, A., & Huber, L. (2018). Pigs (*Sus scrofa domesticus*) categorize pictures of human heads. *Applied Animal Behaviour Science*, *205*. <https://doi.org/10.1016/j.applanim.2018.05.009>
- Wright, T. F., & Dahlin, C. R. (2018). Vocal dialects in parrots: Patterns and processes of cultural evolution. *Emu - Austral Ornithology*, *00*(00), 1–17. <https://doi.org/10.1080/01584197.2017.1379356>

- Xin, H., Leger, D. W., Deshazer, J. A., & Leger, D. W. (1989). Pig Vocalizations Under Selected Husbandry Practices. *Facult Publications, University of Nebraska*.
- Xu, N., Fu, Z.-Y., & Chen, Q.-C. (2014). The function of offset neurons in auditory information processing. *Translational Neuroscience*, 5(4), 275–285.
<https://doi.org/10.2478/s13380-014-0235-5>
- Yvert, B, Crouzeix, a, Bertrand, O., Seither-Preisler, a, & Pantev, C. (2001). Multiple supratemporal sources of magnetic and electric auditory evoked middle latency components in humans. *Cerebral Cortex (New York, N.Y. : 1991)*, 11(5), 411–423.
<https://doi.org/10.1093/cercor/11.5.411>
- Yvert, Blaise, Fischer, C., Bertrand, O., & Pernier, J. (2005). Localization of human supratemporal auditory areas from intracerebral auditory evoked potentials using distributed source models. *NeuroImage*, 28(1), 140–153.
<https://doi.org/10.1016/j.neuroimage.2005.05.056>
- Yvert, Blaise, Fischer, C., Guénot, M., Krolak-Salmon, P., Isnard, J., & Pernier, J. (2002). Simultaneous intracerebral EEG recordings of early auditory thalamic and cortical activity in human. *The European Journal of Neuroscience*, 16(6), 1146–1150.
<https://doi.org/10.1046/j.1460-9568.2002.02162.x>